Numerical Study of Thermophilic Anaerobic Digestion Enhancement Using Parabolic Solar Collector Integrated With Paraffin Wax Based Thermal Energy Storage

Beyisa Bogale Defaru

A Thesis Submitted to the Department of Thermal and Aerospace Engineering

School of Mechanical, Chemical, and Material Engineering

Presented in partial fulfillment of the Requirement for the Degree of Master of Science in Thermal Engineering

Office of Graduate Studies

Adama Science and Technology University

August, 2021

Adama, Ethiopia

Numerical Study of Thermophilic Anaerobic Digestion Enhancement Using Parabolic Solar Collector Integrated With Paraffin Wax Based Thermal Energy Storage

By

Beyisa Bogale Defaru

Advisor: Dr.Dawit Gudeta Gunjo

A Thesis Submitted to the Department of Thermal and Aerospace Engineering

School of Mechanical, Chemical, and Material Engineering

Presented in partial fulfillment of the Requirement for the Degree of Master of

Science in Thermal Engineering

Office of Graduate Studies

Adama Science and Technology University

August, 2021

Adama, Ethiopia

DECLARATION

I hereby declare that this Master thesis entitled **"**Numerical Study of Thermophilic Anaerobic Digestion Enhancement Using Parabolic Solar Collector Integrated with Paraffin Wax Based Thermal Energy Storage**"** is my original work. That is, it has not been submitted for the award of any academic degree, diploma, or certificate in any other university. All sources of materials that are used for this thesis have been duly acknowledged through citation

Beyisa Bogale

______________________	___________________	_______________________
Name of candidate	Signature	Date

RECOMMENDATION

I, the advisor of this thesis, hereby certify that I have read the thesis entitled **“**Numerical Study of Thermophilic Anaerobic Digestion Enhancement Using Parabolic Solar Collector Integrated with Paraffin Wax Based Thermal Energy Storage**”** prepared under my guidance by **Beyisa Bogale Defaru** submitted in partial fulfillment of the requirements for the degree of Mater’s of Science in Thermal engineering. Therefore, I recommend the submission of the thesis to the department following the applicable procedures.

Dr.Dawit Gudeta

Advisor	Signature	Date
____________________	______________________	_________________________

APPROVAL SHEET

I, the advisors of the thesis entitled **"**Numerical Study of Thermophilic Anaerobic Digestion Enhancement Using Parabolic Solar Collector Integrated with Paraffin Wax Based Thermal Energy Storage**"** and developed by Beyisa Bogale Defaru; hereby certify that the recommendation and suggestions made by the board of examiners are appropriately incorporated into the final version of the thesis.

______________________	______________	______________________
Advisor	Signature	Date

We, the undersigned, members of the Board of Examiners of the thesis Beyisa Bogale Defaru have read and evaluated the thesis entitled **"** Numerical Study of Thermophilic Anaerobic Digestion Enhancement Using Parabolic Solar Collector Integrated with Paraffin Wax Based Thermal Energy Storage **",**and examined the candidate during the open defense. This is, therefore, to certify that the thesis is accepted for partial fulfillment of the requirement of the degree of Master of Science in Thermal Engineering.

Chairperson	Signature	Date
Internal Examiner	Signature	Date
External Examiner	Signature	Date

Finally, approval and acceptance of the thesis is contingent upon submission of its final copy to the Office of Postgraduate Studies (OPGS) through the Department Graduate Council (DGC) and School Graduate Committee (SGC).

Department Head	Signature	Date
School Dean	Signature	Date
Office of Postgraduate Studies, Dean	Signature	Date

DEDICATION

this thesis is dedicated to my father Bogale Defaru

ACKNOWLEDGMENTS

First and above all, I praise the almighty God for his grace to do this work, blessings, wisdom, protection and helps me throughout my life. All these people deserve heartfelt gratitude. My sincere apologies, if I fail to mention some who deserve to be acknowledged.

My Advisor Dr. Dawit Gudeta has been an enormous resource to me in all facets of my academic life during my Master's study. I am grateful to him for his continuous encouragement and constructive comments from the beginning of the research up until the thesis was made to this final form including the final edition and proofreading. He made every effort possible to help me develop as a successful researcher in a multidisciplinary environment for which I am sincerely indebted.

I extend my deep gratitude to Adama Science and Technology University for its willingness in providing and supporting me financially, At last, but not least, I am grateful to extend my deepest and heartfelt gratitude towards my family who was always on my side in my academic life. This long academic life involved lots of difficulties, hope, despair, and needed immense moral and material support. Thank you all for your persistent support all along.

ABSTRACT

Energy is one of the main inputs for the economic growth of any country. It is a well-known fact that the growth of a given nation has a direct relationship with the quantity of energy utilization. The renewable energy sector is one of the main sources of energy that can give a crucial role in the development of a nation. Biogas is a promising technology is produced from the anaerobic digestion of organic waste raw material. Temperature is the main factor that can affect the production and performance of an anaerobic digestion system. The amount of produced biogas is increased with digester temperature. In order to achieve and maintain a constant process temperature and to compensate for possible heat losses, digesters are heated by external heating sources. Solar energy may well be integrated within the process then a high gas production rate can be accomplished. However, the main drawback of this resource is the intermittency and unpredictability of solar energy, so thermal storage is a key issue to be addressed to allow the intermittence of solar energy.

The objective of this study was to investigate the numerical performance of thermophilic anaerobic digestion enhancement utilizing a parabolic solar collector integrated with paraffin wax-based thermal energy storage (TES) that is designed to digest cow dung at Bale Robe weather conditions. The system is composed of an anaerobic digester, parabolic trough solar collector, latent heat thermal storage, and a thermal model developed for those main components. The thermophilic anaerobic digester produced the daily cooking and lighting energy demanded by my family and nearby householder (50). The parabolic trough solar collector is used as an external source of energy to provide the heat energy required to maintain the digester temperature at the desired level. TES used as a storage unit to store solar energy that was later used by digestion during the absence of solar radiation. An anaerobic digester design to produce $30.5m^3$ *biogas per day. Water used as heat transfer fluid and Paraffin wax n-Hentriacontane used as phase change material. Transient One dimensional heat transfer model developed each component of system and PYTHON and MATLAB script also written to solve iteratively using finite difference scheme. The numerical simulation results showed that* $4.9\ m^3$ *spherical capsule paraffin wax phase change material and 5 units of parabolic trough solar collector is fulfilled the energy required by the digester.*

Key Word: Thermophilic, Anaerobic digestion, parabolic trough solar collector, solar radiation Heat transfer fluid, Phase Change Material, Thermal Energy Storage

TABLE OF CONTENTS

CONTENTS PAGE

LIST OF FIGURES

LIST OF TABLES

ABBREVIATIONS

HRT	hydraulic retention time
GIS	Geographic Information System
CFD	Computational Fluid Dynamics
HBS	Hybrid Biomass System
TRNSYS	Transient System Simulation
EPDM	**E**thylene Propylene Diene Terpolymer
SR	substrate-feeding rate
PTC	Parabolic solar Collector
HCE	Heat collecting element
HTF	Heat transfer fluid
TES	Thermal Energy storage
LHS	Latent heat storage
SHS	Sensible Heat Storage
STAR	Solar Thermophilic Anaerobic Reactor
PCM	Phase change Material

SUBSCRIPTS

T	Total volume of digester	f	working fluid
m	Mass flow of manure	g	glass envelope
s	surrounding	in	internal
Dg	Digestate	cv	convection
F	Feed	eff	effective
L	Leaving from digester	s	PCM
Bg	Biogas	m1	solid-solid transition
r	radiation	s1	solid PCM
Co	cover	s2	liquid PCM
At	Atmosphere	ini	initial
So	solar irradiation’s	elem	Element
w	water	fu	Fusion

st	standard meridian	st	Storage tank
loc	longitude of the location	min	minimum
sr	sunrise	am	ambient
ss	sunset	a	aperture
max	maximum	ri	Rim angle
ex	External	ro	Outer radius of absorber
cnv	convection	m2	solid-liquid transition

NOMENCLATURE

Q	Heat flow (W)
T	Temperature (K or ^{o}C)
V	Volume (m3)
C	Specific heat capacity (J/kgK)
h	Convective heat transfer coefficient (W/m^{2}K)
S	Absorbed solar radiation (W/m^2)
u	Speed (m/s)
G	Global radiation (W/m^2)
E	Equation of time
k	Thermal conductivity (W/mK)
n	Day of the year
ST	Solar time (hr)
N	Day time duration
DH	Diffused radiation on horizontal (W/m^2)
BH	Beam radiation on horizontal (W/m^2)
t	Time (s)
R	Radiation factor
I	Incidence solar radiation (W/m^2)
U	Overall heat transfer coefficient (W/m^{2}K)
A	Area (m^2)
FR	Collector heat removal factor
e	Porosity

D	Diameter (m)
Re	Reynolds number
H	Enthalpy (J/kg)

GREEK SYMBOLS

ρ	Density (kg/m^3)	ν	Kinematic viscosity (m^2/s)
β‘	Coefficient of thermal expansion (1/K)	μ	Dynamic viscosity (kg/ms)
ε	Emissivity	θi	Incidence angle (^{o})
σ	Stefan-Boltzmann constant	θz	Zenith angle (^{o})
δ	Declination angle (^{o})	β	Inclination angle ($^{o)}$
ω	Solar hour angle (^{o})	α	Thermal absorptivity
ψsoil	Ground albedo	Δ	Change
γ	Bond thickness (m)	η	Efficiency
τ	Transmissivity	γ’	Melt fraction of phase changing material

CHAPTER 1: INTRODUCTION

1.1. Background of the study

Energy is one of the main inputs for the economic growth of any country. It is a well-known fact that the growth of a given nation has a direct relationship with the quantity of energy utilization. The high standards of living in the developed nations are the manifestation of high-energy utilization levels. For the reason of the exhaustible nature of primary energy sources or nonrenewable energy sources; such as (coal, oil, and natural gas) and their repeatedly reducing supply with increasing consumption causes the rising prices **(Radoičić et al, 2016).** Not lone this, the drastic increment of global warming implies that the increased effect of greenhouse gases (carbon dioxide) emission **(Surendra et.al, 2014).** As the studies, point out combustion of fossil fuels is accountable for more than 62% of global warming **(Okuo et al, .2014)**. These and other factors are the driving forces, which driven us to looks for renewable energy sources and result in the development of renewable energy production technologies**.**

1.1.1. Role of Renewable Energy Technology

In practice, renewable energy refers to hydropower, biomass energy, solar energy, wind energy, geothermal energy, and ocean energy. Except ocean energy, all forms of renewable energies are relevant in Ethiopia. These resources are constantly replenished by nature and cleaner source of energy. Renewable energies are; suitable for decentralized application, environment friendly (pollution-free), help to fight global climate change and directly associated with sustainability. Moreover, they have short lead-time for planning and construction; they can increase energy security in diversifying energy supply and they contribute to local or regional economic development, because money spent on non-renewable energy stays at home **(Benjamin, 2004).**

1.1.2. History of Biogas Initiation in Ethiopia

In October 1962, the first biogas plant in Ethiopia was installed in Ambo agricultural college, located 115km west from Addis Ababa. This floating drum biogas system comprised of 7 m^3 digester size and with daily loading rate of about 100 liter of dung with water in a 1:1 ratio. Currently the total biogas plants installed in Ethiopia is estimated to be nearly 120. In 1970's most of the biogas plants installed were floating drum systems and built by the then Ethiopian National Energy Committee (ENEC). Some rural technology promotion centers also build the same type of digesters in different parts of the country. But the number of biogas systems installed is not much relative to the large potential of available feedstock within different institutions. This may be attributed to the lack of awareness of people regarding the technology or the high cost of the metallic biogas system then in use. The other reason might be the availability of fuel-wood at a relatively cheaper price; hence making the cost benefit analysis of the systems unattractive. Hence, even four decades after the introduction of biogas technology to the country, its dissemination has been observed to be rather sluggish **(Tadesse, 2010)**

1.1.3. Biogas plant in Ethiopia

The size of biogas plants installed in the institutions ranged from 12m^3 to 350m^3. There was an incidence to observe plants connected in series; including the one with 350m^3. The size of visited biogas plants installed in different organizations is listed in Figure 2-1. The most common capacity is 100m^3 accounting for 20 percent of the installation and the 30m^3 plants accounting for 11percent**(leta,2009).**

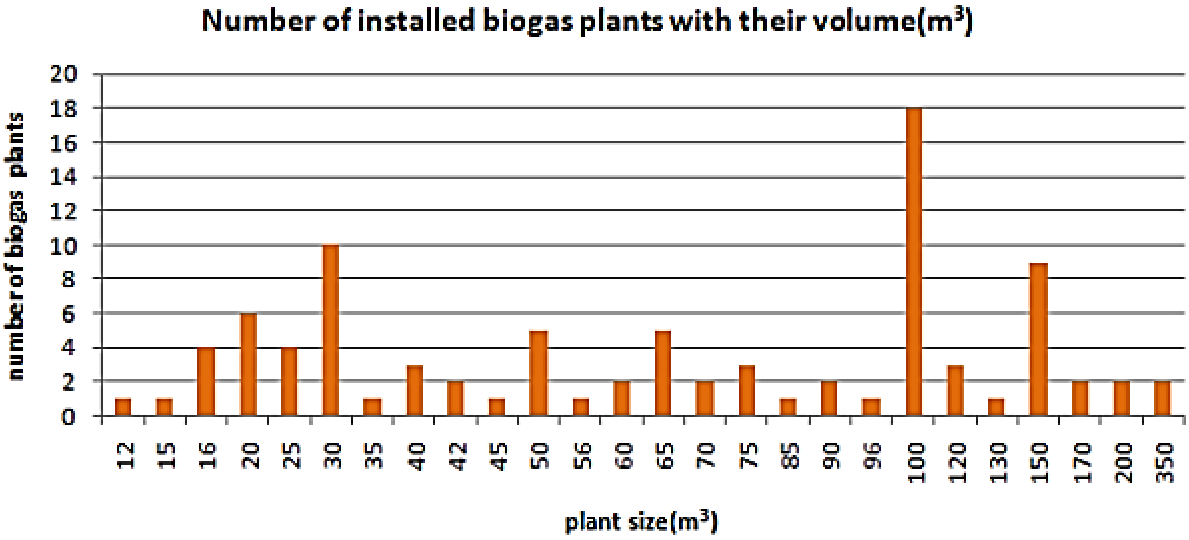

Figure 1. 1:Distribution of biogas plants in size (Leta, 2009)

1.1.4. Applications of biogas in Ethiopia

Most of the biogas plants are installed for cooking, some for lighting, waste stabilization, demonstration, agricultural fertilizer, milk processing, heating, or in combination of the above mentioned. However, institutions are observed using the biogas system apart from the initial purpose of the plant. In contrast, some biogas systems give service in addition to the purpose that the plant aimed to give service.

Table 1. 1:Purpose of installing biogas plats and their number (leta,2009)

Purpose	Number of plants
Cooking	89
Waste Stabilization	11
Agricultural Fertilizer	6
Lighting	4
Demonstration	3
Other	3
Lab use	2
Run engine	1
Milk/meat processing	1
Heating	1

1.1.5. Energy policy and plans, and Biogas Programme in Ethiopia

(A) Energy policy and plans

With over 94% of the total energy consumption for domestic activities supplied by biomass, wood contributing the lion share, Ethiopia is third in the list of countries using traditional fuels. However, Ethiopia is endowed with a variety of energy resources potentials. These include all forms of biomass, hydro, geothermal, solar, wind and substantial economically exploitable natural gas and coal. Despite the immense available resource, except the woody biomass, which is unsustainably exploited, much of the other energy resource has yet to be developed. The country is engaged aggressively in developing and promoting indigenous energy resources. The energy development programs are being implemented within the framework of the Government's national development policy and strategy. It is guided by the energy policy issued in 1994 that gives high emphasis to the development of hydropower for meeting the national modern energy demand and aiming at bringing rapid socio- economic development **(Tadesse, 2010)**

Moreover, among the energy resource and technology development programs the country has given emphasis and implementing a number of programs and projects on biomass demand and supply side areas. These areas are also given priority, because the forest resource of the country is depleted that caused land degradation. The use of energy inefficient cooking devices coupled with population growth has escalated the demand for woody biomass substantially. Scarcity of woody biomass fuel resources has forced low-income households, in particular women and children to spend their considerable time and effort for searching, collecting and transporting fuels. To avert this situation and to enhance the woody biomass resource of the country, the Government has been undertaking intensive forestation and reforestation programs. In addition to this, the country is now promoting energy efficiency and conservation measures at the supply and consumer side **(Tadesse, 2010).**

The National Energy Policy in Ethiopia aims to satisfy the basic (energy) needs of all households. The energy policy recognizes the importance of energy as a means for sustainable development. Key areas include: a) Priority development of hydro and traditional energy resources, b) Diverse and enhanced biomass based technologies (biogas, agricultural residue briquetting, and ethanol production), c) energy conservation technologies and measures. This is vital to the development of the energy sector to ensure self-reliance on indigenous resources, formulation of a conducive sector regulations and directives and ensuring of environmental sustainability. Dissemination of domestic biogas in rural areas is seen as another intervention area with considerable potential impacts for both the energy and agriculture sectors. Ethiopia has the largest cattle population in Africa. An integrated system of energy and fertilizer production from biogas digesters has the potential to address two key problems in rural areas. The government in the past decade has pursued promotion of the biogas technology, mainly for rural domestic applications. Now the government is working with development partners to upgrade the dissemination to the next level with the proposed development of many thousand domestic biogas units in rural areas within the next five years **(Tadesse, 2010).**

Due to the renewed interest in biogas, and in order to unleash the potential for biogas in Ethiopia, a feasibility study to assess the potential for domestic biogas plant was commissioned. The positive outcome of the feasibility study of a National Biogas Programme (NBP) for Ethiopia resulted in a formal partnership between the Ethiopian Rural Energy Promotion and Development Centre (EREDPC) and SNV/Ethiopia to develop a Programme implementation document for mass dissemination of domestic biogas.

1.1.6. Types of Biogas plants

There are various types of plants. Concerning the feed method, three different forms can be distinguished: Batch plants, Continuous plants, and Semi-batch plants. **Batch plants:** are filled and then emptied completely after a fixed retention time. Waste is fed into the system in batches, usually with a starter (5 percent to 30 percent by volume) and left for gas production until thorough degradation occurs. The digester is then emptied and a new batch of feedstock is added. Each design and each fermentation material is suitable for batch filling, but batch plants require high labor input. As a major disadvantage, their gas-output is not steady.

Continuous plants: are fed regularly once the first feed starts generating gas**.** They empty automatically through the overflow whenever new material is filled in. Therefore, the feedstock is fed after mixing with water and in course of time, the digested slurry overflows through the outlet. Once the digestion process gets established, the gas production rate becomes fairly constant, and higher than in batch plants. Today, nearly all biogas plants are operating on a continuous mode. If straw and dung are to be digested together, a biogas plant can be operated on a **semi batch** basis. The slowly digested straw-type material is fed in about twice a year as a batch load. The dung is added and removed regularly **(Tadesse, 2010).**

Concerning the construction, although, various types of biogas plants have been developed, the two most familiar types in developing countries are the fixed-dome plants and the floating-drum plants (GTZ, 1999). In developing countries, the selection of appropriate design are determined largely by the prevailing design in the region. Typical design criteria are space, existing structures, cost minimization, and substrate availability

1.2. Biogas

Biogas is a gas created from the anaerobic breakdown of natural waste materials. It is essentially a mix of methane and carbon dioxide, a combustible product that can be utilized as a renewable and effortlessly controlled fuel. The fundamental step in the production of biogas:

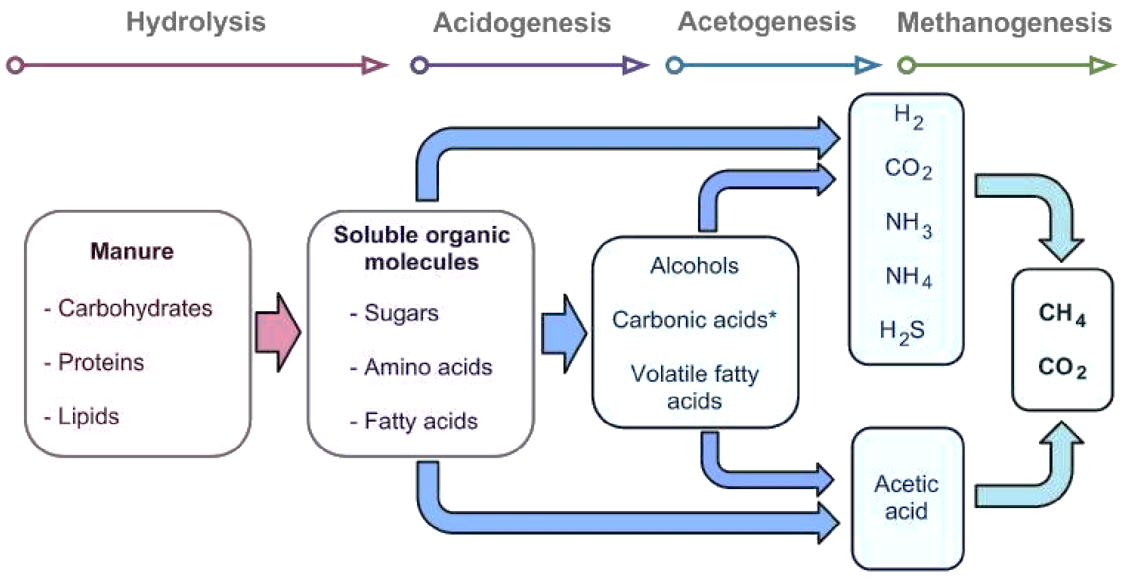

Table 1. 2: The fundamental steps in the production of biogas (Yousef et al, 2016.)

Yousef et al., (2016) since it can be produced from locally accessible raw materials, it offers a potentially affordable and sustainable implies for rural householders to meet their energy needs.

Table 1. 3:Typical content of biogas

Compound	Formula	%
Methane	CH_4	50-75
Carbon dioxide	CO_2	25-50
Nitrogen	N_2	0-10
Hydrogen	H_2	0-1
Hydrogen sulfide	H_2S	0-3
Oxygen	O_2	0-0

1.3. Anaerobic Digestion

The process of degradation of organic material in every step is done by a range of bacteria as already stated above, which are specialized in the reduction of intermediate products formed. The efficiency of the digestion depends on how far the digestion happens in these three stages. Better digestion, shorter retention time, and efficient gas production. The biogas production process involves three stages namely **(Kamp & Bermúdez Forn, 2016).**

Hydrolysis: The complex organic molecules as fats, starches, and proteins, which are water-insoluble, contained in cellulosic biomass are broken down into simple compounds with the help of enzymes secreted by bacteria. This is the stage where the complex polymers break into simple monomers.

Acid formation: The resultant product (monomers) obtained in the hydrolysis stage serve as input for acid formation stage bacteria. Products produced in the previous stage are fermented under anaerobic conditions to form different acids. The major products produced at the end of this stage are acetic acid, propionic acid, butyric acid, and ethanol.

Methane formation: The acids produced in the previous stages are converted into methane and carbon dioxide by a group of microorganisms called "*Methanogens*". In other words, it is the process of the production of methane by methanogens. They are obligatory anaerobic and very sensitive to environmental changes.

Anaerobic digestion relies on the activity of methane-producing microorganisms called methanogens. Although digester design may vary, the ultimate goal remains to produce as much useable methane as possible. Digesters must be designed and operated to maintain the optimum conditions necessary for the growth of these organisms. There are numerous factors to take into account. According to **Cheng, (2010),** these conditions can be separated into two general areas: chemical and physical environments, as shown in Table 1.2:

Table 1. 4:: Chemical and Physical factor of Anaerobic Digestion (Cheng, 2010).

CHEMICAL	PHYSICAL
Anaerobic Conditions	Temperature
Substrate	Water
Nutrients	Particle Surface Area
pH	Loading Rate
Toxics	Retention Time
	Mixing

1.4. Temperature

The physical environment provides a platform for chemical reactions. Maintaining a constant temperature in the optimal range for the bacteria is critical for maximizing gas production. Anaerobic bacteria can endure temperatures ranging from below freezing to above 70°C but thrive best at mesophilic temperatures of about 36.7°C (98°F) or thermophilic temperatures of about above 50°C (122°F). In the thermophilic range, decomposition and biogas production occurs more rapidly than in the mesophilic range. However, digesters operated in the mesophilic range are less sensitive to upset or change in operating routine

Table 1. 5:Comparison of Anaerobic Processes phase (Cheng, 2010)

Anaerobic Process	Operating Temperature (°C)	Operating HRT (days)	Microbial Growth and Digestion Rates	Tolerance to Toxicity
Psychrophilic	10 – 25	> 50	Low	High
Mesophilic	30 – 37	25 – 30	Medium	Medium
Thermophilic	50 – 70	10 – 15	High	Low

Table 1.5 **Cheng, (2010)** appeared that the temperature ranges, operating hydraulic retention time (HRT), the average length of time liquids and solvent compounds stay within the digester, growth and digestion rates, and tolerance to toxicity for the three anaerobic processes. Increasing HRT permits more contact time between substrate and bacteria but requires a slower feeding rate or larger digester volume.

According to **Hamed et al. (2004),** the temperature is a critical factor that can influence the performance of anaerobic digestion, and the sum of gas produced increases with an increase in digester temperature, with retention time, and with the percentage of total solids in the slurry. Anaerobic digestion can be achieved under psychrophilic (5 – 25 ^oC), mesophilic (25 – 40 ^oC) or thermophilic (> 45 ^oC) conditions .Digestion under thermophilic conditions has many advantages such as higher metabolic rates and higher destruction of pathogens and weed seeds (**Varel et al., 1980**). The major drawbacks of thermophilic treatment compared with mesophilic treatment are less stability and higher energy requirements.

To preserve the optimum biogas yield and anaerobic digestion condition temperature, the thermal management of biogas digester ought to apply. The foremost common methods of thermal management of heating biogas digester are as follows **(Dawit et al., 2019).**

I. **Direct heating** in form of steam or hot water and

II. **Indirect Heating** via the heat exchanger, whereby the heating medium, usually hot water, imports heat while not mixing with the substrate

Indirect heating methods incorporate renewable energy resources such as thermal solar energy that might be integrated within the process at that point high gas production can be accomplished with high-energy efficiency **(Hamed et al., 2004).** The combination of solar energy and biogas production represents a kind of solar energy storage in the form of fuel.

1.5. Statement of Problem

Steady process temperature inside the digester is one of the most crucial conditions for stable operation and high biogas yield. Digestion under higher temperature conditions has many advantages such as higher metabolic rates and a higher destruction of pathogens and weed seeds. Temperature fluctuations, together with fluctuations determined by season and weather conditions as well as nearby fluctuations, in different areas of the digester, must be kept as low as possible. The causes of temperature changes are different: Addition of new feedstock, with different temperature than the one of the process. Inadequate placement of heating elements. Extreme outdoor temperatures during summer or winter.

In order to achieve and maintain a constant process temperature and to compensate for possible heat losses, digesters must be insulated and heated by external heating sources. Solar energy may be well integrated within the process then a high gas production rate can be accomplished with the High-energy efficiency of the digestion system. Solar energy storage is a key issue to be addressed to permit intermittent energy sources, typically renewable sources, to match energy supply with demand. Depending on the weather condition of Ethiopia, integrating solar energy and thermal energy storage to biogas digester researches and studies are stills few reports found.

1.5. Description of the Study Area

The Robe is the capital town of Bale Zone. A suffix Weleshe is sometimes used to name as Robe- Weleshe to differentiate it from Robe-Dida of Arsis Zone. The town has been established in, 1931 as a settlement area. Robe town is located in Oromia National regional state, in Bale Zone, Sinana Woreda. Astronomically, it is located at 70 3’30” to 70 10’ 45” North Latitude, and 340 57’ 38” to 400 2’ 38” East Longitude **(Bale Robe, 2021).**

The average elevation of this town is 2,492 m above mean sea level and Bale Robe (figure.1.2) is located about 430 km from the capital city Addis Ababa. The average daily duration of sunshine is approximately 8-10 hours, and the mean annual maximum and minimum temperatures are 22.20 and 7.750 respectively **(Abebe.Ch & Ababu G, 2018)**. It is characterized by cold climate type with annual rainfall of about 1200 mm.

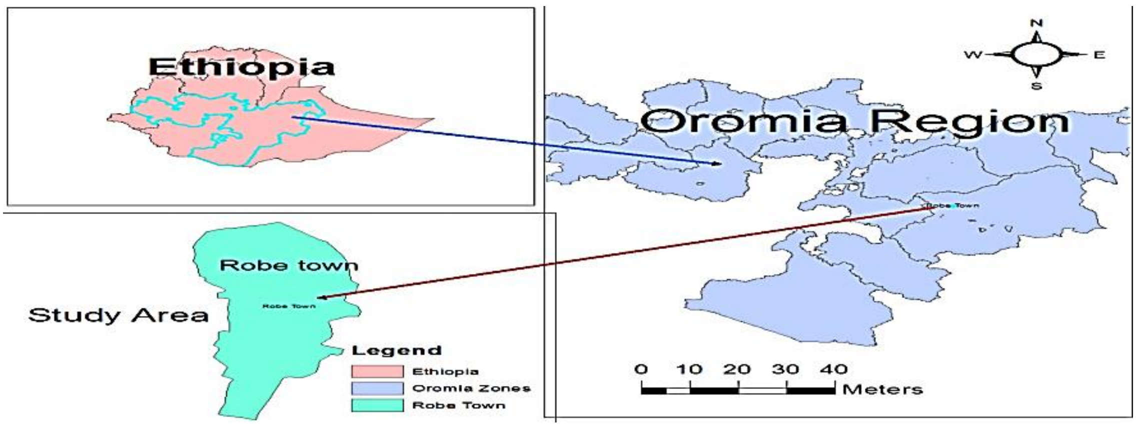

Figure 1. 2:The map of the study area of Robe town (Source: GIS)

In the present study, the thermal performance of thermophilic anaerobic digestion enhancement utilizing parabolic solar collector Integrated with paraffin wax-based thermal energy storage (Paraffin wax n-Hentriacontane) will numerically investigate. The digester is designed to digest cow dung at Bale Robe weather conditions. Produced biogas gas ought to fulfill the energy request of my family plus nearby householders (total 50) round Robe town for cooking and lighting purpose.

1.6. Generally Objective of this study

The general objective is numerical study of thermophilic anaerobic digestion enhancement utilizing parabolic solar collector integrated with paraffin wax-based thermal energy storage that is designed to digest cow dung at Bale Robe weather conditions.

1.6.1. The specific objectives of the study are

- Estimate the anaerobic digester size and energy demand of a select number of householders for their cooking and lighting application.
- Simulate parabolic solar collector and thermal energy storage using MATLAB and ANACONDA PYTHON script
- Numerically investigate the transient thermal performance of the thermophilic anaerobic digester major components using numerical method i.e.
    - Transient thermal simulation and performance of anaerobic digestion system under selected weather conditions.
    - Transient thermal performance of the parabolic solar collector system that fulfills the energy demand of the digester.
    - Transient thermal performance of energy storage device with integrating paraffin wax investigated with the digester.

1.7. Theoretical /Conceptual Framework

The system considered in this study consisted of parabolic solar collectors, anaerobic digester, heat exchanger /coil, and paraffin wax-based thermal energy storage device. The parabolic collector is the main component of the heating system and it converts solar energy into heat. The heat storage device accumulates the surplus heat and supplies heat when there is not sufficient heat-collecting capacity. Furthermore, the storage device reduces the influence of the relatively unstable solar energy heat source and increases the stability of the system **(Lu et al., 2015).** The collected useful heat is transferred to thermal energy storage device at the time the temperature of thermophilic anaerobic digestion system is higher than 60°C. When temperatures of digestion system is lower than 60°C, it is used for heating the anaerobic digestion system.

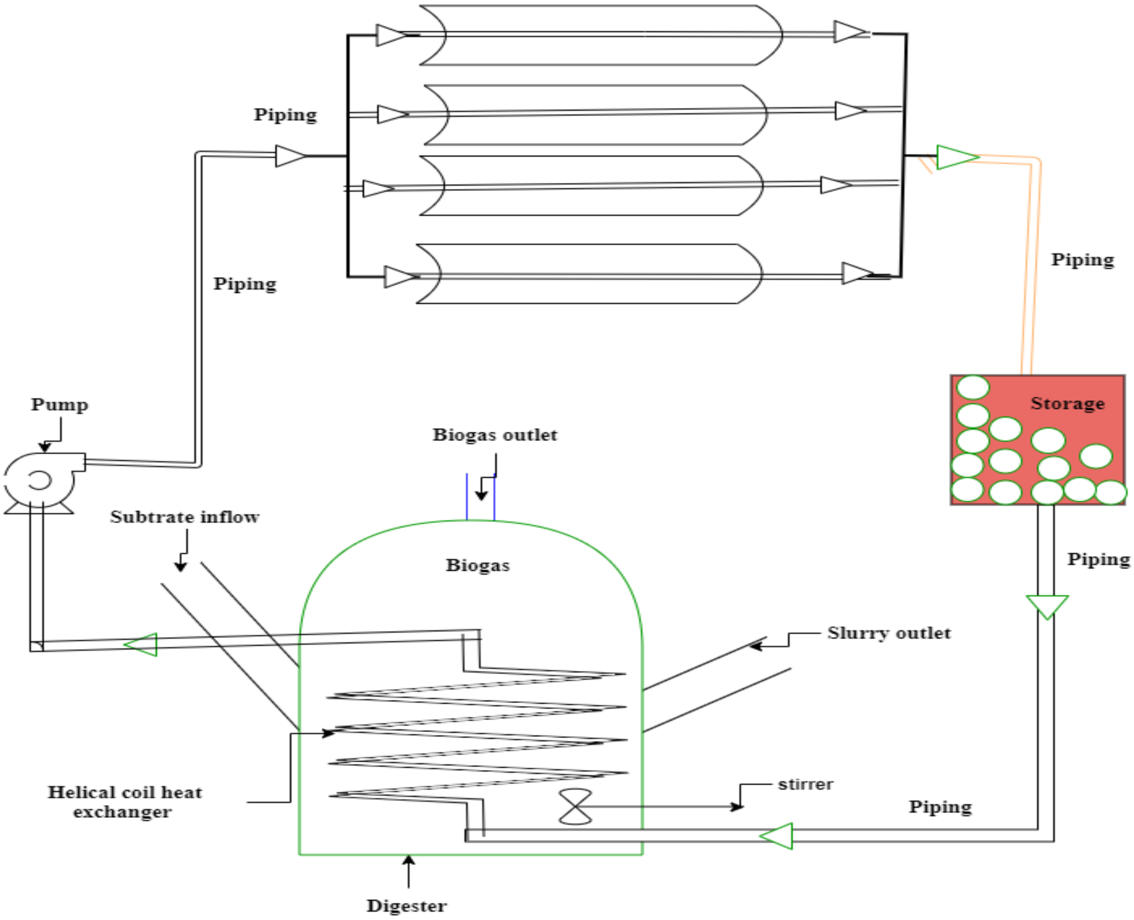

Figure 1. 3:Schematic diagram of anaerobic digester integrated with PTC and TES

1.8. Scope and Limitations

1.8.1. Scope of Study

This study mainly focuses on the numerical study of thermal performance of a thermophilic anaerobic digester that is designed to treat animal waste (cow dung) and it is designed to work at weather condition Bale Robe, This investigation also includes the performance analysis of Paraffin Wax a phase-changing material based thermal storage integrated with the parabolic solar collector to storage energy needed to maintain digester temperature of anaerobic digestion.

1.8.2. Limitations of the study

This study is delimited to numerical investigate the transient thermal performance of a parabolic solar collector, transient thermophilic anaerobic digester, transient thermal energy storage system. The analysis of helical coil heat exchanger, solar tracking system of PTC, and experimental study and cost-effectiveness analysis of a system is not included here. The multi-dimensional heat transfer phenomenon in the digester, solar collector, and thermal energy storage system complicates the analysis. Thus in this study, a one-dimensional heat flow model is used to investigate the systems.

1.9. Significances of the Study

Now day biogas is one of renewable energy source has been used all over the world and in Ethiopian this technology slowly used by household and especially farmer in a rural area for different application. Temperature is one factor that inhabits the production of biogas

To maintain temperatures in the mesophilic or thermophilic ranges during anaerobic digestion, energy investment in a system that supplies heat to the digester is necessary. This involves an extra cost at the operation of anaerobic digesters.

An alternative to solve this problem is the use of solar energy by implementing a solar collection parabolic type with a thermal storage tank that would supply heat to the anaerobic digester by using an internal coil. Using a solar collector allows heat supply to the anaerobic system at a low cost and with a very low environmental impact because digester is not necessary to use fuels.

1.10. Organization to this study

Once going through a numerous amount of literature on each part of the system in chapter 2, a method approaching the solution has been developed and the methodology of study will layout in chapter 3. The mathematical modeling for biogas digester-based on mass, energy will be in chapter 4 and the developed model will be validated against an experimental test conducted on the thermophilic anaerobic digestion heat transfer heat requirement in chapter 7.

Available solar radiation on the surface for different representation day of each month of the year required and design parabolic trough solar collector with the implementation of the model in PYTHON script is studied in Chapter 5.Chapter 6 is focused on developing a mathematical model for the latent heat storage unit based on the energy balances and heat transfer equations. Same as the PTCs, the model will be implemented in MATLAB software, Charging, and discharging time of latent heat storage integrated with the parabolic trough solar collector will be studied and result is validated to others work in chapter.

CHAPTER 2: LITERATURE REVIEW

2.1. Introduction

Researches and developments have been done in biogas technology to improve the efficiency and performance of anaerobic digestion, There are different ways to maximize both the efficiency of biogas plants and the usefulness and effectiveness of digesters. As mentioned earlier the temperature is one of many factors that affect the anaerobic digestion system. To overcome temperature problems using a different auxiliary heating system such as utilizing solar thermal technology and heat exchanger as an energy source. In this section, previous works are associated with solar assisted biogas systems are reviewed

2.2 Thermophilic Anaerobic Digestion

Anaerobic digestion (AD) will take place at any temperature over approximately 10 degrees Celsius. Over the years research has set up that there are two temperature ranges that are the most efficient for biogas production by utilizing the normal bacteria and other synergistic organisms which contribute, which are the most efficient for the process and for biogas production. Those two temperature ranges are known as the mesophilic and the thermophilic temperature ranges. The mesophilic is the cooler range, and the thermophilic range is the hotter one**. (Thermophilic Digester, 2019)** a thermophilic digester or thermophilic biodigester could be a kind of biodigester that works in temperatures above 50 °C producing biogas. In reality, it can be as much as six to ten times faster than a normal biodigester.

2.3. Application of solar thermal energy technology in the heating biogas plant

CFD simulation of flat plate collector was done for preparation of hot water utilized to produce biogas system by the solar water heater **(Negera Woyessa et al., 2020).** The detailed study was done on an average of solar radiation heater absorbers by $2m^2$ flat plate collectors under Jimma weather conditions and 122 number of the collector required to produce the heat needed for the fermentation of system at 35℃ temperature with 44.7 m^3 according to mathematical calculation design. A CFD simulation to predict the result of different parameters on the solar collector heater system to validate thermal performance, pressure drop, flow velocity water, and temperature output for a different type of mesh and flow types in the collector has been conducted. The maximum outlet water temperature of 333.2K. Moreover, based on the output temperature the efficiency of the flat plate collector was validated.

Darwesh & Ghoname,(2021) the study aimed to evaluate the technical and design feasibility of using solar energy to heating the digestion unit's .measure and determined the contribution of solar energy to heat the system. This study was conducted in the central area of Coastal Delta, Egypt (30.5ºN, 30.6E; 8.5 m a.s.l.).The result revealed that the contribution of solar energy to biogas production was 75.21%, 60%, and 53.58% when using three settings temperatures of (37, 40, and 45ºC) of the energy consumed via cattle dung solution heating. Furthermore, increasing the set temperature inside the horizontal and vertical digesters from 37 ºC to 45 ºC augmented their daily average volumetric biogas production by 87.12% and 59.45%, respectively. Finally, the current study says that solar energy has reduced energy consumption by 61.28%. In addition, the economic analysis indicates that the estimated return profit was $ 177.41 (USD), which represents 45.15% of the total income per operation.

El-Husseini et al., (2019) carried out an experimental study on enhancing the fermentation temperature inside the digester by supplying the required thermal energy collected by PTC to maintain the optimum range (mesophilic range) for biogas production during winter. A parabolic trough solar collector thermally enhances one digester, while the other digester used as control operated the ambient temperature. The result showed that the average temperature of the control digester experiment was 21.5°C, while the enhanced digester was at 27.08°C.PTC enhanced the fermentation temperature of the digester by 20.6%. The temperature in the treatment digester by 20.6%. The total biogas yield of the control digester and the treatment digester was 9684.7 mL/kg. T.S. and 24649.69 mL/kg. T.S. respectively. The productivity of biogas in enhanced digester was about 2.5 times more than control digester.

Amro et al.,(2011) In this research, one digester under the ground was used as a study object, which is located at Runzhen middle school in Chunhua county, Shannxi province, and its volume is100 m^3. The raw material was human manure, which was fed to the system every day. The average temperature in January was -1.6ºC, the lowest temperature was -15ºC and the average solar radiation in the Runzhen area was 4.5 kWh/m^2. Because in the winter the biogas yield without a heating system will almost stop, the objective of this study is to investigate the feasibility of using solar energy for increasing biogas production. The system includes a 120m^2 greenhouse and 8 flat solar thermos tube heaters with a total surface area of 20 m^2 to reach optimum temperature. Results show that in the winter the solar system can increase biogas yield by 12 m^3 per day with a cost of 1.5 Yuan/m^3, all the gas yield can be used in the school kitchen by the designed pipe for cooking. In addition, the parabolic trough solar concentrator (PTC) with tracking system was developed for the heating system, which is expected for higher gas production per day without daily additional cost.

Terakegn, (2018) in work investigated the thermal performance of solar-assisted biogas digestion, system integrated with phase change material. This system consists of a flat plate solar collector, helical coil heat exchanger, biogas digester, and thermal energy storage unit. The flat plate solar collector was used to deliver energy demand by biogas digester to maintain fermentation temperature. The result showed that for 100 people the energy demand for their cooking can be fulfilled by 31 flat plate collectors to maintain digestion system,3m^3 paraffin wax filled in packed bed thermal storage unit can store energy for later use for biogas digester during solar disappear.

The application of the solar heating system in the anaerobic digestion of cow dung and the feasibility of the integrated solar thermal energy in the anaerobic digestion was investigated **Badr et al., (2017)** in their study, a simulation model of the mesophilic digester (35 ± 2^oC) having a volume of 70 liters coupled with a new design of the solar water thermal system has been developed using TRNSYS. Under Kenitra Morocco's climatic condition, the thermal performance and dynamic behavior of the systems are investigated. It found that the solar system covers 90% of the energy consumed by anaerobic digestion during the year. In addition, the result showed that the integration of solar thermal energy to the anaerobic digester has a feasible benefit. When it integrates with an anaerobic digester a daily temperature fluctuation, becomes 0.8^oC in summer and 2.3^oC in the winter season.

M. Sain & Anita A, (2014) thermal simulation for MIT biogas plant has been developed using MATLAB in order to determine the heat transfer from the slurry and gasholder to the surrounding earth and air respectively. The computation has been performed when the slurry is maintained at 20℃and 30℃, the optimum temperature of anaerobic fermentation. If the slurry is considered to be at 35℃, the optimum temperature of anaerobic fermentation, the total heat loss from the plant is higher than the heat loss when the slurry is maintained at 20℃. The heat calculations provide an appraisal for the heat, which has to be supplied by external means to compensate for the net heat losses, which occur if the slurry is to be maintained at 35℃.A solar system with an auxiliary electric heater is designed for maintaining the slurry at 35℃.In conclusion; the results of the thermal analysis are used to define a strategy for operating a biogas plant at optimum temperatures.

Gutiérrez-Castro et al., (2014) deal with an analytical study on a fixed collector or tracking collectors for maintenance the temperature anaerobic digester at 55°C and have a better atmosphere into the digester to the microorganism generate the biogas in a minor time. The analytic method evaluates the used to flat plate solar collector, one case is fixed and another one having a solar tracking system. The goal of analytic analysis to achieve greater energy saves to the methane generation was achieved. If the tracking system is installed to MGTS, the built costs savings to be about 20 to 25% more than the fixed system. In other words, the tracking solar system was evaluated to can see if there is more saving in building costs and propose it in the future biogas plants in Mexico City using the organic fraction of the municipal solid waste.

Alkhamis et al., (2000) developed a heat transfer model to investigate the design parameters for heating digester using solar collectors coupled with a heat exchanger. The model accounts for the useful energy gained from solar collectors and the heat losses through the side, bottom, and top of the solar collectors. The experiment was performed using solar collectors in the laboratory made of less expensive materials. It was found that the digester temperature increases to 40℃ after 1 hour of operating the solar collector. Comparing the efficiency of the solar collector shows good agreement with the experimental values (61 % compared to 62 %).

They investigate the potential of integrated solar heating techniques to raise the slurry temperature within a low-cost tubular digester and its impact on biogas yield. Two similar digesters were used, the first one (D1) was heated by thesolar greenhouse integrated with a solar water heating system and a capillary heat exchanger, while the second (D2) was heated by the only solar greenhouse, and both digesters were above ground and were fed with cattle manure. The results showed an average slurry temperature of 9.5 and 4.9 °C above the mean ambient temperature for D1 and D2, respectively. Furthermore, the mean specific biogas production of D1 and D2 were 247 and 181 L/kg VS, respectively, with no significant variations in the methane content (62.7%). The study indicated that using integrated solar energy is efficient to achieve the optimum temperature for the process of biogas production roughly most of the year **(Gaballah, Eid, et al, 2020).**

Further, the use of phase change heat storage material has been reported, **Lu et al. (2015)** to determine the heat demand of the digester system located in the Anhui Province mathematical model is developed, in Central China. The model considers the heat loss from the digester, and the loss through the pipe connecting the digester and the heat storage tank. The size of the solar collector panel surface area and the storage tank volume are estimated. The required insulation material and thickness are determined. In addition, it was found that when the solar fraction is 0.8, the 20-m^2 solar collector area and 3m^3-heat storage volume could achieve the mesophilic slurry temperature in the winter. The determination of the suitable insulation material and thickness suggests that the use of 200 mm polyurethane is ideal for the digester system. However, some drawback of the study includes the assumption of a 5^{o}C ambient temperature during winter.

Similarly, **Lu & Lu ,(2016)** demonstrated that the impact of insulation of the heat storage tank with a phase change is an additional benefit. A thermal model was developed in fluent (v3.3.26) to simulate the impact of a solar collector and heat storage on the digester temperature. It was validated with a laboratory study, which uses an electric heater to supply hot water to a storage tank with paraffin wax placed between an internal and external polyurethane insulated material. The results obtained from both experimental studies agree with the simulated result as it shows that at air temperatures between 0 and 10℃, the storage tank maintained the hot water temperature above 50℃, thus providing a mesophilic temperature in the biodigester. However, it was found that the simulation result over predicted the water and paraffin temperature.

Lu, Wang, (2016) & Lu, Tian, (2015) illustrated the impact of the phase change material in upgrading the digester temperature when integrated with the solar collector and heat storage tank. The difference is that the paraffin wax was the exchange liquid within the case of **Lu, Tian, (2015),** and whereas within the consider of **Lu et al., (2016)** paraffin wax is utilized as the insulation material.

The simulation study was compared the heat balances of system A and a system that had no heating resource. Both systems were assumed found in Xianyang, Shaanxi province, northwest China. The simulation and modeling were undertaken to utilize EPBSS, OpenStudio, and Sketch Up. The simulation had the following results appeared that within system A, the monthly normal temperature of the process during the winter was kept up (>9.8^{o}C) and in opposite to system which had a temperature of <8^{o}C. The result showed that system A seems only to be practical in regions where the average temperature during the winter is over -5^{o}C. The validation study was conducted on an actual digester with the model and location as system A and the results were within the range of result from simulation results (<0.34) ^{o}C difference found. Economic investigation of System A appeared that installation of the two greenhouses could increment income from biogas by

US$1,290 per year, which could cover the costs of the greenhouse within 14 months of operation (**Hassanein et al., 2015).**

A novel over-ground household solar heating thermostatic biogas system was developed in this study to improve the biogas generation rates in winter in cold districts of China. Tests were conducted on seven batches process for more than a year and a semi-continuous process experiment for about four months during winter in cold districts of China, alongside the amount of day-by-day heat consumed by the digester within the semi-continuous process digestion. The economic feasibility of the system was moreover assessed. The result appeared average biogas generation rates of 0.63, 0.68, 0.44, 0.64, 0.93, 1.09 and 1.08 m^3/ (m^3 slurry) at T80 were decided in seven batches. Within the semi-continuous, prepare try, four daily biogas generation peaks. The biogas generation rate increased rapidly when the amount of time consumed during slurry temperature after reloading was little. The heat consumed by the digester was 15 MJ/d–30 MJ/d during the worst time of the year **(Feng et al., 2016).**

Youzhou, J., et al., (2016) developed a solar collector heating pipe system to assess its impact on the anaerobic digestion of cow manure in winter. The developed thermal model incorporates the heat gain from the solar collecting pipe, the losses from the wall, and the cover of the fermentation tank, and the heat exchanger the model was validated with an experiment using the model conditions. The measurement of the methane yield, methane and carbon dioxide content, digester temperature, the hot water temperature was recorded. The study found that the system was able to maintenance mesophilic temperature while achieving stable methane production. The slurry temperature increases by 5°C during the sunny day and decreases to 0.6°C at night. Also. It was reported that during the day, there are no heat losses from the digester since it is surrounded by the heat collection system, while at night the digester losses heat.

This paper presented the transient analytical study of a fixed dome type biogas plant, which incorporates a water heater concept in the design for higher biogas production, particularly in the winter season. Further improvement in the performance of the system has been investigated by using insulation on the walls and the base of the digester. An explicit expression for the slurry temperature, as a function of time (depending upon various parameters), has been developed**(Gupta et al., 1988).**

The results showed the feasibility of implementing this type of anaerobic digestion system assisted by solar energy at different scales for use of debit form, parks, gardens, and businesses and reducing the volume of contamination by organic waste and reducing costs generated disposal. At the same time, biogas is obtained as a product of anaerobic digestion resulting in the generation of a product with high benefit from the use of a residue considered polluting and thus contributing to the reduction of emissions of greenhouse gases. Increased biogas production estimated temperature increase of 10.14°C using solar energy is approximately 16.6 %. This result suggests the possibility of scaling the system**(Quinto et al., 2016)**.

In order to maintain a certain degree of temperature for rural household biogas digester in winter especially in north China, a solar-assisted heating system was designed. In the system, the biogas digester was heated by hot water from the solar collector through a spiral heat exchanger. A mathematical model was established and the operation of the system was simulated to evaluate the effect of the system. The results showed that the solar-assisted heating system can effectively increase the temperature of the household biogas digester**(Chen et al., 2011).**

This paper investigated the concept of a Hybrid Biomass System (HBS) consisting of solar thermal flat plate collectors (FPC) providing heat energy to the (55°C) anaerobic digestion process and the potential energy yield of the hotel OFMSW in Kolkata. The methodology comprises the development and assessment of a theoretical model representing the anaerobic digestion process for optimum biogas yield and TRNSYS simulation of a $5m^2$ and $10m^2$ FPC. This concluded that FPCs could support thermophilic digester heating requirements with heat store or direct integration**(Pollard & Blanchard, 2014).**

This work deals with design and fabrication biogas digester with simple solar heater (built-in solar reverse absorber heater) are presented where the reverse absorber heater is installed under the methane tank. The result showed that maximum temperature of 50^0C inside of the methane tank, using energy balance equation for the case of a static mass of fluid being heated the thickness of thermos insulating material was determined. The temperature of the slurry-solar irradiance and ambient temperature relationships were investigated experimentally. The biogas up-gradation scheme for the removal of carbon dioxide, hydrogen sulfide, and water vapor from biogas and conversion of biogas energy conversion into electric power are discussed**(Karimov & Abid, 2012).**

El-Mashad et al., (2004) examined the effects of preheating, insulation material, and solar energy on the performance of a continuously stirred tank reactor in Egypt. In the experiment, two stirred tank reactors are operated at 55^{o}C and 60^{o}C, to attain a steady-state in the digester. The digesters were later subjected to daily temperature fluctuation, which causes a reduction in the methane production rate by 12 % (50ºC) and 20 % (60ºC). Fitting the experimental results into the model developed revealed solar and insulation is effective for a small digester, and less effective for larger digesters.

Yiannopoulos et al., (2008b) proposed a system consisting of a solar collector, digester, and a heat storage tank. The model was developed to estimate the heat demand of the digester, consisting of the useful heat gained from the heat storage tank, heat loss to the surface of the insulator, heat loss to the surroundings, and the losses from the pipe linking the digester and the storage tank. It was found that the solar collector was able to meet the heat demand of the digester for the different locations considered.

Simple heating of the digester with either solar energy or biogas has been reported to be unsustainable, especially during the cold season. Hence, a sustainable way involves the combination of both heating sources. **Rennuit & Sommer, (2013)** developed a decision support model to evaluate the heat demand of household biogas in Vietnam, considering the size of the digester plant, the number of pigs, and the hydraulic retention time. The model includes the heat gained by the digester using solar and biogas. The results of the simulation show that a combination of solar and 10 % biogas will meet the heating demand of the digester while providing surplus biogas. Further, to meet the heat demand, the digester must be operated a hydraulic retention time of fewer than 40 days with a dilution rate of 1:3.

Presented designs solar heating biogas fermentation system of $6m^3$ volume and calculates digester's heat load based on Hohhot's weather data. Using U-tube solar collector tests results were collected for 5 months. The relationship between solar collector system and biogas fermentation system heat load s matched. The result appeared that at Hohhot, in October, the heat was absorbed by $2m^2$ solar collectors that were run 8 hours can meet the fermentation heat demands of $6m^3$ digester **(Yuan et al., 2011b)**

(Lu et al., 2015) developed a mathematical model to determine the heat demand of the digester system located in Anhui Province, in Central China. The model considers the heat loss from the digester, and the loss through the pipe connecting the digester and the heat storage tank. The size of the solar collector panel surface area and the storage tank volume are estimated. The required insulation material and thickness are determined. In addition, it was found that when the solar fraction is 0.8, the 20-m^2 solar collector area and $3m^3$-heat storage volume could achieve the mesophilic slurry temperature in the winter. The determination of the suitable insulation material and thickness suggests that the use of 200 mm polyurethane is ideal for the digester system. However, some drawback of the study includes the assumption of a 5°C ambient temperature during winter

2.4. Solar collector

The major component of any solar system is the solar collector. A solar collector is a device designed to absorb incident solar radiation and to transfer the energy to a fluid (usually air, water, or oil) passing in contact with it **(Tian&Zhao., 2013).** The major components of any solar collector include the reflector, absorber, and heat transportation medium. Solar collectors are usually classified into two categories according to concentration ratios: non-concentrating collectors and concentrating collectors **(Mohammed, 2012).** A non-concentrating collector has the same intercepting area as its absorbing area, whilst a sun-tracking concentrating solar collector usually has concave reflecting surfaces to intercept and focus the solar irradiation to a much smaller receiving area.

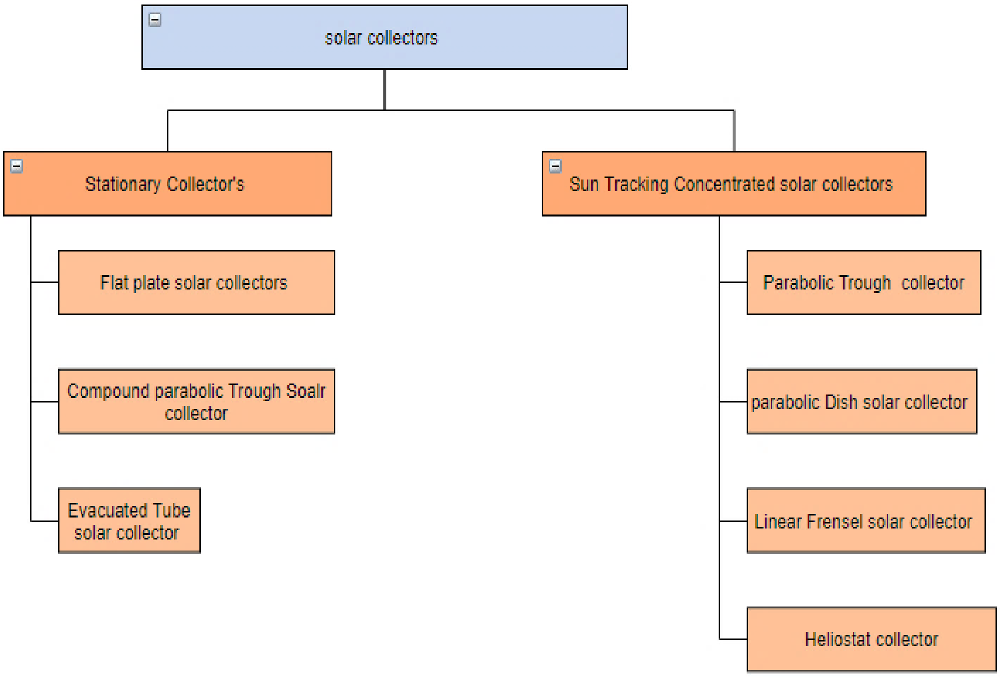

Figure 2. 1: Classification of solar collectors

2.4.1. Parabolic trough collector

Parabolic troughs are devices that are formed like the letter “u”. The troughs concentrate sunlight onto a receiver tube that is positioned along the central line of the trough. Parabolic trough collectors are made by bending a sheet of reflective material into a parabolic shape. A black metal tube, covered with a glass tube to diminish heat losses, is placed along the central line of the receiver (figure 2.2). When the parabola is pointed toward the sun, I reflected parallel beam occurrence on the reflector onto the receiver tube. The concentrated radiation coming to the receiver tube heats the liquid that circulates through it, in this way changing the solar radiation into valuable heat.

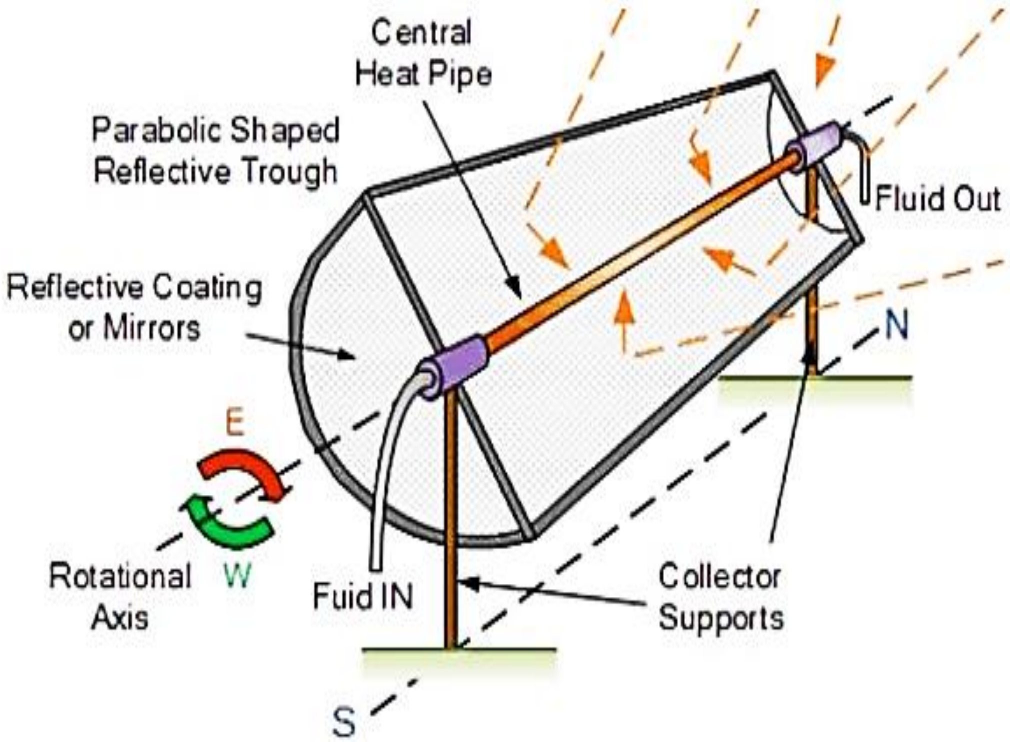

Figure 2. 2: Principle of parabolic Trough Collectors

2.5. Thermal energy storage system for water heating

Solar energy is a form of renewable energy that is found clean, abundant, and easily accessible. However, its intermittent and dynamic nature makes it difficult to utilize the energy effectively. TES system becomes a solution to those natures and the time-mismatch between energy demand at night and the external solar energy available during the day **(KOUSKSOU et al., 2007).**TES stores energy by heating, melting or vaporizing a storage medium and the stored energy is utilized during the night for various applications by or solidifying the storage medium. Due to the fluctuating nature of solar radiation throughout the day, a TES is required to be designed properly to achieve a continuous supply of heat**.** Thus, TES systems are used to fully utilize solar energy and cover off-peak periods.

From all the TES's, sensible heat storage (SHS) and latent heat storage (LHS) systems are the most common in storing solar energy for solar applications. As appeared within the figure, **(Ashish, 2019)** classified warm vitality capacity framework as latent and sensible heat. As shown in figure 2.3, (**Ashish, 2019)** classified thermal energy storage systems as latent and sensible heat.

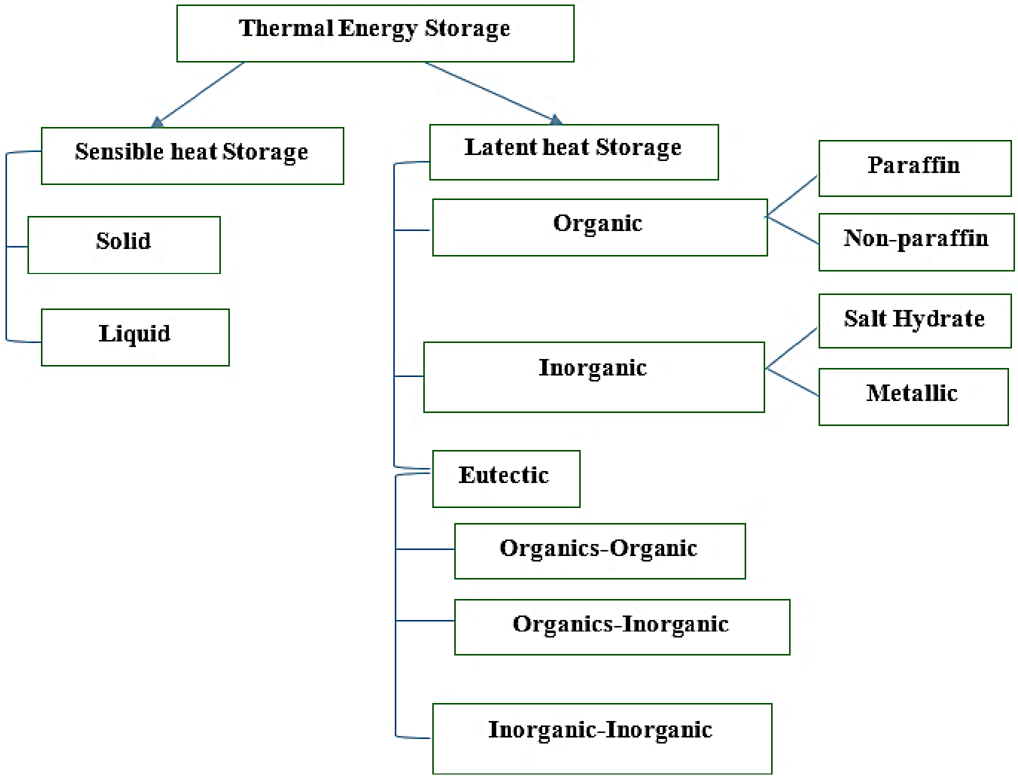

Figure 2. 3: General classifications of thermal energy storage materials.

1. Sensible heat storage

In sensible heat storage (SHS), thermal energy is stored by raising the temperature of a solid or liquid. SHS system utilizes the heat capacity and the change in temperature of the material

during the process of charging and discharging. The amount of heat stored depends on the specific heat of the medium, the temperature change, and the amount of storage material.

$$Q = \int_{T_i}^{T_f} mC_p dT = mC_{pa}(T_f - T_i) \text{ ....(2.1)}$$

Where:

- m is the mass of storage material (kg)
- C_{pa} is the average specific heat between Ti and T_f (J/kg K)
- T_i and T_f are the initial and final temperature of material respectively (°C)

Water appears to be the best SHS liquid available because it is inexpensive and has a high specific heat capacity. However, above 100°C, oils, molten salts, and liquid metals, etc. are used. For air, heating applications rock bed type storage materials are used **(Sharma et al., 2009).**

2. Latent heat storage

Latent heat storage (LHS), is based on the heat absorption or release when a storage material

undergoes a phase change from solid to liquid or liquid to gas or vice versa. The storage capacity of the LHS system with a PCM medium is given by:

$$Q = \int_{T_i}^{T_m} mC_{ps}dT + ma_m L_{fuss} + \int_{T_m}^{T_f} mC_{pl}dT \quad \text{………………..(2.2)}$$

$$Q = m\left[C_{ps}(T_m - T_i) + a_m L_{fuss} + Cp_l(T_f - T_m)\right] \quad \text{………………..(2.3)}$$

The ideal PCM to be used for a latent heat storage system must meet the following prerequisites: tall, sensitive heat capacity and warm of combination, steady composite on, high density and heat conductivity, chemical inactive, non-toxic and non-inflammable, sensible, and cheap **(Arabacigil et al. 2015)**.

2.5.1. Thermal energy storage using paraffin-based PCMs

Paraffin-based PCMs can be integrated with solar thermal collectors to improve the system thermal efficiency, meanwhile serving as on-site TES. Alternatively, they can be used as independent TES units coupling with solar thermal collectors to provide continuous heat supply for the demand side. In both approaches, the charging of paraffin with the heat generated needs to be fulfilled first, followed by the retrieval of the heat using heat transfer fluids (HTFs) for specific applications e.g. space heating or cooling **(Lin et al., 2019).**

2.5.2. Storage system configurations

Progress in LHS systems mainly depends on heat storage material investigations and on the development of heat exchangers that assure a highly effective heat transfer rate to allow rapid charging and discharging. Latent heat TES systems are broadly classified into the capsule-type and the shell-and-tube type, according to the method of containing the thermal energy storage material and to the mode of exchanging heat energy within the container **(Dinker et al., 2017).** The various studies carried out by the researchers on different configurations are classified under i) Tubular exchanger ii) packed bed unit iii) system with different heat transfer enhancement techniques.

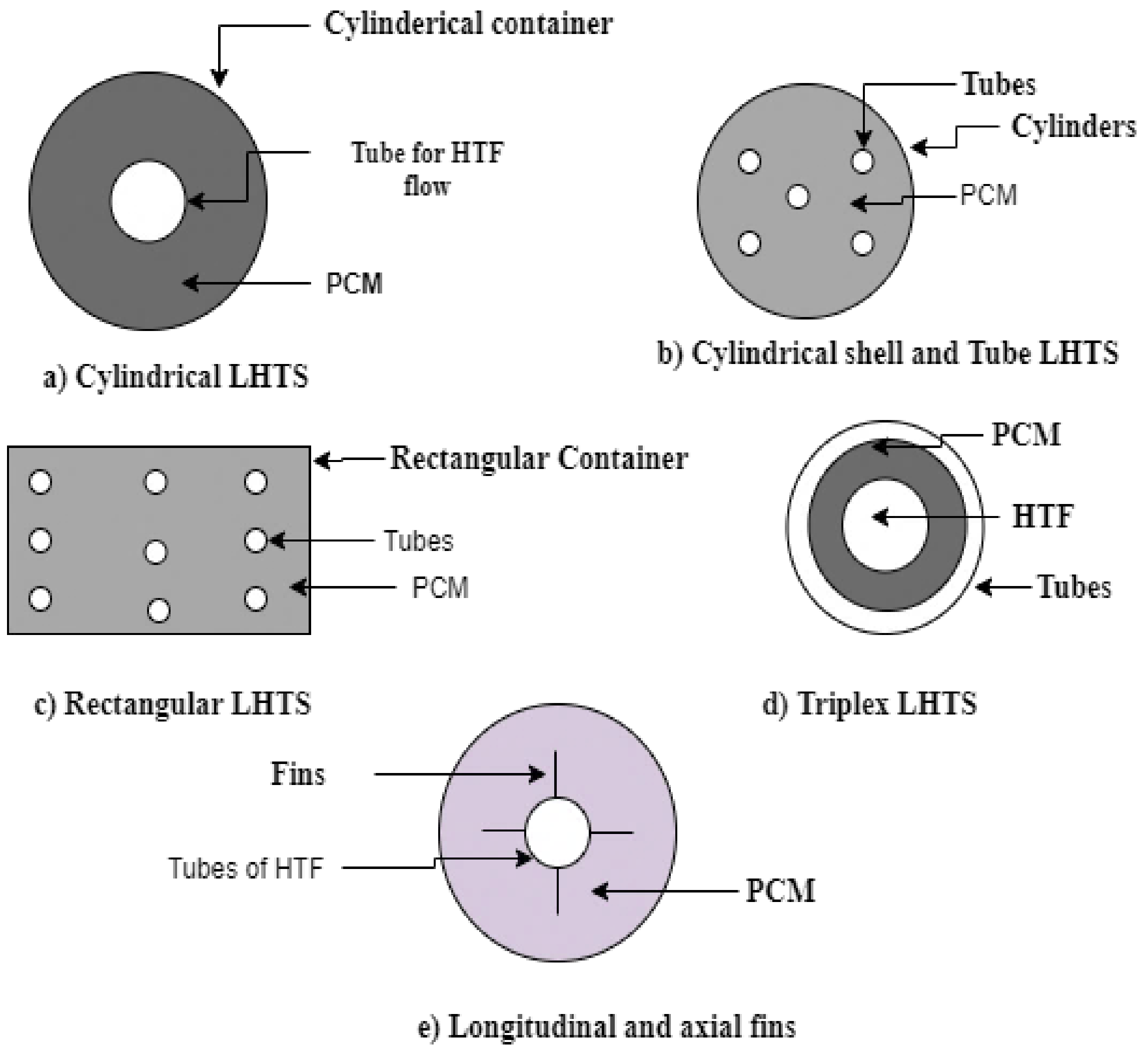

Figure 2. 4: The geometrical design of various thermal storage Units **(Dinker et al., 2017)**

2.6. Summary of Literature

As literature reviewed earlier, anaerobic digestion is a popular technology to produce biogas. Maintaining temperature is very important for an efficient anaerobic digestion process. A well-built heating source can improve the activity of the bacteria. A huge number of research studies have been conducted on the utilization of the solar system to heat the slurry in digesters. It seems like a natural solution for solar radiation to facilitate the generation of a high-grade form of energy (biogas). Therefore, the utilization of a solar component to maintaining the temperature can significantly enhance biogas production. Most reviewed papers are experimental and numerical studies on utilizing solar thermal energy for anaerobic digestion. In addition to solar energy integration, thermal storage to this is few in the report. Solar radiation supplies heat to maintain the reactor at the desired temperature.

CHAPTER 3: METHODOLOGY

3.1. Research method

In order to model and simulation the thermophilic anaerobic digestion enhancement Using Parabolic solar collector integrated with paraffin wax-based thermal energy Storage, some input data will be provided atmospherics temperature, wind speeds, and monthly solar radiations data, articles, transactions, journals, and books related to the title "Numerical Study of Thermophilic Anaerobic Digestion Enhancement Using Parabolic Solar Collector Integrated With Paraffin Wax Based Thermal Energy Storage" has been reviewed.

Data Collection: In order to model and simulate the system:-

- Daily atmospheric temperature, wind speed, and monthly solar radiation is collected from the Meteorology agency.
- To the specific number of householders and sizing digester related articles are used.

Model and simulation: Based on the collected data and applying empirical formulas system is simulating using PYTHON code script and MATLAB Script.

System Analysis and Interpreting the result: The aforementioned collected data have been organized to model and simulations the system.

The following important point is discussed in detail:

- Specific the anaerobic digester size according to energy demanded by the householder.
- PYTHON code Script is written to estimate the energy demand by biodigester to maintain the thermophilic range of fermentation.
- Estimation of solar irradiance of selected location (Bale Robe) using excel and PYTHON code script.
- Parabolic trough solar collector standard specification and transient model of heat transfer analysis also evaluated using PYTHON code script.
- Geometrical configuration PCM and Mathematical model are simulated by MATLAB script.

INPUTS

- Atmospheric Temperature
- The total mass of digestate
- Thermophysical properties of digester and digestate
- Wind speed
- irradiance
- latitude and altitude of Bale Robe
- Thermophysical properties of working fluid
- Engineering and optical specification of PTC
- Thermophysical properties of Phase change

MODELING AND ANALYSIS

- Sizing digester size and determine energy demanded by the house holder
- Heat transfer modeling of the thermophilic digester and thermal analysis
- Solar energy required estimation
- Parabolic trough size required and thermal analysis
- PCM thermal modeling

OUTPUTS

- Temperature drop in the digester
- Amount of heat lost out from digester and determine amount heat energy demanded by the digester.
- solar radiation collected and useful heat gained by PTC
- Temperature variation of PTC
- Sizing of PTC, Optical and thermal efficiency of PTC
- Total Charging and discharging time of thermal energy storage
- The result, discussion, and Validations
- Conclusion ,Recommendation and Future Work

Figure 3. 1: Methodology flow chart

CHAPTER 4: THERMAL MODELING OF THERMOPHILIC ANAEROBIC DIGESTER

4.1. Thermophilic Anaerobic Digester

A thermophilic digester or thermophilic biodigester is a kind of biodigester that operates in the temperature above 50^0 C that producing biogas. **Hreiz et al., (2017),** the anaerobic digester is semi-buried (only covered part of the digester is exposed to the environment) to digest cow dung at Bale Robe weather conditions. Its walls are made of reinforced concrete and having 20 cm thickness. The reactor's cover is a deformable black EPDM (Ethylene Propylene Diene Terpolymer) membrane whose thickness is 3-mm. The operating pressure is maintained approximately equal to atmospheric pressure. The digester is equipped with a mechanical mixing system, powered by an electrical motor. Indeed, an efficient stirring of the digestate is required for homogenization (i.e. temperature, species, and biomass concentrations, etc.), minimizing heavy solids sedimentation, and reducing the formation of floating scum or straw blankets.

According to **Madamarwar et al, (1990)** the optimum temperature for thermophilic anaerobic digestion of cattle dung is 60^oC. Hot water coming from the parabolic trough solar collector is used to heat the digestate through an immersed helical-coil heat exchanger. The digestate temperature is designed to maintain at 60^oC.

This thermophilic anaerobic biogas digesters reactor is a community type to digestate cow dung per day to produce biogas and the reactor is designed to produce biogas that can fulfill the energy demand of family plus householder (50) for their cooking and lighting application. To perform a heat requirement analysis, the biogas production rates have to be determined. According to (**Wassie & Adaramola, 2020**) analyzing household biogas utilization and impact in rural Ethiopia biogas for cooking and lighting purpose per household average is estimated as 0.5 m^3 per day and 0.11 m^3per day respectively. The total energy demand to fulfill both cooking and lighting per household is 0.61 m^3 per day. The designed thermophilic biogas reactor is responsible to produce 30.5m^3 of biogas per day for my family plus householders (50).

Varel et al., (1980) report that utilizes cattle waste with 8% of volatile solid content, in this study the concentration of volatile solid within cow dung that is added to the reactor is the same as utilized by (Varel et al., 1980).

The amount of biogas production per kg of cow dung was measured at 0.023-0.04 m^3 or average 0.031 m^3 **(Gunter U, 2011).**To produce 30.5 m^3 of biogas per day for 50-

householder 983.9 kg cow dung have to feed into reactor per day. There is 983.87 kg weight of moist biomass and total solid content is 0.2 with dry matter (D_m) of fresh discharge is 196.77 kg. To make favorable condition for fermentation the concentration of organic dry matter should be 8% i.e. 8kg Organic dry matter should be available in 100kg influent.

$$x = \frac{196.77 * 100}{8} = 2459.677 \frac{kg}{day}$$

Water should be added to make the discharge 8% concentration of organic dry matter is:

M_{water}=2459.677-983.87=**1475.8 kg/day**

The total daily substrate feed into the reactor is 2459.677 kg/day. In this analysis, the density of water and cow dung mixture has been calculated as the weighted average of water and cow dung densities and has been evaluated to be 952.5 kg/m^3.

Digester volume is determined based on the chosen retention time and daily substrate input quantity. The retention time, in turn, is determined by the digesting temperature. Practical experience shows that retention times is 20 days.

The digester volume can be calculated using the following formula:

$$V_{digester} = SRxHRT \quad \text{………….……………….……………} (4.1)$$

Where:

- V_{digester} is digester volume,
- SR is the substrate-feeding rate
- HRT is the hydraulic retention time of substrate within a digester.

Therefore $V_{\text{disgester}=}$20*2.5822=51 m^3.

Ibn et al.,(2012), investigation of thermophilic anaerobic digestion of cow dung the Digester volume can only cover 70% of the total volume of anaerobic digester. The total volume of digester can be calculated as:

$$V_T = \frac{V_{\text{digester}}}{0.7} = \frac{51}{0.7} = 74\text{m}^3 \quad \text{………………………….……………} (4.2)$$

From total volume of digester 30%, left for holding produced biogas, and it covers 23m^3. The gasholder has a hemispherical shape and its diameter is calculated from the volume of the biogas holder:

$$\text{volume of gas holder } V_h = \frac{1}{12}\pi d^3 = 23\text{m}^3 \quad \text{……………………………………….} (4.3)$$

Where d is the diameter of a gasholder, solving equation (4.3) to get the diameter of gasholder, gives to be d= **4.43 m**

Similarly, the height h of the digester is calculated from the volume of the digester:

$$\text{Volume of digester } V_{digester} = \frac{1}{4}\pi d^2 h = 51 m^3 \quad \text{………………………………..(4.4)}$$

The height (h) of the digester from equation (4.4) is **3.31 m**

4.2. Climatic Condition

Bale Robe region is characterized by a climate condition of tropical and it has a medium intensity of solar radiation. The monthly average temperature of Robe ranges between 16.4℃ February and 18.6 ℃ October. Ten-year average monthly average temperatures in Robe are presented in the chart. Meteorological data are required for evaluating heat transfer between the digester and its surroundings. In this present study, Ten-year average climatic conditions of Robe town are used to analyze different parameters.

Table 4. 1: Monthly average annual climatic condition of Robe (Ethiopia national meteorology)

Month												
Temp(℃)	Jan	Feb	Mar	Apr	May	Jun	July	Au	Sep	Oct	Nov	Dec
Ave(ºC)	17.6	16.4	16.7	17.8	16.9	18.7	17.4	18.3	17.5	18.6	17.4	17.2
Min(ºC)	12.4	11.6	12.8	11.8	11.5	13.8	11.4	15.1	10.7	12.3	10.7	10.7
Max(ºC)	22.8	21.1	20.5	23.9	22.4	23.5	23.4	21.5	24.4	24.9	21.6	23.7
speed	3.5	2.7	3.5	3.5	3.5	2.8	2.8	2.7	2.8	3.4	4.3	3.4

4.3. Heat Balance Equations for the Digester

Zupančič and Roš, (2003) reported that the heat and energy requirement for anaerobic thermophilic digestion of cow dung is consist of three parts: first part heat required for raising the temperature of incoming substrate for digestion, second, for compensating heat loss through the boundaries digester and, third, for compensating losses that might occur in the piping between the heat source and the digester. By appropriate construction, the heat losses in the piping (the third part) can be minimized to the point where such losses can be neglected. Solar water heating is only responsible for heating the anaerobic digestion of cow dung. The energy for mixing and pumping electrical energy is supplied. The heat energy requirements considered were the heat losses of the digester and the heat necessary for raising the incoming sludge temperature.

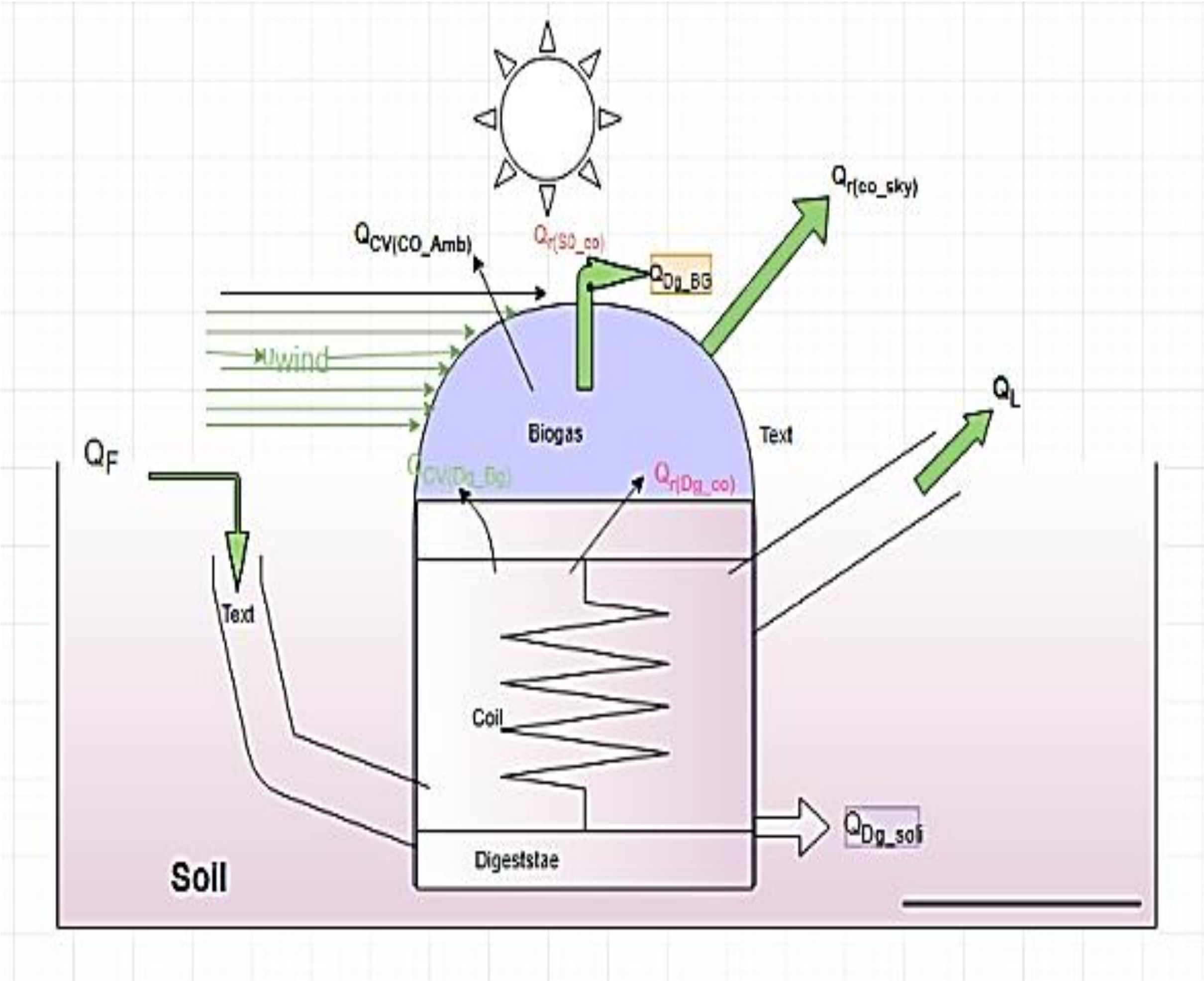

Figure 4. 1: Schematic Diagram of a physical model of biogas digester and Heat Transfer

$$Q = Q_m + Q_s \quad \ldots\ldots\ldots\ldots\ldots\ldots\ldots\ldots\ldots\ldots\ldots\ldots(4.5)$$

Where: Q: rate of heat to maintain digester temperature

Q_m: rate of heat transfer to manure the heat needed to raise influent temperature to the temperature (in this study it is 60^{o}C)

Q_s: rate of heat loss through digester walls, floor, and top to the surrounding environment

To study the heat transfer phenomena of digester and heat required for the slurry model is based on an energy balance, which is one-dimensional. The assumptions considered for the modeling of the heat transfer in the digester are as follows **(K. G. Gebremedhin et al., 2005).**

1. The digester is completely buried except for the top surface or cover

2. Microbial heat generation is considered negligible.
3. The temperature of the manure inside the digester is maintained constant (There is no gradient in slurry temperature inside the digester).
4. Physical properties of the soil, digester material, the insulation material is uniform.
5. Heat outgoing by biogas is neglected
6. Negligible atmospheric long-wave radiation.
7. Evaporative and convective losses from the surface of the slurry inside the digester is negligible because they have an insignificant influence on digestate temperature compared with heat transfer from soil and air and heat loss to rainwater dripping on the cover and the heat lost by the cover due to rainwater evaporation **(Terradas-Ill et al., 2014).**

Depend on the schematic diagram and assumption the transient energy balance of slurry or digestate, biogas, and biogas cover is present below section.

A. Digestate Phase

To investigate the heat transfer between slurry and it is surrounding applying the energy conservation principle to the slurry contained in the digester gives **(Hreiz et al., 2017).**

$$\rho_{Dg} V_{Dg} C_{Dg} \frac{dT_{Dg}}{dt} = Q_F - Q_L - Q_{cnv(Dg\text{-}Bg)} - Q_{r(Dg\text{-}co)} - Q_{(Dg\text{-}soil)} + Q_{Dg-HE} \quad \ldots(4.6)$$

Where:

- ρ represents density,
- V the volume, C
- the constant pressure heat capacity,
- T the temperature and t the time
- Subscript Dg refers to the digestate, F to the feed, Bg to the biogas, Co to the cover,
- HE to the heat exchanger,

The left side term of equation (4.6) represents energy stored in digestate or slurry and the right side term represents heat in to and out of digestate.

- Q_F represents the heat carried by the feed (slurry and solid manure).
- Q_L denotes the heat lost due to the digestate leaving the reactor by overflow
- Therefore, the term (Q_F-Q_L) corresponds to the heat required to warm the inputs up to the digestate temperature.

- $Q_{Dg\text{-}Bg}$ - represents heat loss by mass transfer from the digestate to biogas.
- $Q_{cnv\ (Dg\_Bg)}$ - is the convective heat transfer from the digestate to the biogas.
- $Q_{Dg\text{-}soil}$- represents heat transfer from the digestate to the soil across the walls.
- $Q_{r\ (Dg\_co)}$ - represents the net radiative heat transfer from the digestate to the cover.

All radiative heat transfer phenomena from/with the biogas are neglected. Indeed, gases have very low thermal emissivities and are almost transparent to infrared rays.

B. **The Biogas Phase**

Similarly, the dynamic heat balance around the biogas phase gives **(Hreiz et al., 2017).**

$$\rho_{Bg}V_{Bg}C_{Bg}\frac{dT_{Bg}}{dt}=Q_{Dg\_Bg}-Q_{Bg}+Q_{cnv(Dg\_Bg)}-Q_{cnv(Bg\_co)} \quad \ldots\ldots\ldots\ldots..\ldots(4.7)$$

Where:

- Q_{Bg} denotes the heat carried by the outgoing biogas
- $Q_{Bg\text{-}Co}$ is the convective heat transfer from the biogas to the cover

The heat carried by the outgoing biogas is small compared to the other heat transfer terms, because the mass flow rate of the outgoing biogas is small.

C. **The cover**

The heat balance over the cover gives **(Hreiz et al., 2017**):

$$\rho_{co}V_{co}C_{co}\frac{dT_{co}}{dt}=\begin{bmatrix} Q_{cnv\,(Bg\_co)}-Q_{cnv\,(co\_At)}-Q_{r\,(Dg\_co)}- \\ Q_{r\,(co\_At)}+Q_{r\,(so\_co)} \end{bmatrix} \quad ..\ldots(4.8)$$

Where the subscript At refers to the atmosphere (and the ambient air), So to solar irradiation's represents density, V the volume, C constant heat capacity T the temperature, and t the time

- $Q_{cnv(co\text{-}At)}$ represents convective heat transfer from the cover to the ambient air
- $Q_{cnv(Bg\_co)\text{-}}$ represents convective heat transfer from the biogas to the cover
- $Q_{r(Dg\_co)\text{-}}$ represents convective heat transfer lost from the to the cover to digester
- $Q_{r\ (Co\text{-}At)}$ corresponds to long-wave radiations emitted by the cover to the ambient
- $Q_{r(Co\text{-}So)}$ denotes the cover heat gain from solar irradiation

4.4. Modeling of the heat transfer terms

4.4.1. Modeling of the heat carried by the feed, Q_F, and the heat lost due to the digestate leaving the, Q_L

The digester was fed with a daily average of 2459.677 kg of feed (manure) and water mixture. As the mass flow rates of the generated biogas are small compared thereto of the feed, the mass flow rate of the feed and the outgoing digestate could be thought of equal **(Hreiz et al., 2017):**

$$Q_F = \dot{m}_F C_w T_{At} \qquad (4.9)$$

$$Q_L = \dot{m}_L C_w T_{dg} \qquad (4.10)$$

Where:

- $\dot{m}_F$ the feed mass flow rate equal to mass flow out of the digester $\dot{m}_L$
- C_w the water heat capacity at constant pressure and temperature and
- T_{At} is the ambient air temperature.

4.4.2. Modeling of the heat loss by mass transfer from the digestate to the biogas, $Q_{(Dg-Bg)}$, the heat carried by the outgoing biogas, Q_{Bg}

$$Q_{(Dg\_Bg)} = \dot{m}_L C_{Bg} T_{Dg} \qquad (4.11)$$

$$Q_{Bg} = \dot{m}_{Bg} C_{Bg} T_{Bg} \qquad (4.12)$$

Where: **(Hreiz et al., 2017):**

- $\dot{m}_{Bg}$ represents the mass flow rate of biogas
- C_{Bg} the specific heat capacity of biogas and
- T_{Dg} the temperature of digestate and TBg the temperature of biogas

Thermo-physical properties of Biogas determine by the composition of (60% CH_4 by volume, 36% CO_2, and 4% water vapor). **(Axaopoulose et al., 2001),** experimentally found a medium size digester thermophilic digester (45m^3), under mild weather conditions, the temperature difference between the biogas and the digestate can exceed 10℃. The operating pressure being nearly atmospheric, the biogas density was estimated as 1.06 kg/m^3. Its heat capacity was taken as the mass-weighted average of the CO_2, CH_4 and water vapor heat capacities and hence, was estimated at 1376 J/kg, at the biogas temperature of 50^{o}C.

4.4.3. Modeling of the convective heat transfer from the digestate to the biogas, $Q_{cnv\,(Dg-Bg)}$

The convective heat flux from the digestate to the biogas is given by **(Hreiz et al., 2017):**

$$Q_{cnv\,(Dg\_Bg)} = h_{Dg\_Bg} S_{Dg\_Bg} (T_{Dg} - T_{Bg}) \quad \text{.........................(4.13)}$$

Where S_{Dg_Bg} is the digestate free surface (equals the digester's cross-section, 15.97 m^2) and h_{Dg-Bg} the convective heat transfer coefficient between the digestate surface and the biogas. Considering the biogas phase, given the low gas velocities, forced convection effects may be neglected. Thus, it is assumed that $h_{(Dg\_Bg)}$ is due to free convection in the biogas phase. Thermally driven natural convection flows occur if the thermal gradients lead to unstable density stratification and the Rayleigh number, Ra, exceeds a critical value. Ra is defined as follows:

$$Ra = \frac{g\,\beta'_{Bg}\,|\Delta T|\,L^3}{\nu_{Bg}^2}\,pr \quad \text{.......................................(4.14)}$$

Where:

- g is the constant of gravity
- $|\Delta T|$ the absolute value of a characteristic temperature difference
- β'_{Bg} the fluid coefficient of thermal expansion
- a characteristic length scale and is taken as $D_{Dg}/4$ (the ratio of the area over the perimeter of the digester cross surface
- ν the fluid kinematic viscosity and
- Pr the Prandtl number

In the current study, P_{rBg} has been taken as 0.75 which is a typical value for gases, and β_{Bg} as 1/TBg (ideal gas assumption given the moderate biogas pressure). Note that T_{Bg} should be expressed in K; ν_{Bg} was calculated as the volume-weighted average of the CH_4 and CO_2 kinematic viscosities, and thus, have been estimated to be 1.5×10^{-5} m^2 s^{-1} (evaluated at 45^{o}C). The convective heat transfer coefficient between the digestate surface and the biogas h_{Dg_Bg} is calculated using the correlations presented below **(Hreiz et al., 2017).**

$$Nu = \frac{h_{Dg\_Bg} L}{k_{Bg}} = 0.54 x Ra^{0.25} \text{ if } 2x10^4 \le Ra \le 8x10^6 \quad \text{...............(4.15)}$$

$$Nu = \frac{h_{Dg\_Bg} L}{k_{Bg}} = 0.15 x Ra^{0.33} \text{ if } 8x10^6 \le Ra \le 10^{11} \quad \text{...............(4.16)}$$

Where Nu is the Nusselt number and kBg is the biogas thermal conductivity

Free convection flow type is encountered in three situations:

- Heat transfer between the biogas and the digestate if T_{Dg} is higher than T_{Bg}.
- Heat transfer between the biogas and the cover if TBg is greater than T_{co}.
- Heat transfer between the ambient air and the cover if Tco is greater than T_{At}.
- k_{Bg} has been calculated as the volume-weighted average of the CH_4 and CO_2 thermal conductivities and has been estimated to be 27×10^{-3} W/mK (evaluated at 45 °C). k_{At} has been taken as 25×10^{-3} W/mK (evaluated at 20ºC).

4.4.4. Modeling of the convective heat transfer from the biogas to the cover, $Q_{cnv\ (Bg\_co)}$ (Hreiz et al., 2017)

Give the convective heat flux from the biogas to the cover:

$$Q_{cnv(Bg\_co)}=h_{Dg\_co}S_{co}(T_{Bg}-T_{Co}) \text{ ………………………...(4.17)}$$

Where – S_{co} is the cover single-sided surface and h_{Dg_co} the associated heat transfer coefficient. S_{co} equals 19 m^2 this value has been calculated by assuming that the cover has a spherical cap shape. If T_{Bg} is higher than T_{co} and the associated Ra greater than 2×10^4, free convection on the lower surface of a cold plate flow type occurs in the gas near the cover

4.4.5. Modeling of the net radiative heat transfer from the digestate to the cover, $Q_{r\ (Dg\text{-}Co)}$

The cover's internal surface and the digestate free surface delimit a closed domain. Considering that both surfaces behave as gray bodies, and since the digestate free surface is planar, $Q_{(Dg\text{-}Co)}$, the net radiative heat transfer between the digestate and the cover is given by **(Hreiz et al., 2017):**

$$Q_{r\,(Dg-co)} = \sigma \frac{T_{Dg}^4 - T_{Bg}^4}{\frac{1-\varepsilon_{Dg}}{\varepsilon_{Dg} S_{Dg-Bg}} + \frac{1}{S_{Dg-Bg}} + \frac{1-\varepsilon_{co}}{\varepsilon_{co} S_{co}}} \text{ …….……………(4.18)}$$

Where:

- σ is the Stefan–Boltzmann constant and
- ε designates thermal emissivity

The emissivities of both the EPDM cover and the digestate have been taken as 0.9. Note that

temperatures values should be expressed in K and not in .

4.4.6. Modeling of the long-wave radiations emitted by the cover to the atmosphere, $Q_{r\ (Co\text{-}At)}$

The cover loses heat to the atmosphere by long-wave radiation through its external surface. This heat loss, $Q_{(co\_At)}$, is calculated as follows **(Hreiz et al., 2017):**

$$Q_{r(co\_At)} = \varepsilon_{co} \sigma S_{co} (T_{co}^4 - T_{sky}^4) \quad \text{……..…….……………….(4.19)}$$

Where:

- $Tsky$ the equivalent sky temperature is evaluated according to Swinbank (1963)

  correlation (as reported by Hreiz et al., 2017):

$$T_{sky} = 0.0552\, T_{At}^{1.5} \quad \text{……………….………………….…….(4.20)}$$

Temperatures values should be expressed in K.

4.4.7. Modeling of the convective heat transfer from the cover to the ambient air, $Q_{cnv\ (Co\text{-}At)}$

The convective heat transfer from the cover to the ambient air is given by

$$Q_{cnv(co\_At)} = h_{co\_At} S_{co} (T_{co} - T_{At}) \quad \text{……………….….….(4.21)}$$

In the presence of wind, forced convection is assumed when u_{wind} greater than 0.5 m/s, correlations used to estimate h_{co_At} are given below: In the presence of wind, for wind speeds, $uwind$, lower than 0.5 m/s, mixed convection occurs an h_{co_At} is evaluated using the correlation proposed by Okada & Kusaka (2013) **(as reported by Hriez et al., 2017)**

$$h_{co\_At} = 0.0065 \rho_{At} C_{At} (T_{co} - T_{At}) u_{wind} \quad \text{…………………….(4.22)}$$

For greater wind speeds, forced convection is assumed. The heat transfer coefficient is calculated using the correlation of **Rao (2004) (as reported by Hriez et al., 2017)** for u_{wind} lower than 7 m/s, and using the correlation of McAdams (1954) (as reported by Hriez et al.,(2017) for larger wind speeds:

$$h_{co\_At} = 0.025 \rho_{At} C_{At} u_{wind}^{0.3}, if\ 0.5 \text{ m/s } \leq u_{wind} \leq 7 m/s \quad \text{…(4.23)}$$

$$h_{co\_At} = 7.2 u_{wind}^{0.78}, \text{if } u_{wind} \geq 7 m/s \quad \text{………………...…(4.24)}$$

Air properties are considered constant. ρ_{At} is taken as 1.1924 kg/m^3, and C_{At} as 1006 J/kgK (evaluated at 21℃, the average annual temperature in Bale Robe). In the absence of wind, if Ra is sufficiently important, free convection occurs whether T_{co} is greater or lower than T_{At}.

4.4.8. Modeling of the cover heat gain from solar irradiation

Solar radiation reaching the digester's cover consists of (1) Beam–or direct–radiation coming on a straight path from the sun, i.e. its trajectory does not deviate during its passage through the atmosphere. (2) Diffuse radiation, which is the fraction of solar radiation that reaches the earth after being scattered by the atmosphere (Rayleigh and aerosols scattering, reflections and scattering by the cloud cover, multiple reflections between the ground and the atmosphere, etc.).This radiation component has no preferential path, i.e. is isotropic. (3) Albedo radiation, which is the fraction of solar radiation reaching the cover after diffuse reflection on the ground (thus, it can be considered isotropic) the thermal model for calculating the cover's heat gain from solar radiation performance. Several steps:

1. **Determine global daily solar irradiation (J/m^2/day) received by a horizontal surface located at the upper limit of the earth.**

An astronomical model is used for determining the sun's position in the sky (as seen from Bale Robe) as a function of the day of the year and of the time of the day. This model allows calculating for each day of the year, G_0, the global daily solar irradiation (J/m^2/day) received by a horizontal surface located at the upper limit of the earth's atmosphere.

The first step for modeling the incident solar irradiation is to determine the sun's position and path in the sky, as seen from the digester geographic position, as a function of the day of the year and time of the day. Solar time is a time based on the apparent angular motion of the sun across the sky with solar noon the time the sun crosses the meridian of the observer and it is given by.

$$\text{solar time} = \text{standard time} + 4(L_{st} - L_{loc}) + ET \quad \ldots\ldots\ldots\ldots(4.25)$$

Where Lst is the standard meridian for the local time zone, L_{loc} is the longitude of the location in question, and longitudes are in degrees west, that is, $0^o < L < 360^o$. The parameter ET is the equation of time (in minutes), and is given by **(Kalogirou, 2014):**

The values of the ET as a function of the day of the year (N) can be obtained approximately from the following equations

$$ET = 9.97\sin(2B) - 7.53\cos(B) - 1.5\sin(B)[\min] \ldots\ldots(4.26)$$

$$B = (N - 81)\frac{360}{364} \ldots\ldots\ldots\ldots\ldots\ldots\ldots\ldots\ldots\ldots\ldots\ldots\ldots(4.27)$$

The sun declination angle, δ (°), the angular position of the sun at solar noon (i.e., when the sun is on the local meridian) with respect to the plane of the equator, north positive; -23.45° ≤ δ ≤ 23.45° **(Kalogirou, 2014).**

The declination, d, in degrees for any day of the year (N) can be calculated approximately by the equation

$$\delta = 23.45 \sin\left[\frac{360}{365}(284+N)\right] \text{……..……………………}(4.28)$$

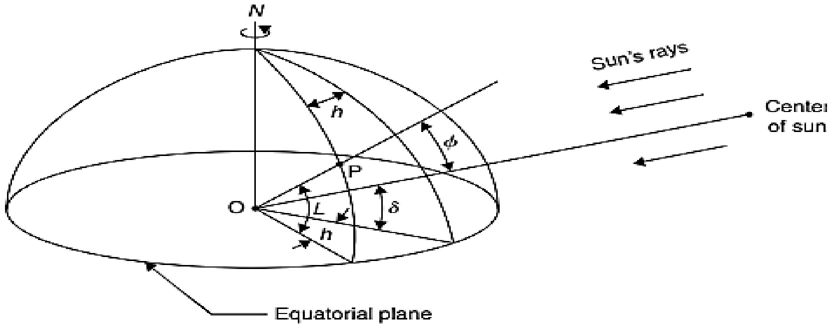

Figure 4. 2: Declination angle (Kalagor.2014)

The **solar hour angle ω**, the angular displacement of the sun east or west of the local meridian due to rotation of the earth on its axis at 15 per hour; morning negative, afternoon positive. In addition, **(Kalogirou, 2014)** .given by

$$\omega = 15(\text{solar time} - 12) \text{…………………………………}(4.29)$$

The solar elevation angle, H (°), is evaluated using:

$$\sin(H) = \sin(L)\sin(\delta) + \cos(L)\cos(\delta)\cos(\omega) \text{ …..…….}(4.30)$$

Where L refers to the latitude (°) is equal to 7.1333° (Bale Robe latitude)

At sunrise, the hour angle magnitude**,** ω_{sr} (°), and the local solar time, ST_{sr}, is calculated as follows:

$$\cos(\omega_{sr}) = -\tan(L)\tan(\delta) \text{ ………… ……..………………….}(4.31)$$

$$ST_{sr} = 12 - \frac{\omega_{sr}}{15} \text{ ……………….……….………………………}(4.32)$$

The local solar time at sunset, ST_{ss} is given by:

$$ST_{ss} = 12 + \frac{\omega_{ss}}{15} \text{ …………………………….…………....}(4.33)$$

Thus, the daytime duration, d (h), equals

$$d = 2\frac{\omega_{sr}}{15} \quad \ldots\ldots\ldots\ldots\ldots\ldots\ldots\ldots\ldots\ldots\ldots\ldots\ldots(4.34)$$

G_{0H}, the global daily solar irradiance received by a horizontal surface at the upper limit of Earth atmosphere, is calculated as follows expressed in J m^{-2} day^{-1} **(Kalogirou, 2014):**

$$G_{0H} = \frac{24x3600G_{sc}}{\pi}\left[1+0.033\cos\left(\frac{360N}{365}\right)\right] x \left[\begin{array}{l}\cos(L)\cos(\delta)\sin(\omega_{sr})+ \\ \frac{\pi\omega_{sr}}{180}\sin(L)\sin(\delta)\end{array}\right] \quad ..(4.35)$$

Where G_{sc} is the solar constant, is 1367 W/m^2

2. Calculation of the global daily solar irradiation on a surface at ground level

Solar energy reaching the earth's surface is attenuated while crossing the atmosphere because of absorption, reflection, and scattering by liquid and solid aerosols, etc., especially in the case where a cloud cover is present. This attenuation factor is estimated based on the daily sunshine duration experimental data, which allows calculating G_H(J/m^{2}day), the global daily solar irradiation received by a horizontal surface at ground level and is given by **(Duffie &Beckman, 2013):**

$$\frac{G_H}{G_{0H}} = a + b\left(\frac{n_s}{N_s}\right) \quad \ldots\ldots\ldots\ldots\ldots\ldots\ldots\ldots\ldots\ldots\ldots\ldots\ldots(4.36)$$

Where G_H global daily solar radiation on a horizontal surface, G_{0H}, is the global daily solar radiation outside of the atmosphere for the same location, a, and b are empirical constants, (values are evaluated by regression), ns is the daily hours of bright sunshine and Ns is the maximum possible daily hours of bright sunshine.

The regression parameters a and b can be determined from:

$$a = -0.110 + 0.23\cos\varphi + 0.323\left(\frac{n_s}{N_s}\right) \quad \ldots\ldots\ldots\ldots\ldots\ldots\ldots\ldots(4.37)$$

$$b = 1.449 - 0.533\cos\varphi - 0.694\left(\frac{n_s}{N_s}\right) \quad \ldots\ldots\ldots\ldots\ldots\ldots\ldots\ldots(4.38)$$

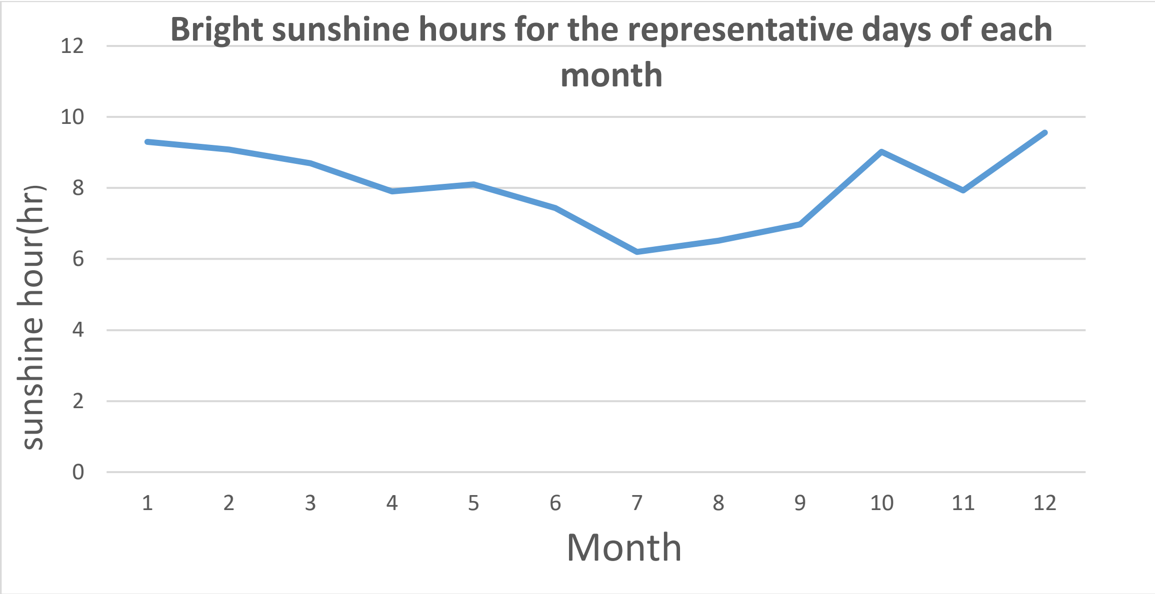

Figure 4. 3: Daily hours of bright sunshine

3. **Calculation of the beam and diffuse daily solar irradiation on a surface at ground level.**

B_H and D_H (J/m^{2}day), the beam and diffuse components of G_H.The average daily diffuse radiation on a horizontal surface can be determined from the average daily global radiation on a horizontal surface and the number of bright sunshine hours **(Duffie & Beckman, 2013):**

$$\frac{D_H}{G_H} = 0.931 - 0.814\left(\frac{n_s}{N_s}\right) \qquad (4.39)$$

The daily beam solar radiation hitting a horizontal surface at ground level, B_H (J/m^{2}day.

$$B_H = G_H - D_H \qquad (4.40)$$

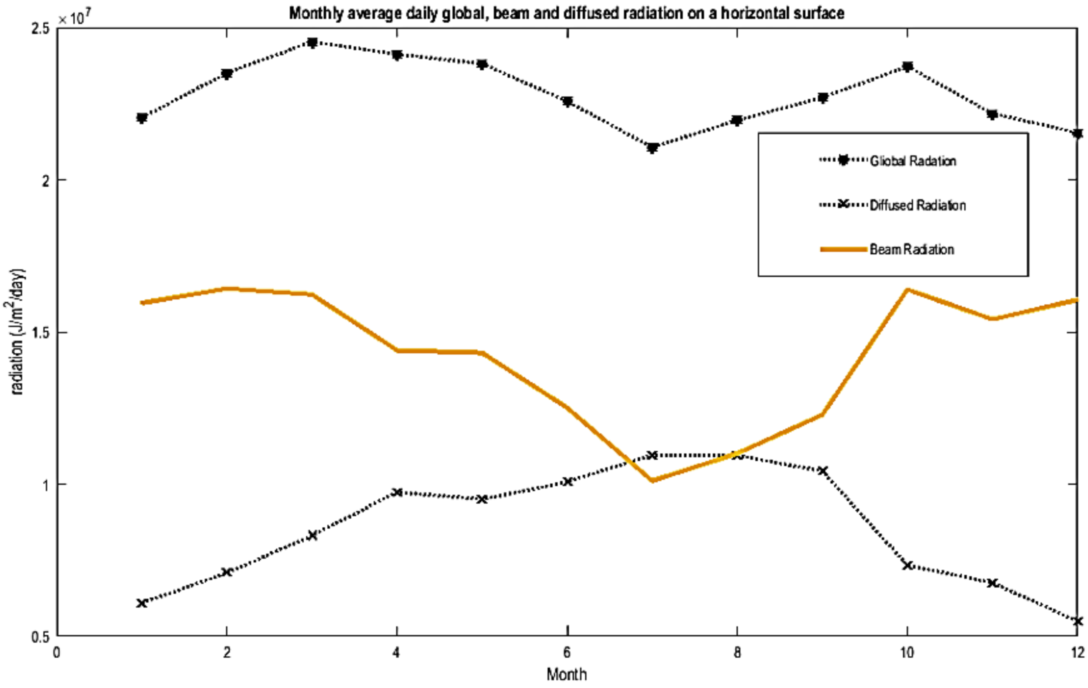

Figure 4. 4: Monthly average daily global, beam and diffused radiation on a horizontal surface

4. **Calculation of the beam and diffuse solar irradiances on a horizontal surface at ground level**

B_H And D_H are daily average quantities. However, the knowledge of the instantaneous solar heat flux is required for the transient thermal model. Therefore, the Collares-Pereira and Rable, (1978) model is used to calculate B^*_H and D^*_H, the beam and diffused solar irradiances (W/m^2) on a horizontal surface at ground level, as a function of the time of the day. During daytime (i.e.$ST_{sr} \leq ST \leq ST_{SS}$), B^*_H and D^*_H are given by (they are nil the remainder of the day) **(Hriez et al., 2017):**

$$D_H^* = \frac{\pi}{24x3600}\left[a+b\cos(\omega)\right]\frac{\cos(\omega)-\cos\left(\omega_{sr}\right)}{\sin(\omega_{sr})-\frac{\pi\omega_{sr}}{180}\cos\omega_{sr}} * D_H \quad \text{.........(4.41)}$$

$$B_H^* = \frac{\pi}{24x3600}\left[a+b\cos(\omega)\right]\frac{\cos(\omega)-\cos\left(\omega_{sr}\right)}{\sin(\omega_{sr})-\frac{\pi\,\omega_{sr}}{180}\cos\omega_{sr}} * D_H \quad \text{.......(4.42)}$$

Where:

$$a = 0.409 + 0.502\sin(\omega_{sr} - 60)$$
$$b = 0.661 - 0.477\sin(\omega_{sr} - 60) \quad \text{..} (4.43)$$

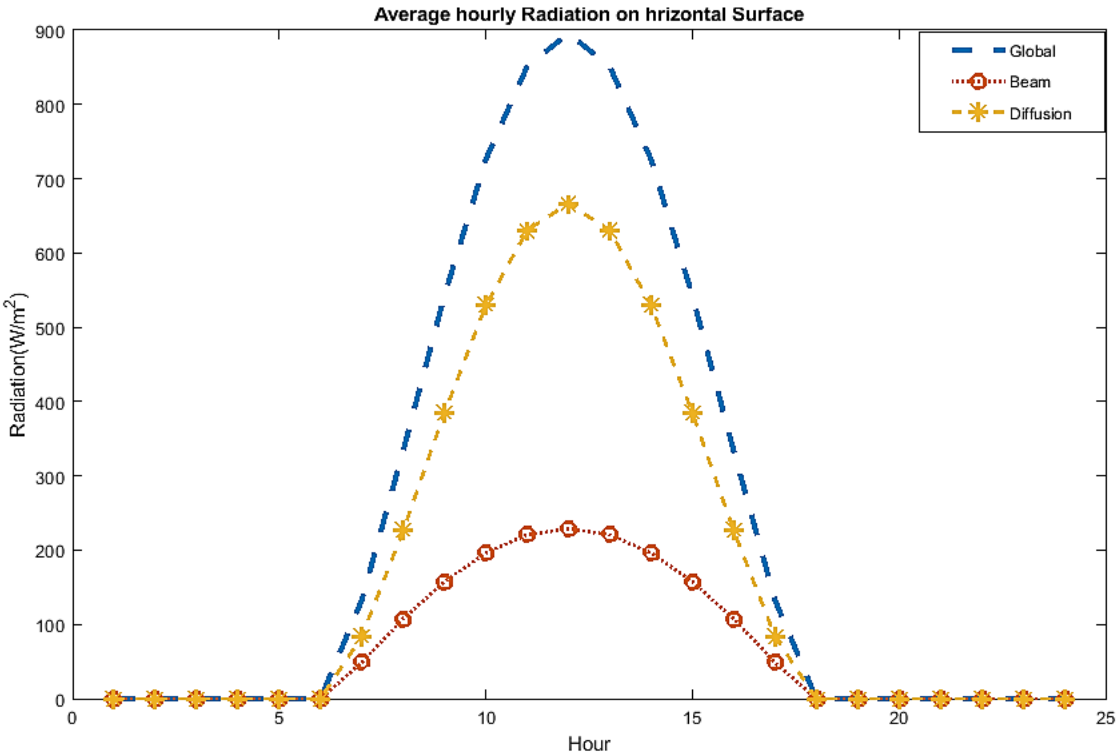

Figure 4. 5: Global, beam and diffused radiation on a horizontal surface on January 17

5. Calculation of the solar heat flux absorbed by the cover

The diffuse solar irradiance on a tilted plan D_I^* (W/m^2) is given by:

$$D_I^* = \frac{D_H^*}{2}(1 + \cos\beta) \quad \text{..} (4.44)$$

Where β the inclination angle from the horizontal. Thus, assuming no shading effects since there is no buildings, trees, or other obstacles nearby the digester, the diffuse solar heat flux absorbed by the digester cover, D_{cov}^* (W/m^2), is calculated as follows **(Hriez et al.,2017):**

$$D_{co}^* = \alpha_{co}\frac{D_H^*}{2}\iint[1 + \cos\beta]d^2S \quad \text{..} (4.45)$$

Where α_{co} is the cover thermal absorptivity taken as 0.9 in the current study, (integration is performed on the cover's external surface). Considering that the cover has a spherical cap shape, solving the above equation in spherical coordinates gives (the azimuthal angle γ being equal to the inclination angle:

$$D^*_{co} = 0.626\pi r^2_{co}\alpha_{co}D^*_H \qquad (4.46)$$

Where r_{co} the cover's radius of curvature equal 1.787 m,The, reflected solar irradiance on a tilted plan R^*_I (W/m^2) is given:

$$R^*_I = \varphi_{soil}\left(\frac{D^*_H + B^*_H}{2}\right)*\left[1-\cos\beta\right] \qquad (4.47)$$

Where, Ψ_{soil} is the ground albedo, taken as 0.4 in the current study. Thus, the ground-reflected solar flux that is absorbed by the cover R^*_{co} (W/m^2) equals:

$$R^*_{co} = \psi_{soil}\alpha_{co}\left(\frac{D^*_H + B^*_H}{2}\right)\iint\left[1-\cos\beta\right]d^2 = 0.0586\psi_{soil}\,\pi r^2_{co}\alpha_{co}(D^*_H + B^*_H) \qquad (4.48)$$

Contrary to diffuse and albedo solar radiations, beam radiation is anisotropic: the part of the cover surface that is exposed to beam radiation depends on the solar elevation angle. Thus, it is difficult to derive an analytical relationship between the beam solar heat fluxes absorbed by the digester cover, considering that the cover has a spherical cap shape when θz equals 0^o, the projection of the cover surface on a plane perpendicular to the direct rays (i.e. a vertical plane) is a circular segment which area is 4.84 m^2. For θz equal to 90^o, the projection of the cover surface on a plane perpendicular to the direct rays (i.e. on a horizontal plane) is a disk which surface is 9.69 m^2 (equal to the digester cross-section). For simplicity, assuming a linear relationship between θz and B^*_{co} gives **(Hriez et al., 2017):**

$$B^*_{co} = \alpha_{co}B^*_H(4.67 + \frac{\theta_z}{1.185}) \qquad (4.49)$$

Finally, $Q_{r(co\_so)}$ (J/hr), the cover total heat flux gain from solar irradiation is given by:

$$Q_{r(co\_so)} = B^*_{co} + D^*_{co} + R^*_{co} \qquad (4.50)$$

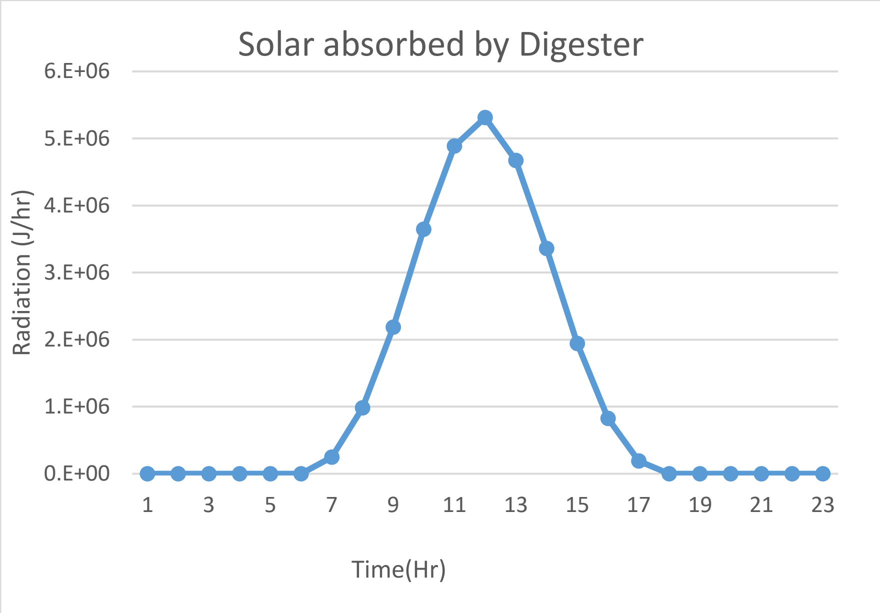

Figure 4. 6: Solar heat flux absorbed by the cover on January 17

4.4.9. Modeling of heat Transfer from Digestate to the soil across the walls

The heat transfer from the digestate to the soil across the walls can be expressed as **(Hreiz et al., 2017):**

$$Q_{Dg\_soil} = U_{Dg\_soli} A_{Dg} (T_{Dg} - T_{soil}) \quad \text{.......................................(4.51)}$$

Where U_{Dg_soil} is the overall heat transfer coefficient for each wall and can be calculated as:

$$\frac{1}{U_{Dg\_soli}} = \frac{1}{h_{Dg}} + \frac{L_{wall}}{k_{wall}} \quad \text{.......................................(4.52)}$$

Where h_{Dg} is the interior surface heat transfer coefficient (i.e. the convective heat transfer coefficient of the digestate), L_{wall} is the thickness of the concrete wall, A_{Dg} is the surface area of the digester, and k_{wall} is the thermal conduction. The soil temperature is affected by the long-term operation of the digester: it increases with time due to heat transfer from the digester (and thus Q_{Dg_soil} decreases), until equilibrium, state is reached. So it becomes more complicated to analyze. A pseudo-steady state analysis is used, using annual monthly average weather conditions. Based on this assumption the undisturbed soil temperature can be calculated as follows Ouzzan et al., (2015), as reported by **Hreiz et al., (2017):**

$$T_{soil} = 17.898 + 0.951\bar{T}_{At} \quad \text{.......................................(4.53)}$$

Where $\bar{\bar{T}}_{At}$ annual average air temperature Bale Robe

4.4.10. **Modeling of the heat supplied by the heat exchanger, QDg-HE**

The HE is a helical-coil pipe forming three turns .The helix diameter is about 4.23 m, and its pitch 0.2 m. The pipe external diameter is 6 cm. Thus the HE external surface, *SHE*, is around 19 m^2 **(Hriez et al., 2017):**

Cogenerated hot water is mixed with warm water returning from the HE in a three-port valve before entering the HE: the total water flow rate in the HE,V_w is maintained at 0.604 m^3 h-1.Water temperature at the HE entrance may be modified using the three-port valve, by passing more or less cogenerated water in the circuit. Thus, the heat power delivered to the digestate may be controlled. When the HE is operated at maximum capacity, i.e. the cogenerated water port is held opened at its maximum, $T_{W,I}$ is about 80 °C. Under these operating conditions, water enters the HE at about 80 °C, and leaves it at about 60 °C. Thus, the heat flux transferred to the digestate equals:

$$Q_{Dg\text{-}HE}(T_{Dg}=60\ °C)= \boldsymbol{\rho}_W v_W c_W(T_{fin}-60°C)\ldots\ldots\ldots\ldots\ldots\ldots\ldots(4.53)$$

If the actual digestate temperature is less than 58 °C, the operator opens the cogenerated water port at its maximum, so $T_{W,I}$ is about 80 °C. For *TDg* greater than 58 °C, it is considered that the operator ‘acts as a proportional controller’, and sets the daily value of $T_{W,I}$ (in °C) according to **(Hriez et al., 2017):**

$$T_{w,I} = 5(58 - TDg) + 55 \ldots\ldots\ldots\ldots\ldots\ldots\ldots\ldots\ldots\ldots\ldots..(4.54)$$

Hence, if *TDg* at 7 am is 58 °C for example, *TW,I* is lowered to 55 °C in order to balance heat losses while avoiding the digester overheating.

4.5. Estimation of Hourly Variation of Atmospheric Temperature.

In modeling, and simulation of digester and parabolic trough solar collector atmospheric temperature is one of the necessary inputs. A mathematical model that uses the minimum and the maximum temperatures of the day estimates the hourly variation of the outdoor temperature. Estimation of hourly dry-bulb temperature can be approximated from the daily mean maximum and daily mean minimum temperatures. A sinusoidal variation of the dry-bulb temperature throughout the day and the maximum temperature at 15:00 hour sun time is assumed. The hourly variation of temperature, given by a report by **(Sitotaw, 2019).**

$$T_{am}(t) = T_{\max} - \frac{(T_{mam} - T_{\min})}{2}\left[1 - \sin\frac{(\pi t - 9\pi)}{2}\right]\ldots\ldots\ldots\ldots\ldots(4.55)$$

Where:

- T_{max} = mean daily maximum temperature at 15:00 hr sun time

- T_{min} = mean daily minimum temperature
- t = Time of the day

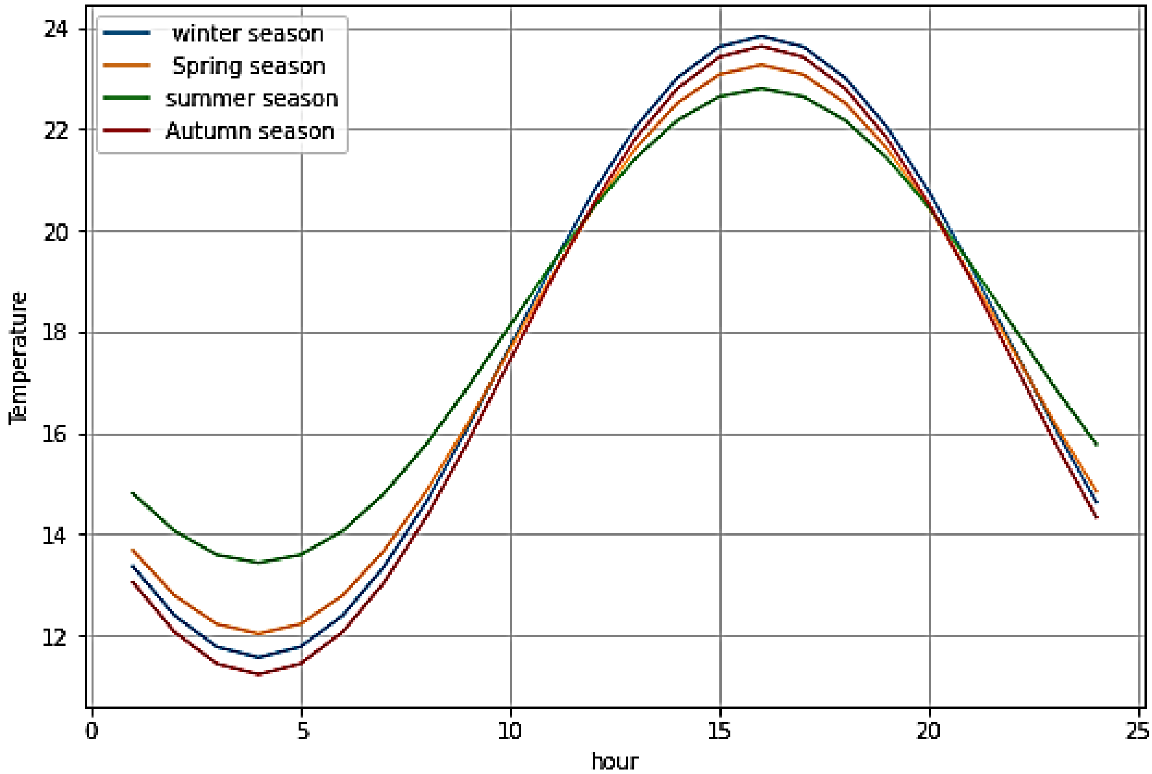

Figure 4. 7: Diurnal ambient temperature variation of Bale Robe Town seasons

4.6. Transient Thermal Simulation of a Digester Using a numerical method

The Transient simulations using monthly average weather conditions of the differential equation describing the energy balance equations are solved using (ODE integrator) PYTHON Script. The thermal model has been written in ANACONDA (SPIDER). Integration with respect to time was performed through the ODEINT scheme module. Substitute heat transfer terms equation (4.10-4.51) into equation (4.6-4.8)

Digestate phase

$$\rho_{Dg} V_{Dg} C_{Dg} \frac{dT_{Dg}}{dt} = \begin{bmatrix} \dot{m}_F C_w T_{At} - \dot{m}_L C_w T_{dg} - h_{Dg\_Bg} S_{Dg\_Bg} (T_{Dg} - T_{Bg}) - \\ \sigma \dfrac{T_{Dg}^4 - T_{Bg}^4}{\dfrac{1-\varepsilon_{Dg}}{\varepsilon_{Dg} S_{Dg-Bg}} + \dfrac{1}{S_{Dg-Bg}} + \dfrac{1-\varepsilon_{co}}{\varepsilon_{co} S_{co}}} - U_{Dg\_soil} A_{Dg} (T_{Dg} - T_{soil}) \end{bmatrix} \quad ..(4.56)$$

Biogas phase

$$\rho_{Bg}V_{Bg}C_{Bg}\frac{dT_{Bg}}{dt}=\begin{bmatrix}\dot{m}_{Bg}C_{Bg}T_{Dg}-\dot{m}_{Bg}C_{Bg}T_{Bg}+h_{Dg\_Bg}S_{Dg\_Bg}(T_{Dg}-T_{Bg})\\ -h_{Bg\_co}S_{co}(T_{Bg}-T_{co})\end{bmatrix}\text{.................}(4.57)$$

Cover Phase

$$\rho_{co}V_{co}C_{co}\frac{dT_{co}}{dt}=\begin{bmatrix}h_{Dg\_co}S_{co}(T_{Bg}-T_{co})-h_{co\_at}S_{co}(T_{co}-T_{At})-\\ \sigma\dfrac{(T_{Dg})^4-(T_{co})^4}{\dfrac{1-\varepsilon_{Dg}}{\varepsilon_{Dg}S_{Dg\text{-}Bg}}+\dfrac{1}{S_{Dg\text{-}Bg}}+\dfrac{1-\varepsilon_{co}}{\varepsilon_{co}S_{co}}}-\varepsilon_{co}\delta S_{co}(T^4_{co}-T^4_{sky})+Q_{r(so\_co)}\end{bmatrix}..(4.58)$$

In the computational program, solar radiation, ambient temperature, soil temperature are the function of times has to be supplied. The temperatures T_{Dg}, T_{Bg}, and T_{co} are constrained to return to their starting values at the end of a 24-hr period **M.Sain & Anita A,(2014).** This is equivalent to,

$$\int_0^{24hr}(\text{rate of heat input to maintain digester temperature})dt$$
$$=\int_0^{24hr}(\text{rate of heat transfer to manure })dt+ \quad \ldots(4.59)$$
$$\int_0^{24hr}(\text{rate of heat loss through digester})dt$$

Table 4. 2: The thermophysical properties of digestate, digester cover, and biogas are considered independent of temperatures

Properties	Digestate	Biogas	digester	Cover	air	Unit
Density	983.3	1.075		1125		Kg/m^3
Specific heat capacity	3976.7	1376.5		1900		J/kg-K
emissivities	0.9		0.9	0.9		

4.7. Thermal Performance of Solar Thermophilic Anaerobic Digestion System

According to **El-Mashad et al., (2004)** specific net thermal energy production of digestion system of Solar Thermophilic Anaerobic Reactor (STAR) defined as the net daily energy production per unit volume of an anaerobic digester, it is the caloric value of the produced biogas minus the total energy required for heating the anaerobic digestion system. The daily net thermal energy production can be calculated using a biogas calorific value. To calculate specific net thermal energy production after applying solar energy (ET), the following equation can be used. To calculate the system SNTEP after applying the solar energy (*ET*), the following equation can be used:

$$ET = \frac{E-(1-P)I}{E} \qquad (4.60)$$

Where: P is the percentage of daily heat requirements that can be covered by solar energy; I

is the daily heat requirements to heat the digester at the desired digester temperature level; and E the potential energy production based on daily biogas production in the anaerobic digestion system.

CHAPTER 5: THERMAL PERFORMANCE ANALYSIS OF PARABOLIC TROUGH SOLAR COLLECTOR

5.1. Introduction

Parabolic-trough solar water heating is a well-proven technology that directly substitutes renewable energy for conventional energy in water heating. A parabolic trough solar collector with a sun tracking system to maximize solar radiation absorptions is leading to increasing the hot water temperature and system efficiency. To enhance the density of solar radiation in a certain area, the solar focus should be used in large areas. The most frequently solar-focus technology contains point-focus and line-focus. Parabolic-trough solar concentrator (PTC) is one of the typical line-focus systems; compare to surface solar energy, PTC has higher heat efficiency and lower cost widely in solar air condition, distillation. However, few reports combine solar energy and anaerobic digester technology. **Hassanein et al., (2019)** experimentally found that parabolic through solar concentrators (PTC) with tracking system for improving the solar system efficiency and increasing biogas production per day without daily additional costs

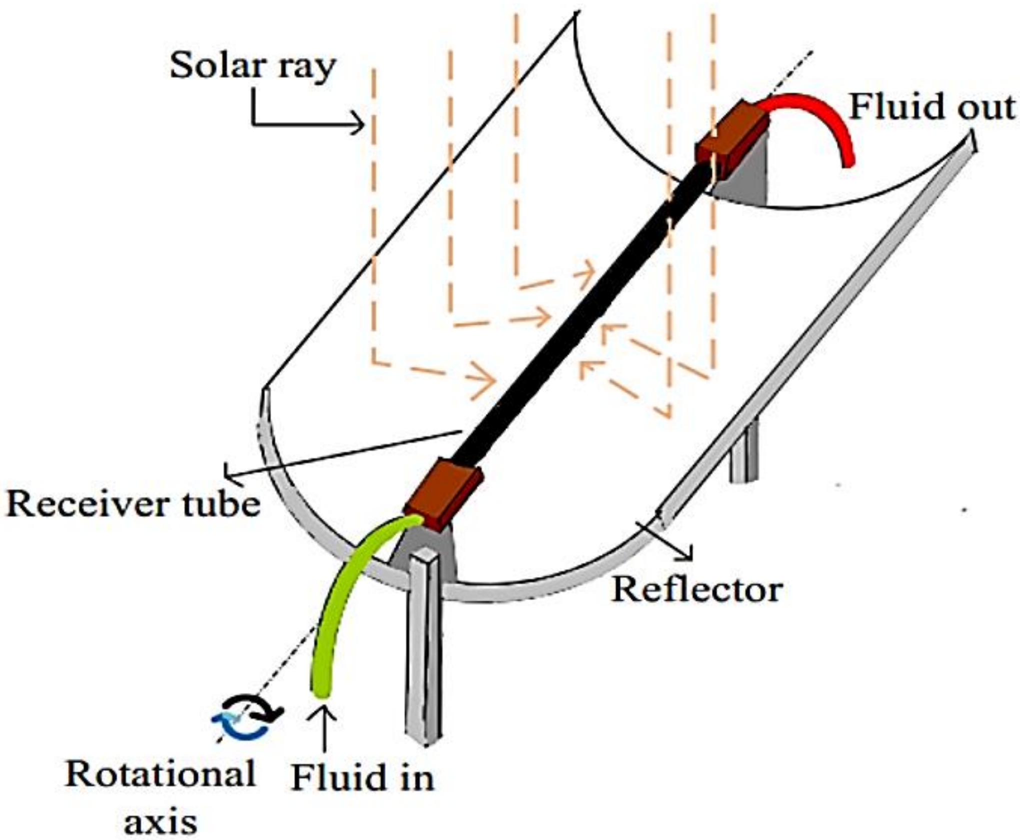

Figure 5. 1: Parabolic Trough Solar Collector Dabiri, Soroush. (2016).

Report of Sandia National Laboratories (SAND94-1884) and Characteristics of the (PTC) used in this study **(Lamrani et al., 2018)**

Table 5. 1: Specification of PTC

Engineering parameters		Optical properties	
Length of collector	5m	Concentration ratio	15.6
Width of collector	3.4m	Cover emittance	0.86
Receiver inner diameter	66mm	Absorber emittance	0.14
Receiver outer diameter	70mm	Trough reflectance	0.93
Focal distance	1.84m	Receiver absorbance	0.906
cover inner diameter	109mm	Cover Transmittance	0.95
cover outer diameter	115mm		

5.2. Collector geometry

A geometrical description of a parabolic trough is commonly used to characterize the form and size of a parabolic trough. The geometry of the collector is obtained using geometrical relations defining the shape that makes up the collector's system **(Padilla et al., 2011).** The profile of the collector is defined using the x and y coordinate.

$$x^2 = 4y\,f \quad \text{……………..…………………………..(5.1)}$$

Where: f represents the focal length (f): Determines the location of the heat collection element. It is the distance between the parabolic center and the absorber tube. **(Padilla et al., 2011)** give the focal length**:**

$$f = \frac{w_a}{4\tan\left(\frac{\varphi_r}{2}\right)} \quad \text{…………………………………..(5.2)}$$

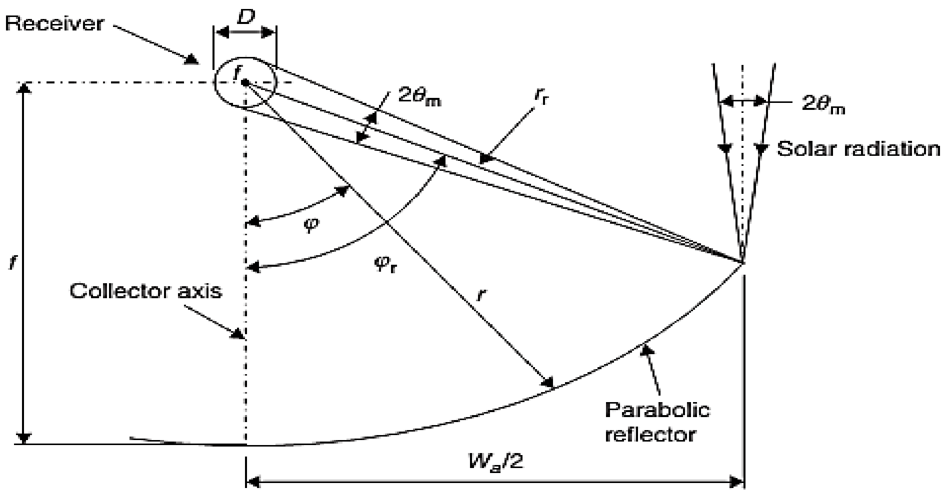

Figure 5. 2:Cross-section of a parabolic trough collector with the circular receiver **(Kalogirou, 2014).**

The rim angle (φ_r): is the angle between the optical axis and the line between the focal point, in addition, the mirror rim has the interesting characteristics that it alone determines the shape of the cross-section of a parabolic trough. That means that the cross-sections of parabolic troughs with the same rim angle are geometrically similar.

Rim angle (φ_r) is calculated using the aperture (W) and the focal distance (f) as below.

$$\varphi_r = \tan^{-1}\left(\frac{8*\frac{f}{w}}{16*\left(\frac{f}{w_a}\right)-1}-1\right) \text{.................................(5.3)}$$

The total collector aperture $(A_a)$is the product of the width (W) and the length (L)

$$A_a = W.L \text{..........................(5.4)}$$

The surface area of a parabolic trough may be important to determine the material need for the trough. The area is calculated as follows:

$$A=\left(\frac{w}{2}\sqrt{1+\frac{w^2}{16f}}+2f*\ln\left(\frac{a}{4f}+\sqrt{1+\frac{w^2}{16f}}\right)*L\right) \text{.........(5.5)}$$

The absorber area (A_{ro}) is the outer area of the tube:

$$A_{ro} = \pi.D_{ro}.L \text{...................................(5.6)}$$

The concentration ratio (C): is defined as the ratio collector aperture to the receiver (absorber) area. Which are the factors increasing the radiation flux on the energy-absorbing surface.

$$C = \frac{A_a}{A_{ro}} = \frac{W * L}{\pi.D_{ro}.L} = \frac{W}{\pi.D_{ro}} \text{......................................}(5.7)$$

5.3. Optical Model

In ideal conditions, 100% of the incident solar energy is reflected by the concentrator and absorbed by the absorber. However, in reality, the reflector does not reflect all solar radiation due to imperfections of the reflector causing some optical losses. The optical efficiency relies on many factors such as tracking error, geometrical error, and surface imperfections.

5.3.1. Optical efficiency

The optical efficiency of PTC is defined as the ratio of energy reaching the absorber tube to that received by the collector. It indicates how much energy is absorbed by its receiver out of the total solar energy incident on the aperture of its mirror. **(A. Allouhi et al., 2018 & Reta, 2020).**

$$\eta_o = \gamma \, \tau \, \alpha \, r_m \, k(\theta) \text{...}(5.8)$$

here γ is intercept factor, τ α is transmittance-absorbance product, r_m is reflectance of the mirror and k(θ) is the incident angle modifier. The incident angle modifier is defined as the ratio of thermal efficiency at a given angle of incidence to the peak efficiency at normal incidence. This can be calculated from the equation as stated below. For the IST collector, the incidence angle modifier k (θ) of the collector is given as follows **(Kalogirou, 2014).**

$$k(\theta) = \cos(\theta) + 0.0003178(\theta) - 0.00003985(\theta)^2 \text{.....}(5.9)$$

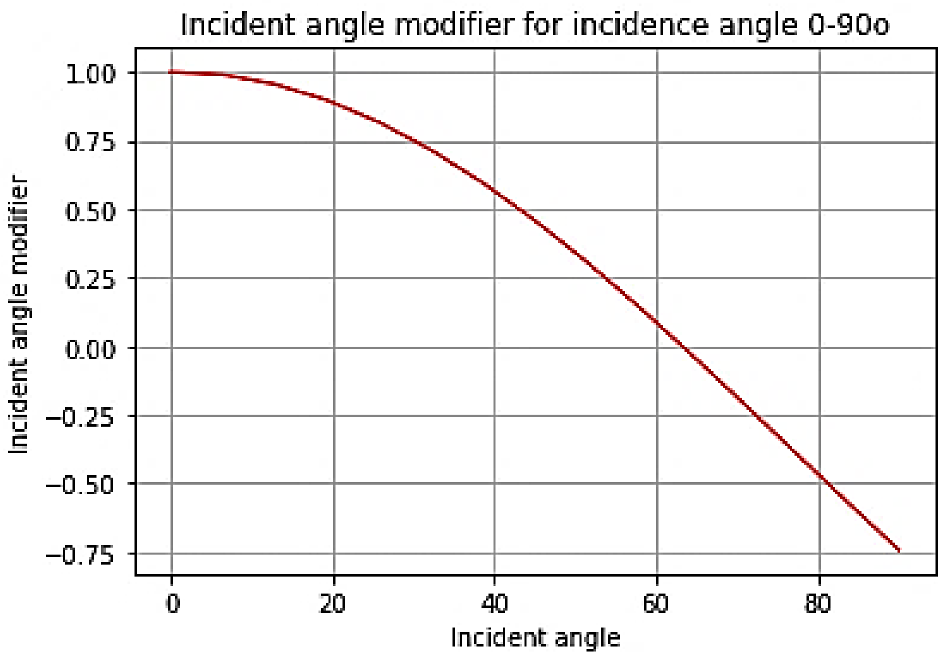

Figure 5. 3: Incident angle modifier for incidence angle 0-90°

5.4. Thermal model

The goal of the thermal model is to determine the energy that is absorbed by the heat transfer fluid (HTF) and describe all the heat losses from the receiver to the atmosphere due to heat transfer mechanisms: conduction, convection, and radiation. Then, the thermal efficiency which is the ratio of the delivered energy to the energy arrived at the reflector can be estimated.

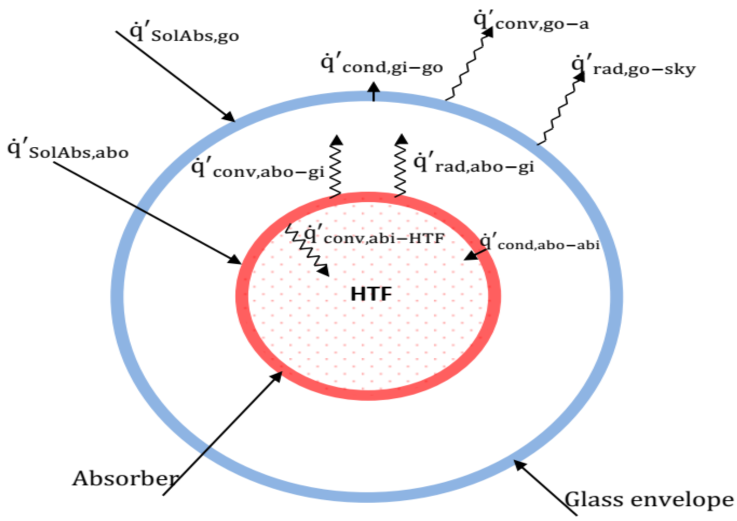

Figure 5. 4: Heat transfer model in a cross sectional area of the HCE **(Al-Oran & Lezsovits, 2020)**

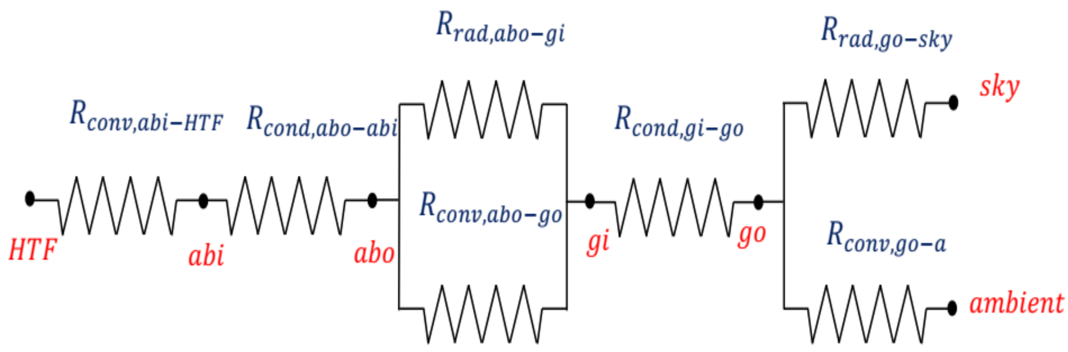

Figure 5. 5.Thermal resistance model

5.4.1. Components of Heat Collection Element

Glass cover: put around the receiver tube to decrease the convective heat loss from the HCE Itis an anti-reflective evacuated glass tube that ensures the absorber from degradation and diminishes the heat losses. The vacuum enclosure is used to reduce heat losses at high working temperatures and to protect the solar-selective absorber surface from oxidation. It is made typically from Pyrex, which keeps up good quality and transmittance under high temperatures **(Ouaguedet al., 2013)**

Receiver tube: is typically stainless steel tube metal black tube set along the focal line of the receiver. Thermal fluid circulates through this tube and gained heat from absorbed solar radiation. It is covered with a particular coating that has a high solar absorptance of 95% for solar radiation, and low thermal emittance (10%, 673 K) for thermal radiation loss **(Ouagued et al., 2013).**

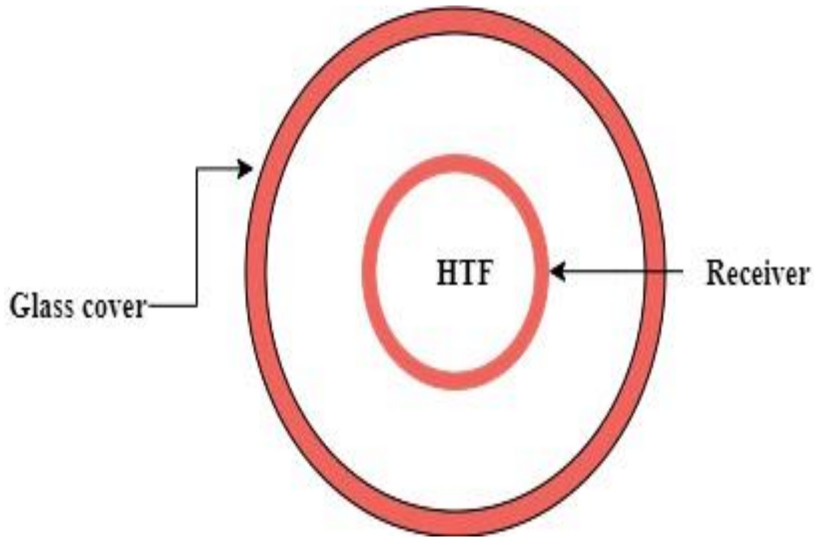

Figure 5. 6: Schematic of HCE in detail

5.4.2. Analysis of Heat Transfer Interactions in HCE

A. Heat transfer between the Glass cover and the atmosphere

Heat transfer from the glass cover to the surrounding ambient air by convection and there is a radiation heat transfer process between Glass cover and sky due to temperature difference.

1. Convection heat transfer

The convection heat transfer is estimated from Newton's law of cooling as shown below **(Padilla et al., 2011).**

$$q_{go\text{-}a}=h_{cv,ext}\pi D_{go}(T_{go}-T_a) \quad \ldots\ldots\ldots\ldots\ldots\ldots\ldots\ldots(5.10)$$

Where

$h_{cv\ ext}$ is the convective heat transfer coefficient between the external surface of the glass cover and the ambient air. Determined by the below equation **(Bellos et al., 2017):**

$$h_{cv,ext} = \frac{8.6 v_{air}^{0.6}}{L^{0.4}} \quad \ldots\ldots\ldots\ldots\ldots\ldots\ldots\ldots\ldots(5.11)$$

Where: v_{air} is the wind speed in m/s and L is the length of the collector in m.

2. Radiation heat transfer.

Assume that the glass envelope is treated as a small gray convex in a large blackbody cavity, which is the sky. **(Lamrani et al., 2018)** give the radiation heat transfer between the glass envelope and the sky

$$q_{go-sky,rad} = \pi D_{go} h_{r,ex}(T_{go} - T_{sky}) \quad \ldots\ldots\ldots\ldots\ldots\ldots\ldots(5.12)$$

The heat transfer coefficient by radiation between the glass envelope and the sky is given as follows

$$h_{r,ext} = \sigma \varepsilon_{go}(T_{go})^2 + (T_{sky})^2(T_{sky} + T_{go}) \quad \ldots\ldots\ldots\ldots\ldots\ldots\ldots(5.13)$$

Where σ is the Stefan–Boltzman constant (5.67x10^{-8} W/m^{2}k^4) and ε_{go} is the emittance of the external surface of the glass envelope. The effective sky temperature is assumed 8°C below the ambient temperature **(Yılmaz & Mwesigye, 2018).**

B. Heat transfer between the receiver tube and the glass cover

Heat transfer between the receiver tube and glass cover occurs by convection and radiation mechanism.

1. **Convection heat transfer**

Convection heat transfer depends on the annulus pressure. For very small Pressure (< 0.013 Pa), the convective heat transfer coefficient is considered as zero. At higher pressures, heat transfer is by free convection. For pressure greater than 0.013 Pa from Raithby and Holland's formula, the convection heat transfer is estimated as follows **(Lamrani et al., 2018):**

$$q_{ro-gi,cv} = h_{cv,\text{int}}(T_g - T_r) \quad \text{..............................(5.14)}$$

Where: $h_{cv,\ int}$ is estimated through natural convection relations between two horizontal, concentric cylinders and given by **(Kalogirou, 2012):**

$$h_{cv,\text{int}} = \frac{2\pi k_{eff}}{\ln\left(\frac{D_{gi}}{D_{ro}}\right)} \quad \text{...(5.15)}$$

(Kalogirou, 2012) gives the effective thermal conductivity k_{eff}:

$$k_{eff} = 0.36 k_{air}\left(\frac{pr_{air}}{0.861}\right)^{0.25}(R_{ac})^{0.25} \quad \text{.........................(5.16)}$$

Where:

$$R_{ac} = h_{cv,\text{int}} = \frac{\left(\ln\left(\frac{D_{gi}}{D_{ro}}\right)\right)^4}{L_{eff}^3\,(D_{gi}^{-0.6} + D_{ro}^{-0.6})^5}(Gr_{air}.\Pr_{air}) \quad \text{..........(5.17)}$$

The critical length is given by $L_{eff} = \frac{D_{gi} - D_{ro}}{2}$ ....(5.18)

2. Radiation Heat Transfer

(Padilla et al. 2011) estimate the radiation heat transfer between the receiver tube and glass cover**:**

$$q_{\text{ro-gi,rad}} = \pi D_{ro} h_{r,\text{int}}\left(T_r - T_g\right) \quad \text{...(5.19)}$$

Where the heat transfer coefficient by radiation between the absorber tube and the glass envelope is expressed as follows **(Kalogirou, 2014):**

$$h_{r,\text{int}} = \frac{\sigma\left((T_r)^2 + (T_g)^2\right)\left((T_r) + (T_g)\right)}{\frac{1}{\varepsilon_r} + \frac{1-\varepsilon_g}{\varepsilon_g}\left(\frac{D_{ro}}{D_{gi}}\right)} \quad \text{...........................(5.20)}$$

C. Conduction heat transfer through the receiver tube wall and glass cover

Fourier's law determines conduction heat transfer through the receiver tube wall of conduction through a hollow cylinder with the assumption that is no thermal resistance and thermal conductivity of the glass is constant **(Kalogirou, 2012).**

$$q_{ri-ro} = \frac{2\pi k_r (T_{ri} - T_{ro})}{\ln\left(\frac{D_{ro}}{D_{ri}}\right)} \quad \text{………………………..………(5.21)}$$

Where k_r is receiver tube thermal conductivity of receiver tube at the average temperature

The conduction heat transfer through the glass cover uses the same equation as the conduction through the receiver tube wall.

D. Heat transfer between the HTF and the receiver tube

From Newton's law of cooling the convection heat transfer from the inside **(Kalogirou, 2012)**

Gives the surface of the receiver tube to the HF.

$$q_{f-r,cv} = h_{cv,f} \pi D_{ri} (T_r - T_f) \quad \text{……………..…..…..……….……(5.22)}$$

The convection heat transfer coefficient at the inside pipe diameter **(Bergman et al., 2020)**

$$h_{cv,f} = Nu_f \frac{k_f}{D_{ri}} \quad \text{…………………….…...………………………(5.23)}$$

Where: Nu_f is Nusselt number based on the inside diameter of the pipe and D_{ri} is the inside diameter of the pipe. The Nusselt number was calculated using the Gnielinski correlation **(Lamrani et al., 2018).**When the Reynolds number is lower than 2300, laminar flow exists in the receiver tube and the Nusselt number is constant. For pipe flow, the constant value, assuming constant heat flux

$$For \ \mathrm{Re}_f < 2300 \quad \mathrm{Nu}_f = 4.36$$

$$For \ \mathrm{Re}_f > 2300 \quad \mathrm{Nu}_f = \frac{\left(\frac{f}{8}\right)(\mathrm{Re}_f - 100)\,\mathrm{Pr}_f}{1 + 12.7\left(\frac{f}{8}\right)^{0.5}\left(\left(\mathrm{Pr}_f\right)^{\frac{2}{3}} - 1\right)} \quad \text{…..(5.24)}$$

With f is the friction factor defined as follows **(Lamrani et al., 2018):**

$$f = (1.82 \log_{10}(\mathrm{Re}_f) - 1.64)^{-2} \quad \text{……………………………..(5.25)}$$

E. Collector heat removal factor

Heat removal factor is defined as the useful energy gained to the energy gained if the entire the absorber is at the inlet temperature of the heat transfer fluid. It is a measure of the thermal the resistance encountered by the absorbed solar radiation is reaching the collector fluid and is expressed as (**Marefati et al., 2018).**

$$F_R = \frac{\dot{m} c_p}{A_r U_L}\left[1\text{-exp}\left(\frac{A_r U_L F^{\bullet}}{\dot{m} c_p}\right)\right] \text{……………….……………..(5.26)}$$

Where k $_f$ is the thermal conductivity of the working fluid (W/m K), D_{ro} is receiver tube inner diameter D_{ri} is receiver tube outer diameter, h_{fi} is convective heat transfer coefficient inside the receiver tube [W/m^{2}K] and U_L is the thermal loss coefficient and given by **(Kumar & Shukla, 2015)**:

Where A_r is the receiver area (m^2) and F′ is the collector efficiency factor is given by:

$$F^{\bullet} = \frac{\dfrac{1}{U_L}}{\dfrac{1}{U_L} + \dfrac{D_{ro}}{h_{fi} D_r} + \dfrac{D_{ro}}{2k_f}\left[\ln\left(\dfrac{D_{ro}}{D_r}\right)\right]} \text{………….….….…..(5.27)}$$

Where k_f is the thermal conductivity of the working fluid (W/m K), D_{ro} is receiver tube inner diameter D_{ri} is receiver tube outer diameter, h_{fi} is convective heat transfer coefficient inside the receiver tube [W/m^{2}K] and U_L is the thermal loss coefficient and given by **(D. Kumar & Kumar, 2015):**

$$U_L = \left[\frac{A_r}{(h_{cv,ext} + h_{r,ext})A_c} + \frac{1}{h_{r,\text{int}}}\right]^{-1} \text{…………………..…..(5.28)}$$

F. Thermal efficiency.

The thermal efficiency of a solar PTC is defined as the ratio of useful heat gain by the HTF and the heat flux received by the concentrator. It is essential to point that only the beam radiation can be exploited from the PTC because these collectors are imaging collectors with a specific image of the sun in the receiver **(Chahine et al., 2018).** The instantaneous thermal efficiency is given by.

$$\eta = \frac{\dot{Q}_u}{I_d A_a} \text{…………………………..………………..(5.29)}$$

A is the unshaded collector aperture area given as $A_r = \pi\ (W_a - D_a)\ L$ *and* the useful energy rate to the working fluid in the receiver tube can be calculated by the use of the Hottel–Whillier equation given as:

$$\dot{Q}_u = \dot{m} c_p (T_{fo} - T_{fin}) = F_R A_a \left[\eta_o I_d - U_L \frac{(T_{fin} - T_a)}{C}\right] \text{…………..(5.30)}$$

The Outlet temperature can be calculated as **(D. Kumar & Kumar, 2015)**:

$$T_{fo} = \begin{bmatrix} T_a + \dfrac{C\eta_o I_d}{U_L} + (T_{fo} - T_a - \\ \dfrac{C\eta_o I_d}{U_L}).\exp\left(\dfrac{-F^{\bullet}U_L A_r}{\dot{m}c_p}\right) \end{bmatrix} = T_{fi} + \frac{\eta A_r I_d}{\dot{m}c_p} \quad \text{.................(5.31)}$$

Mass flow rate analysis Using average daily beam solar radiation of 656 W/m^2 estimated from the solar radiation model analysis. The variation mass flow rate of the collector with outlet temperature and thermal efficiency analyzed.

As shown in Figure. 5.6, as mass flow rate increases outlet water temperature decreases. A mass flow rate of 0.07kg/sec, which corresponds to an outlet temperature of 67.7^{0}C, is selected as the working fluid mass flow rate for this study.

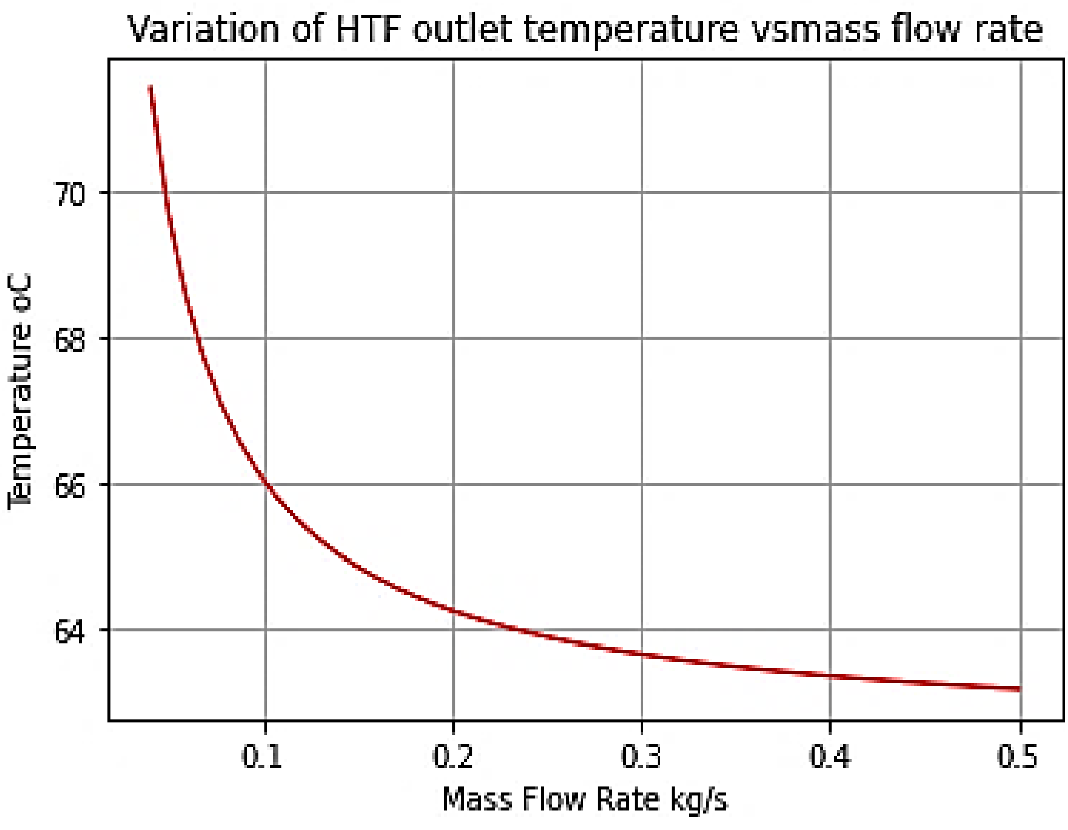

Figure 5. 7: working fluid mass flow rate

5.5. Transient Analysis of Parabolic Trough solar collector

To study the performance collector under fluctuating climatic conditions transient analysis should be done. A one-dimensional mathematical model is introduced to study the transient thermal behavior of the PTC. The inputs of the model are the instantaneous ambient temperature, incident beam radiation, mass flow rate, and physical properties of the glass cover, receiver tube, and HTF. This modeling was used to predict the change in the outlet temperature of the heat transfer fluid (water) versus the beam radiation the thermal exchanges are between the heat transfer fluid, the tube, and the glass tube. The temperature modeling was based on the energy balances characterized by the differential equations of the three temperatures. These equations vary during the illumination time (t) for a length (X) of the absorber. The discretization of method finite difference is used for solving the nonlinear equations of that heat balance at the receiver tubes. A computer program was developed in PYTHON ANACONDA distribution to solve these equations. The mathematical model of energy balance different components of PTC is based on the following assumptions **(Ghodbane & Boumeddane, 2018, Lamrani et al., 2018).**

- The heat transfer fluid is incompressible;
- The heat transfer by conduction in the receiver tube is neglected
- The parabolic shape is symmetrical;
- The ambient temperature around the concentrator is;
- The shadow effect of the absorber tube on the mirrors is negligible;
- The receiver tube and the glass cover are assumed grey bodies.
- The solar flux at the absorber is uniformly distributed;
- The glass is considered opaque to infrared radiation;
- Conduction losses at the ends of the receiver tube are neglected
- The flow is unidirectional.
- The exchanges by conduction in the absorber and the glass are negligible.

A. Energy Balance of Heat transfer fluid.

The energy balance for the heat transfer fluid that circulates in the absorber tube was expressed by the following relationship **(Ghodbane & Boumeddane, 2018, Lamrani et al., 2018).**

$$m_F C_{p,F} \frac{\partial T_F(x,t)}{\partial t} + \dot{m}_f C_f (T_f(x+\Delta x,t) - T_f(x,t)) = Q_u(F)\ . \ (5.32)$$

Where: where *m* is a flow rate working fluid flows inside the absorber, $Q_{F\,u\,()}$ is useful heat transfers to the working fluid by convection. Equation 5.24 can be written as:

$$\rho_f C_{p,f} A_f \frac{\partial T_f(x,t)}{\partial t} = \pi D_{r,i} h_{cv,f} (T_r - T_f) - \dot{m}_f C_f \frac{\partial T_f(x,t)}{\partial x}\ .(5.33)$$

B. Energy Balance of Glass cover

Similarly, **(Ghodbane & Boumeddane, 2018, Lamrani et al., 2018)** gave the energy balance for the glass.

$$\rho_g C_g A_g \frac{\partial T_g(x,t)}{\partial t} = Q_{\text{int}}(x,t) - Q_{ext}(x,t)$$
$$where \;\; Q_{\text{int}}(x,t) = Q_{\text{int},cv} + Q_{\text{int},r} \qquad \text{............(5.34)}$$
$$Q_{ext}(x,t) = Q_{ext,cv} + Q_{ext,r}$$

The equation can be written as:

$$\rho_g C_g A_g \frac{\partial T_g(x,t)}{\partial t} = \pi D_{r,o} h_{cv,\text{int}}(T_r - T_g) + \pi D_{r,o} h_{r,\text{int}}(T_r - T_g) - (\pi D_{g,o} h_{cv,ext}(T_g - T_{amb}) + \pi D_{g,o} h_{cv,ext}(T_g - T_{sky})) \text{ ..(5.35)}$$

Where: ρ_g, C_g, and T_g are the Glass cover density, specific heat, and temperature, respectively and A is the difference between the inner surface and the outer surface of a glass tube (m^2).

C. ***Energy balance for the absorber tube***

The energy balance for the absorber was given by the following equation **(Ghodbane & Boumeddane, 2018, Lamrani et al., 2018).**

$$m_A C_A \frac{\partial T_A(x,t)}{\partial t} = Q_{ab} - Q_{\text{int}} - Q_u(F) \text{ ....(5.36)}$$

Where: Q_{ab} is referring to the solar energy absorbed by the heat-collecting element, Q_{int} is heat loses by convection and radiation and Q_u (F) is useful heat transfers to the working fluid by convection. Write as equation (5.37)

$$\rho_A C_A A_A \frac{\partial T_A(x,t)}{\partial t} = \begin{bmatrix} I_d \, \gamma \, \tau_g \, \alpha_r \, r_m W \, k(\theta) - \pi D_{r,o} h_{cv,\text{int}}(T_r - T_g) - \\ \pi D_{r,o} h_{r,\text{int}}(T_r - T_g) - \pi D_{A,i} h_{cv,F}(T_r - T_F) \end{bmatrix} \text{...(5.37)}$$

The finite difference method is selected. A calculation program PYTHON was established, after the discretization of non-linear equations that allowed us to obtain a set of numerical results. The time derivatives are replaced by a forward difference scheme, whereas the dimensional derivative is replaced by a backward difference scheme. The discretized finite-difference of equation (5.24, 5.26, and 5.28).

For HTF

$$\frac{\partial T_f(x,t)}{\partial t} = \frac{T^{i+1}_{f,n} - T^{i}_{f,n}}{\Delta t} \text{ ....(5.38)}$$

By applying the above derivatives and some rearrangement the following for equation (5.24)

$$T_{f,n}^{i+1} = \begin{pmatrix} T^{i}_{f,n} + \dfrac{\Delta t}{\rho_f C_{p,f} A_f}\left[\pi D_{r,i} h_{cv,f}\left(T^{i}_{A,n} - T^{i}_{f,n}\right)\right] + \\ \dot{m} C_f \dfrac{\Delta t}{2\rho_f C_{p,f} A_f \Delta x}\left[\left(T^{i}_{F,n+1} - T^{i}_{F,n-1}\right)\right] \end{pmatrix} \text{..........(5.39)}$$

$$T_{f,n}^{i+1} = \begin{pmatrix} T^{i}_{f,n}\left(\dfrac{1}{\Delta t} - \dfrac{\pi D_{r,i} h_{cv,f}}{\rho_f C_{p,f} A_f}\right) + T^{i}_{A,n} * \dfrac{\pi D_{r,i} h_{cv,f}}{\rho_f C_{p,f} A_f} \\ + \dfrac{\dot{m} C_f}{2\rho_f C_{p,f} A_f \Delta x}\Delta t\left[\left(T^{i}_{F,n+1} - T^{i}_{F,n-1}\right)\right] \end{pmatrix} \text{.........(5.40)}$$

Rearrange equation (5.30) and abbreviate long terms for simplicity, finally temperature of HTF

$$\mathrm{T}_{\mathrm{f,n}}^{\mathrm{i+1}} = \left[\mathrm{T}_{\mathrm{f,n}}^{\mathrm{i}}\left(\frac{1}{\Delta \mathrm{t}} - \mathrm{AA}\right) + \mathrm{T}_{\mathrm{A,n}}^{\mathrm{i}} * \mathrm{AA} + \mathrm{BB}\left[\left(\mathrm{T}_{\mathrm{F,n+1}}^{\mathrm{i}} - \mathrm{T}_{\mathrm{F,n-1}}^{\mathrm{i}}\right)\right]\right] * \Delta \mathrm{t} \text{ ... (5.41)}$$

Similarly for glass from equation (5.26)

$$T_{g,n}^{i+1} = \begin{bmatrix} T^{i}_{g,n}\left(\dfrac{1}{\Delta t} - CC - DD - EE - FF\right) + T^{i}_{A,n} * (CC + DD) + \\ EE * T^{i}_{amb,n} + FF * T^{i}_{sky,n} \end{bmatrix} * \Delta t \text{ .(5.42)}$$

Again in the same way for absorber tube from equation (5.28)

$$T_{A,n}^{i+1} = \left[\frac{I_d \gamma \tau_g \alpha_r r_m W k(\theta)}{GG} + \left(\left(\frac{1}{\Delta t} - HH\right) T^{i}_{A,n} + II * T^{i}_{g,n} + JJ * T^{i}_{F,n}\right)\right] * \Delta t \text{ ...(5.43)}$$

Coefficient and abbreviated constants are given below:

$$AA=\frac{\pi D_{ri,}h_{cv,f}}{\rho_f C_f A_f}\ ,BB=\frac{\dot{m}C_f}{2\rho_f C_f A_f \Delta x},$$

$$CC=\frac{\pi D_{r,o}h_{cv,\text{int}}}{\rho_g C_g A_g},\ DD=\frac{\pi D_{r,o}h_{r,\text{int}}}{\rho_g C_g A_g},$$

$$EE=\frac{\pi D_{g,o}h_{cv,\text{int}}}{\rho_g C_g A_g},FF=\frac{\pi D_{g,o}h_{r,ext}}{\rho_g C_g A_g},$$

$$GG=\rho_A C_A A_A, HH=\frac{(\pi D_{r,o}h_{cv,\text{int}}+\pi D_{r,o}h_{r,\text{int}}+\pi D_{A,i}h_{cv,F})}{\rho_A C_A A_A}, \tag{5.44}$$

$$II=\frac{(\pi D_{r,o}h_{cv,\text{int}\,g}+\pi D_{r,o}h_{r,\text{int}})}{\rho_A C_A A_A},JJ=\frac{\pi D_{A,i}h_{cv,F}}{\rho_A C_A A_A}$$

Initial Conditions @ t = 0 and x=0 sec or at 12:00 PM morning

- The glass envelope is at ambient air temperature is average temperature Bale Robe (T_{amb}=17.4^{o}C) so, $T_{G(}$x, t) =T_{amb}(x, t).

$$T_{G(x,\,t)}=290.65K$$

- The absorber is assumed to be (10^{o}C) above the ambient air.

$$T_A(x,t)=T_{amb}(x,t)+10^oC$$

- The fluid is assumed to be at an initial temperature of exit fluid temperature of biogas reactor 60 ^{o}C.

$$T_{f(x,\,t)}=(60+273.15)=333.15K$$

CHAPTER 6: THERMAL PERFORMANCE ANALYSIS OF SOLAR THERMAL ENERGY STORAGE

6.1 .Introduction

TES is the temporary storage of high or low-temperature energy for later use, and it is the most appropriate method to reduce the mismatch between the energy. TES can be stored as a change in internal energy of a phase change material as sensible heat, latent heat, thermochemical, and combination of these.

6.1.1. Sensible Heat Storage (SHS)

Sensible Heat Storage (SHS) is a simple and well-developed technology, where, energy is stored by heating or cooling a liquid or a solid, which does not change its phase during the process. A variety of materials has been used in such systems. **Karthikeyan, (2011)** the commonly used materials in the sensible heat storage system are water, pebble beds, packed solid beds, refractory materials, hydrocarbon oils, organics, and metal salts. The amount of heat stored depends on the specific heat of the medium, the temperature change, and the quantity of the storage material. The main advantage of the sensible heat storage system is that energy exchange is possible very easily.

6.1.2. Latent heat storage (LHS)

Latent heat storage (LHS) is based on energy absorption or release when a storage material undergoes a phase change process. **Karthikeyan, (2011)** the LHS unit is particularly attractive due to its high-energy storage density and its isothermal behavior during the energy storing and retrieval process (phase change process). In recent years, there is a keen interest among scientists to develop thermal storage materials for various applications. Wide ranges of PCMs have been investigated, including salt hydrates, paraffin waxes, and non-paraffin organic compounds, for heating and cooling applications.

Any LHS system must possess at least the following three components.

- A heat storage substance (PCM) that undergoes a phase transition within the desired operating temperature range, wherein the bulk of the heat added is stored as latent heat.
- Containment for the storage substance
- Heat transfer fluid (HTF) for transferring heat from the heat source to the storage substance, and from the latter to the application.

6.1.3. Thermo-chemical storage system

In a thermochemical storage system, thermal energy is used to produce a certain endothermic chemical reaction, and the products of the reaction are stored. When the energy is required to be released, the reverse exothermic reaction is made to take place. However, such systems are expensive and are not suitable for most commercial and domestic uses **(Karthikeyan, 2011)**.

6.1.4. Combined storage system

The combined storage system possesses the advantages of both sensible and latent heat storage systems. In this system, the heat transfer fluid that also performs as an SHS material always surrounds the PCM containers/capsules and it is a better alternative. **(Karthikeyan, 2011)** the combined sensible and latent heat storage system has found manifold applications in domestic, commercial, and industrial sectors. In air-conditioning applications, the combined sensible and latent heat storage system has been introduced successfully.

6.2. Thermal energy storage system configuration

Progress in LHS systems mainly depends on heat storage material investigations and on the development of heat exchangers that assure a highly effective heat transfer rate to allow rapid charging and discharging. Latent heat TES systems are broadly classified into the capsule-type and the shell-and-tube type, according to the method of containing the thermal energy storage material and to the mode of exchanging heat energy within the container. The various studies carried out by the researchers on different configurations are classified under i) Tubular exchanger ii) packed bed units iii) system with different heat transfer enhancement techniques.

Packed bed configurations have shown excellent heat transfer characteristics by providing a large surface area for heat exchange. The spherical geometry of encapsulation of PCM is preferred because it presents a larger area of the encapsulated PCM for heat transfer than other geometries encapsulation. It also makes the storage tank have a greater packing density **(Terakegn, 2018).** Packed bed LHTES system, using encapsulated paraffin wax as the PCM and hot water come out solar collector as the HTF. The aim is to investigate the TES system for store thermal energy demanded by the digester to maintain thermophilic temperature.

The use of aluminum spherical capsules for the containment of paraffin in the proposed packed bed thermal energy storage is investigated.

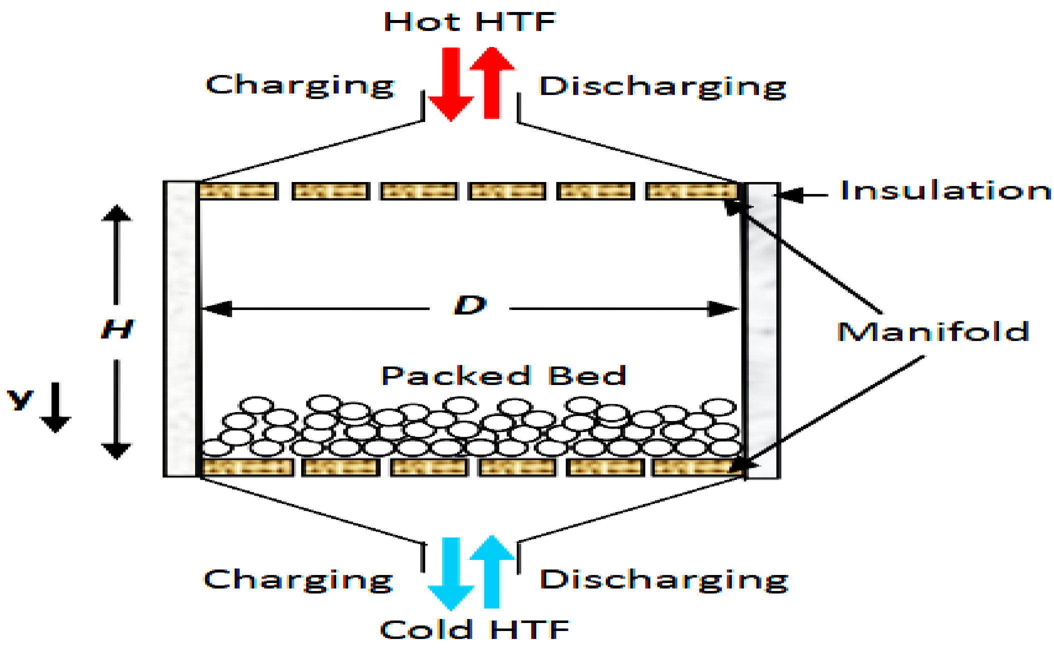

Figure 6. 1: Schematic diagram of the packed bed LHTES system. **(Shobo & Mawire, 2015).**

6.3. Modes of Thermal Energy Storage System

There are three modes of a storage system, which operates on **(Yune, 2019):**

Charging mode: starts with a circulation of the hot HTF heated in the collector system at a temperature higher than the PCM melting temperature. During this period, hot HTF enters the tube side at the top, transfers heat to the solid PCM, and then HTF exits at the bottom of the tubes. This mode occurs during daytime and terminates with a complete melting of the PCM, charging of the store does not terminate with a complete melting of the PCM. If the inlet fluid temperature is above the melt temperature, the charging of sensible heat continues.

Discharging mode: - is started by the circulation of the cold HTF having inlet temperature lower than the PCM melting temperature. The cold HTF enters the system at the bottom is heated by the storage PCM, and then exits at the top. This mode terminates with complete solidification of the PCM.

Standby mode: -This mode occurs when there is no further storage of energy occurring because the thermal storage tank is completely charged or the energy is directly fed to the utility without using storage. There is no flow of HTF in the tube side and heat transfer within the system is dominated by axial conduction, which acts to redistribute the axial temperature gradient formed in the system during charging. This is the transition period between the charge and discharge modes.

6.4. Phase Change Material

Phase Change Material (PCM) is a substance with a high heat of fusion, which melts and solidifies at certain temperatures; is capable of storing or releasing large amounts of energy. Phase change materials are latent heat storage substances, in which energy is stored in the process of changing state, i.e. phase is changed from solid to liquid. When phase change materials attain the temperature at which phase change occurs from solid to liquid, they absorb a large amount of energy and release stored energy when phase change material solidifies **(Bhagat & Verma, 2011).**

Table 6. 1: Thermo-physical properties of phase change material (Paraffin wax n-Hentriacontane)

Melting temperature (°C)	Latent heat of fusion kJ/k	Density (kg/m3)		Specific heat (J/kg°C)		Thermal conductivity (W/m°C)	
		Solid	Liquid	Solid	Liquid	Solid	Liquid
67-68.5	260	912	781	1855	2387	0.216	0.154

The phase change material used in this study is a technical grade Paraffin wax n-Hentriacontane. It has a melting point of 67°C-68.5. The thermophysical properties of Paraffin wax n-Hentriacontane are presented in Table 6.1 **(Reza Vakhshouri, 2020).**

6.5. Mathematical of Modeling of Packed Bed PCM Storage Unit

6.5.1. Modeling of Latent Heat Storage System

The mathematical modeling of physical phase change problems can be broadly classified into two types: i) Variable domain methods (Temperature based method) ii) fixed domain methods (Enthalpy method). The essential difference between the two is that in the former, the total domain is divided into two phases and the intervening interface region, and each region is treated separately. Since the volume of each region changes with time, the method is termed the variable domain method. In this method, the temperature is the sole dependent variable. The energy conservation equations are written separately for each region, and these equations are coupled through energy balance at the interface. The interface, hence, has to be tracked efficiently by solving simultaneously all the three energy equations. The fixed domain method (enthalpy method) does not deal with**,** particular forms of the energy and mass conservations principle for each region. It rather considers the entire domain including all the regions together, and thus, since the total domain does not change with time, the method is termed as the fixed domain method. In this formulation, enthalpy is used as a dependent variable along with the temperature. Enthalpy is continuous only in time, whereas temperature is continuous only in space. Hence, the energy equation, in which, the time derivative is written in enthalpy, the space derivative in temperature, is valid in all the three regions of interest, and the equation can be solved over the whole region as a fixed domain.

A schematic diagram of the packed bed LHTES system, consisting of a perfectly insulated a vertical cylinder of length, H, diameter, D, the ratio of H to D is 1.5 and, with inlet and outlet manifolds at top and bottom ends, is shown in Fig. 6.1. The encapsulated spherical PCM spheres are randomly packed in the tank with porosity, e, through which the HTF flows.

6.6. Design Consideration

The thermal storage material can be chosen based on availability, cost, and compatibility. The major factors to be considered in the design of an LHTES unit containing a PCM include:

- The storage capacity of the tank
- The configurations of the transfer fluid.
- The type of heat transfer fluid.
- Temperature limits within which the units are to operate.
- The thermophysical properties of PCM

6.7. Models Employed in the Present Analysis

The following general assumptions are made in the formulation of the mathematical models

- The hot water thermal storage tank is insulated to reduce heat loss to the surrounding and Radiant heat transfer in the storage is neglected.
- The temperature of the HTF at the entry of the storage tank is equal to the exit of solar PTC.
- The thermal resistance of the encapsulation material is neglected
- The thermos-physical properties for both HTF and PCM were constant with respect to $T_{out.}$

- Both the PCM and the HTF should be chemically non-reactive with the encapsulation material
- The initial temperature of the storage was uniform and it was in melting temperature.
- The HTF entering inside was laminar flow and incompressible fluid
- The thermal conduction in the axial direction is neglected for both PCM and HTF.
- PCM at the same layer has the same temperature and is independent of radial position.
- The thermal resistance of the encapsulation material is neglected.
- The PCM spheres are identical
- There is no internal heat generation in the bed

In this study, a dual phase model for fixed HTF temperature, in which all the PCM capsules are considered to be a saperate domain, and the internal conductive resistance inside the individual PCM capsule and the conduction along the flow direction are considered

6.8. Governing Equations Thermal Energy Storage for Charging and discharging mode

The governing equations for the mathematical model for the HTF and PCM are respectively **(Shobo & Mawire 2015):**

$$\varepsilon \rho_f c_f \frac{\partial T}{\partial t} + \varepsilon \rho_f c_f \frac{\partial T}{\partial y} = \varepsilon \lambda_f \frac{\partial^2 T_f}{\partial y^2} - h_f (T_f - T_s) \text{.............(6.1)}$$

$$(1-\varepsilon)\rho_s c_s \frac{\partial T_s}{\partial t} = (1-\varepsilon)\lambda_s \frac{\partial^2 T_s}{\partial y^2} + h_f \left(T_f - T_s\right) \text{..................(6.2)}$$

The first term on the left-hand side of Equation (6.1), represents the rate of change of the internal energy of the HTF; the second term represents the net energy transported due to the HTF flow in the axial direction. The term on the right-hand side represents the heat transfer by convection between in Equation (6.2), the left-hand side represents the rate of change of the temperature of the PCM, and on the right-hand side, and the term represents the heat transfer by convection between the HTF and the PCM.

The Reynolds number is calculated as:

$$\mathrm{Re} = \frac{\rho_s d_p \varepsilon v_f}{\mu_f} \text{ ....(6.3)}$$

The Prandtl number is calculated using:

$$\mathrm{Pr} = \frac{c_f \mu_f}{\lambda_f} \text{ ....(6.4)}$$

The volumetric heat transfer coefficient is calculated as follows:

$$h_f = \frac{6(1-\varepsilon)*[2+1.1*\mathrm{Re}^{0.6}\,\mathrm{Pr}^{1/3}]\lambda_f}{d_p^{\ 2}} \text{ .... (6.5)}$$

The phase change within the encapsulated PCM is accounted for by the apparent heat capacity method. The PCM undergoes three stages during charging and discharging, namely:

solid stage, solid-liquid phase change, and liquid stage **(Shobo & Mawire, 2015).**

(a) During the solid stage, $T_s<T_{ml}$

$$c_s = c_{s2}; \rho_s = \rho_{s2}; \lambda_s = \lambda_{s2} \text{ .... (6.6)}$$

(b) During solid-liquid phase change, $T_{ml} <T_s<T_{m2}$

$$c_s = \frac{c_{s1}+c_{s2}}{2} + \frac{\gamma_{th}}{T_{m2}-T_{m1}}; \rho_s = \frac{\rho_{s1}+\rho_{s2}}{2}; \lambda_s = \frac{\lambda_{s1}+\lambda_{s2}}{2} \text{ ....(6.7)}$$

(c) During the liquid stage, $T_s>T_{m2}$

$$c_s = c_{s2}; \rho_s = \rho_{s2}; \lambda_s = \lambda_{s2} \text{ ....(6.8)}$$

Initial and boundary conditions

At time t = 0, $T_f = T_s = T_{initial}$ for $0 \le y \le H$,

At time t > 0, $T_f(0, t) = \frac{dT_S}{dy} = 0$ for y=0

$\frac{dT_f}{dy} = 0; \frac{dT_S}{dy} = 0$ for y=H

6.8.1. Discretization

The equations (6.1-6.2) for the HTF and the PCM are discretized by the explicit finite difference scheme. The forward difference approximation for the time derivative and the central difference approximation for the space derivative is used. In particular, the convective term of the HTF equation is resolved by the upwind (or backward difference) scheme, as the flow in the axial direction is convection-dominated. The discretized equation of the HTF and PCM are solved simultaneously, for the new values of the temperature of the HTF and the temperature of the PCM at an increasing time step. The above calculation is repeated by considering this new set of temperature values as the present values for finding the temperature in the next time step. The simulation is continued until the temperature of the HTF and the PCM at all the nodes of the storage tank reach the inlet temperature of the HTF. The discretized form of the equation for the HTF at any interior nodes of the storage tank is

$$\varepsilon\rho_f c_f\left(\left[\frac{T_{f_i}^{n+1}-T_{f_{i-1}}^{n}}{\Delta t}\right]+v_f\left[\frac{T_{f_i}^{n+1}-T_{f_{i-1}}^{n}}{\Delta y}\right]\right)=\left[\varepsilon\lambda_f\left(\frac{T_{f_{i+1}}^{n+1}-2T_{f_i}^{n}+T_{f_{i-1}}^{n}}{\Delta y^2}\right)-h_f\left(T_f^n-T_s^n\right)\right]\ldots.(6.9)$$

The discretized form of the equation for the PCM at any interior nodes of the storage tank is,

$$(1-\varepsilon)\rho_s c_s\left(\left[\frac{T_s^{n+1}-T_{s-i}^{n}}{\Delta t}\right]\right)=\left[(1-\varepsilon)\lambda_s\left(\frac{T_{s_{i+1}}^{n+1}-2T_{s_i}^{n}+T_{s_{i-1}}^{n}}{\Delta y^2}\right)+h_f\left(T_f^n-T_s^n\right)\right]\ldots\ldots(6.10)$$

6.9. Quantity of heat stored

The quantity of heat, Q_{pcm}, stored in an elemental volume of the PCM is calculated by:

$$Q_{pcm,solid}=\rho_{s1}c_{s1}(1-\varepsilon)V_{elem}(T_{m1}-T_{initial})\ldots\ldots\ldots(6.11)$$

For the sensible heat from initial temperature (T_{intial}) to the commencement of phase change,

where is the volume of the element of PCM at a height in the storage tank?

$$Q_{pcm,latent}=\rho_{s1}(1-\varepsilon)V_{elem}\lambda_{fu}\ \ldots\ldots\ldots\ldots\ldots\ldots\ldots\ldots\ldots\ (6.12)$$

Where λfus [J/kg] is the latent heat of phase-changing material. For phase change.

$$Q_{liquid}=\rho_{s2}c_{s2}(1-\varepsilon)V_{elem}(T_{final}-T_{m2})\ \ldots\ldots\ldots\ldots(6.13)$$

Where, Q_{pcm} is the amount of energy stored in PCM, $Q_{pcm,}$ is the amount of energy stored in solid PCM, $Q_{pcm,}$ is the amount of energy stored in the PCM latent phase and $Q_{pcm,}$ is the amount of energy stored in the liquid phase

6.10. Sizing of Packed PCM Capsules Thermal Storage and Quantifying amount of PCM

To model the size of a Packed PCM capsules thermal storage, the amount of energy demand

used for biogas digester and mass flow rate of hot water circulates in the system should be known. For the sensible heating from the end of phase change to final temperature (T_{final})

of the PCM in the element. The total heat that can be stored in the thermal energy storage device can be calculated by summing the heat stored at different stages.

The amount of energy stored in the packed PCM capsules is given as:

$$Q_{pcm} = Q_{pcm,solid} + Q_{pcm,latent} + Q_{pcm,liquid} \quad \text{……………………..(6.14)}$$

Therefore, energy stored in the packed PCM capsules sums up can be given as **(Dejene, 2020):**

$$Q_{pcm} = \int_{T_{init}}^{T_m} m_{pcm} c_{ppcm,s} dT + m_{pcm} \Delta h_{fus} + \int_{T_{init}}^{T_m} m_{pcm} c_{ppcm,l} dT \quad \text{...(6.15)}$$

Where, $mpcm$ is mass of PCM, $cppcm,s$ specific heat capacity of PCM for solid-state, $cppcm,l$ is the specific heat capacity of PCM for the liquid state, ρpcm is the density of PCM and Δhm is change enthalpy in the latent phase.

$$m_{pcm} = \rho_{pcm} V_{st} (1-\varepsilon) \quad \text{…………………….……………(6.16)}$$

From equation **(6.14)**, the volume of the storage tank can be determined as:

$$V_{st} = \frac{E_{store,in\ \mathrm{pcm}}}{\int_{T_{init}}^{T_m} \rho_{pcm}(1-\varepsilon) c_{ppcm,s} dT + \rho_{pcm}(1-\varepsilon)\Delta h_{fus} + \int_{T_{init}}^{T_m} \rho_{pcm}(1-\varepsilon) c_{ppcm,l} dT} \quad \text{…(6.17)}$$

The length of storage as a function of its diameter can be given as:

$$D_{st} = \sqrt{\frac{4V_{st}}{\pi L_{st}}} \quad \text{……………………………………………(6.18)}$$

Know the diameter of the capsule; the number of PCM capsules required for the storage can be given as;

$$n_{pcm,capsules} = \frac{6(1-\varepsilon)V_{st}}{\pi d_{pcm}^3} \quad \text{………………………………. (6.19)}$$

Where d_{pcm} is the diameter of PCM and $n_{PCM,}$ is the number of PCM capsules.

The amount of PCM is determined based on thermophilic anaerobic digester energy demand to maintain the desired level of temperature. The mass of PCM requires is calculated using equation (6.15) and the Volume of PCM is given as:

$$V_{PCM} = \frac{m_{pcm}}{\rho_{pcm}} \quad \text{……………………….………..………(6.20)}$$

CHAPTER 7: RESULTS AND DISCUSSIONS

7.1. Thermophilic Anaerobic Digester Thermal Simulation Result

A thermophilic anaerobic digester has been designed to maintain 60ºC (333.15 K). For a digester to maintain a desired level of temperature it is important to calculate the temperature drop of the digester, to determine the energy requirement of digester that can operate at the desired temperature range. The Temperature drop is occurred due to heat is lost from the inflow digestate to digester at surrounding temperature, from digestate leaving at the digester operating temperature, the heat lost through the boundaries of the digester. Assuming at morning (6:00 AM) the digester is at desired level temperature (333.15 K).

Below the average daily temperature drop of a digestate for the representative days of each month is presented in Figure.7.1.It can see that the highest temperature of digestate drop by 5.45 K in June and the smallest value of temperature drop occur in February by 4.95 K. Similarly ,temperature drop digester cover (Figure.7.2) the minimum average daily temperature drop of cover occurs in February (3.453 K) and a maximum temperature drop occurs in June (4.237 K).

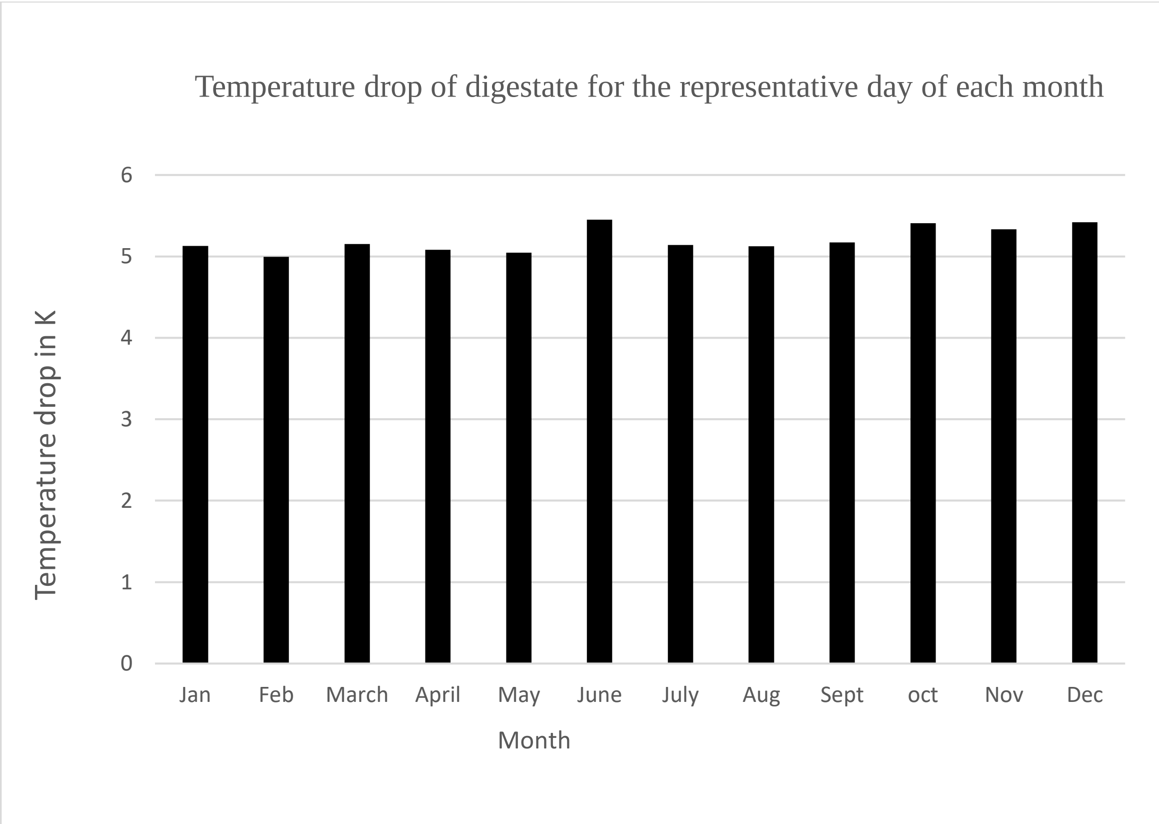

Figure 7. 1: Daily average temperature drop of digestate for the representative day of each

month.

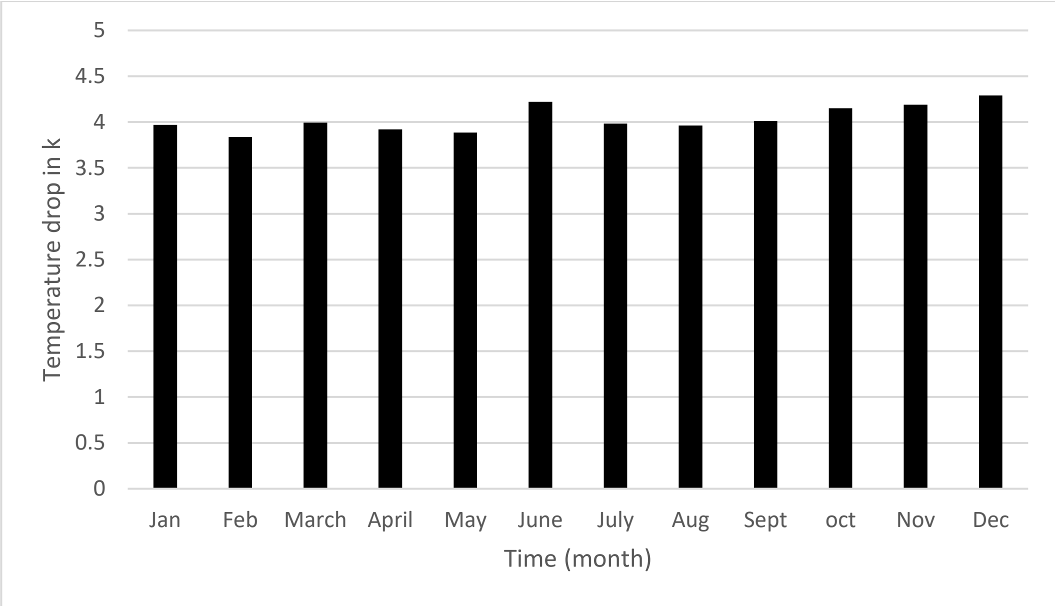

Figure 7. 2: Daily average temperature drop of cover for the representative day of each month

7.2. Heat Requirement

The heat requirements considered were the heat losses of the digester and the heat necessary for raising the incoming sludge temperature. The heat losses have to be calculated on a monthly basis since the outside temperature varies throughout the year. For the calculation, the monthly average outside temperature has to be considered. For our calculations, the 10-year average (2011–2020) monthly average temperatures for Bale Robe were considered (Table 4.1).

7.2.1. Total heat requirement

The total heat loss of the digester is determined from the temperature drop of the digester. Figure 7.3 represents the total energy loss from the anaerobic thermophilic digestion system through the representative day of each month.

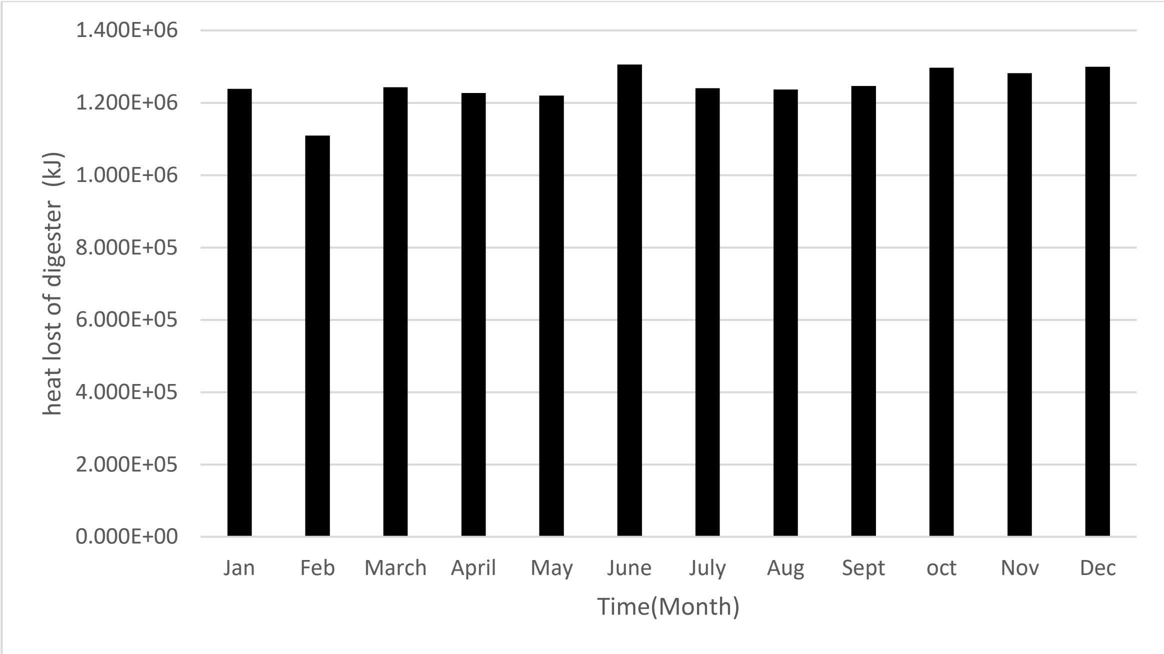

Figure 7. 3: Total energy loss from the digester throughout the representative days of each month

From the above figure, total energy demanded by the digester to maintain the desired temperature level varies 1.109867*10^6 kJ/day on (2^{nd}) month (February) to 1.306175*10^6 kJ/day on the (6^{th}) month (June).

The annual average daily heat requirement of digester:

$$Q_{demand} = \frac{(1.109867+1.306175)*10^6 \frac{kJ}{day}}{2} = 1.208021*10^6 \frac{kJ}{day}$$

7.2.2. Heat Energy required raising the sludge Temperature to the desired level

The heat needed to raise the sludge temperature to the operating temperature (in this case 60 °C); the following equation was used **(Zupančič & Roš, 2003).**

$$Q_{sludge} = \dot{m}_s * C_{ps}(T_s - T_{so}) \ldots\ldots\ldots\ldots\ldots\ldots\ldots\ldots\ldots\ldots(7.1)$$

Where:

- M_s., Mass flow of inflow sludge (kg/day)
- Ts, Temperature of sludge in the digester (60°C)
- T_{so}, Minimum sludge temperature entering the digester on average monthly basis, presented in Table 4.1

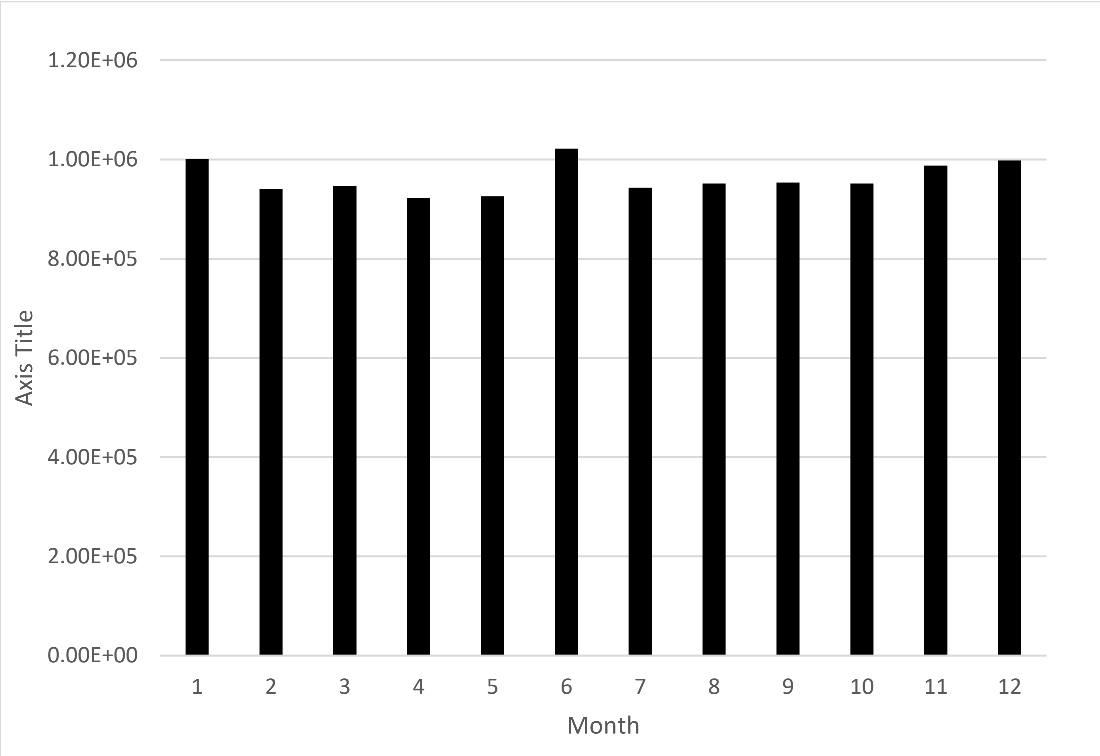

Figure 7. 4: Energy loss from the digester throughout the representative day of each month without considering energy losses through the boundaries of the digester

The percentage of the digester heat losses (compared to sludge) presented below:

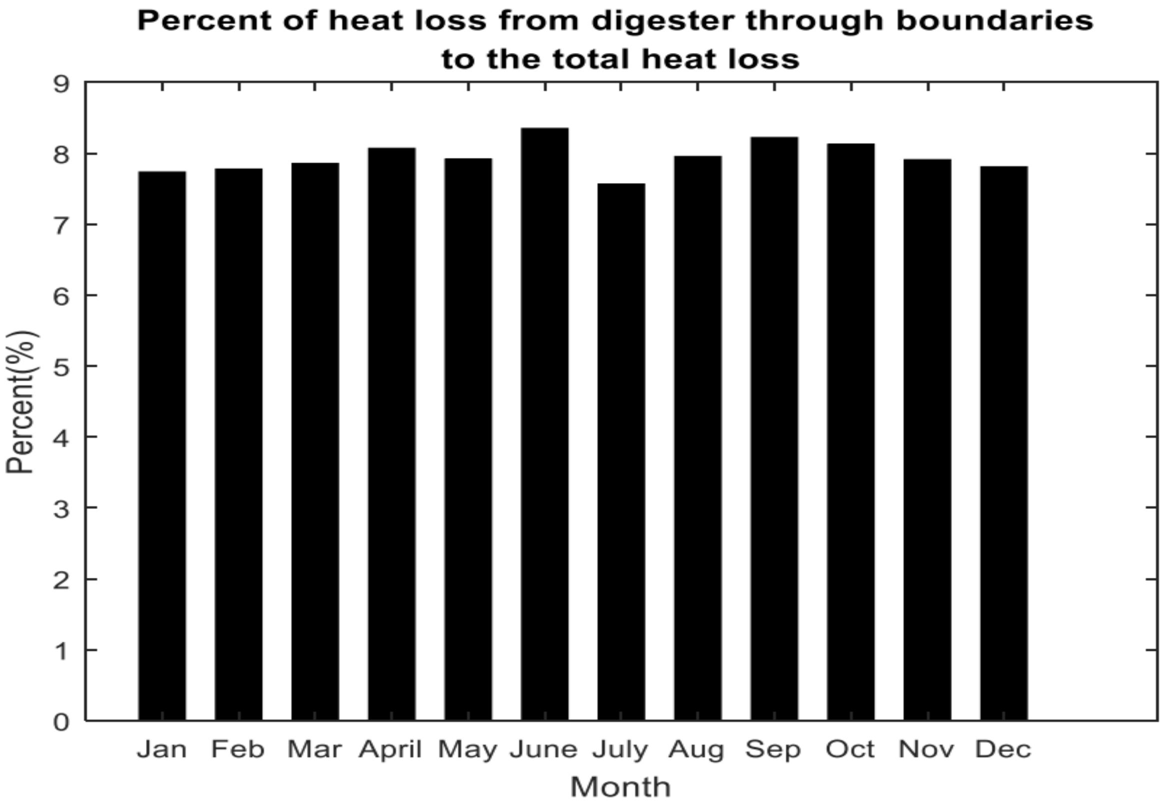

Figure 7. 5: Percent of energy loss from the digester through boundaries to the total energy loss.

From the result, we can conclude that the major part of the energy requirement is used to compensate for the energy loss from the digester by incoming digestate. The energy losses through the walls of the digester are only accounted for 7.65% to 8.7% of the total energy requirement of a digester.

7.2.3. Heat transfer between digestate and Heat exchanger

Below the monthly average heat transfer between digestate and Heat exchanger

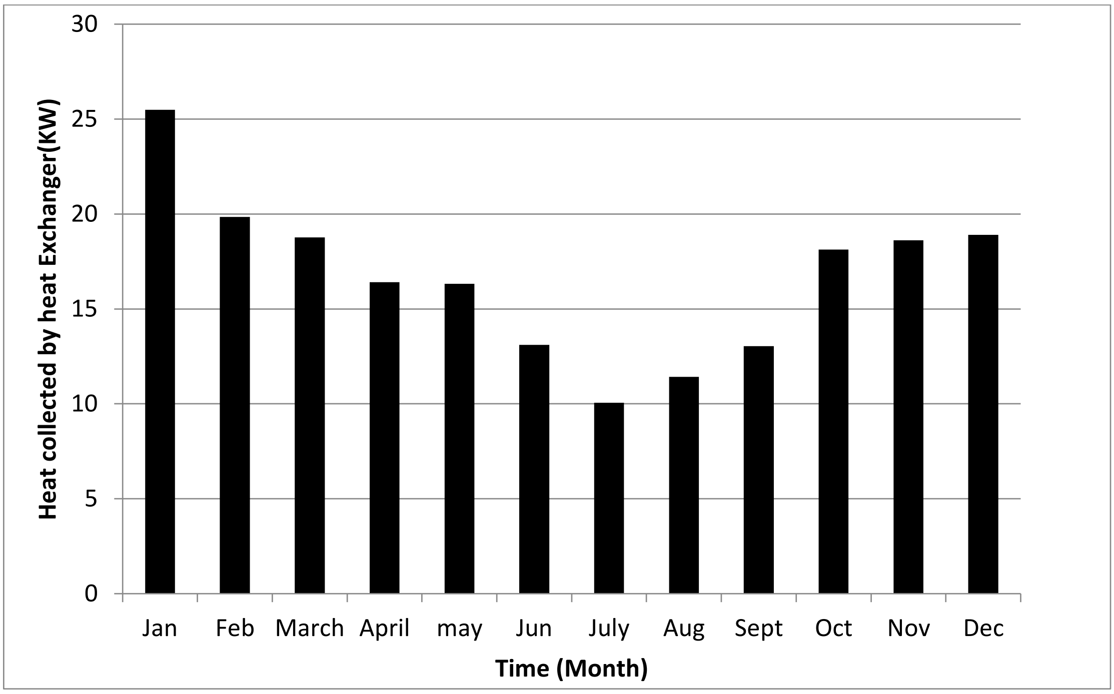

Figure 7. 6:Heat transfer between Digestate and Heat exchanger

Figure 7.6 show that amount heat that delivered to digestate to maintain at given temperature. Average heat is 17.7 kJ/sec

7.2.2.1. Validation

According to **(Zupančič & Roš, 2003)** experiment results of heat and energy requirements in thermophilic anaerobic sludge digestion. The results it is evident that the digester heat losses affect the heat requirements very little. At a certain size of the digester, the heat losses are a small proportion of heat requirements, from only 2–8.5%. Experimental results have a good agreement with the numerical result of this work. There is little variation raised from the desired level temperature of two works, geographical location and weather condition, Slurry for digestion. Take into consideration the difference between, these numerical simulations, the heat losses account for 7.65 –8.7% of the total heat requirement of a digester.

7.3. Hourly Beam Incident Solar Radiation on Horizontal Surface and PTC simulation results

From developed PYTHON code and Excel simulation solar radiation that used as an input variable for thermal and optical analysis of parabolic trough solar collector. Figure 7.6. Show that the maximum and minimum horizontal beam solar radiation that hit the ground surface over 12 months of the selected location of study. From the chart, it is seen that maximum and minimum power is received in October 4.58 KWh/m^2 and July 2.798 KWh/m^2 respectively.

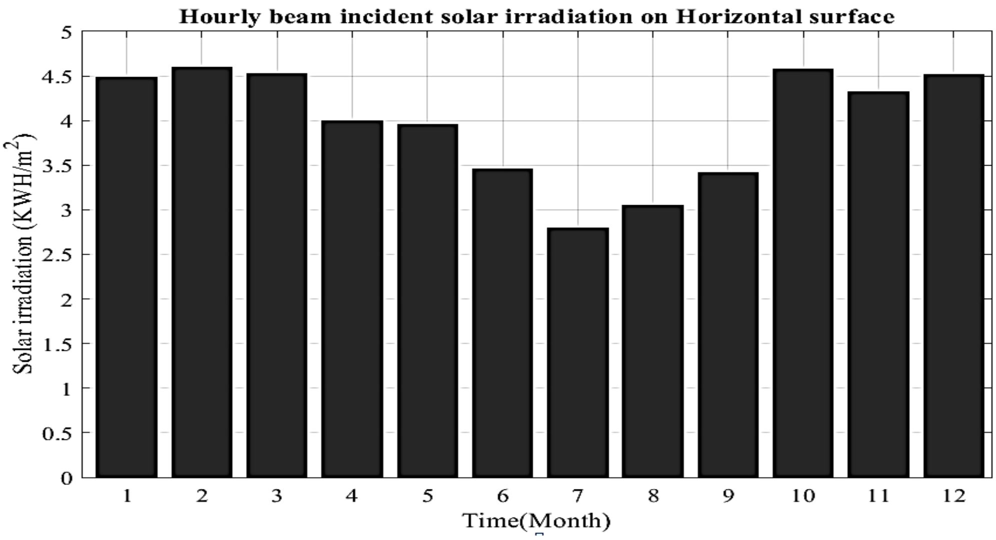

Figure 7. 7: monthly beam incident solar irradiation on Horizontal surface

Similarly, the hourly beam solar radiation on the horizontal surface on the horizontal surface varies significantly with the months of the year. The hourly beam incident solar radiation on a horizontal surface for the winter season is shown in Figure 7.7. The winter season shows that that higher beam solar radiation is received by the horizontal surface. Beam solar radiation for the others season is presented in ANNEX –A.1

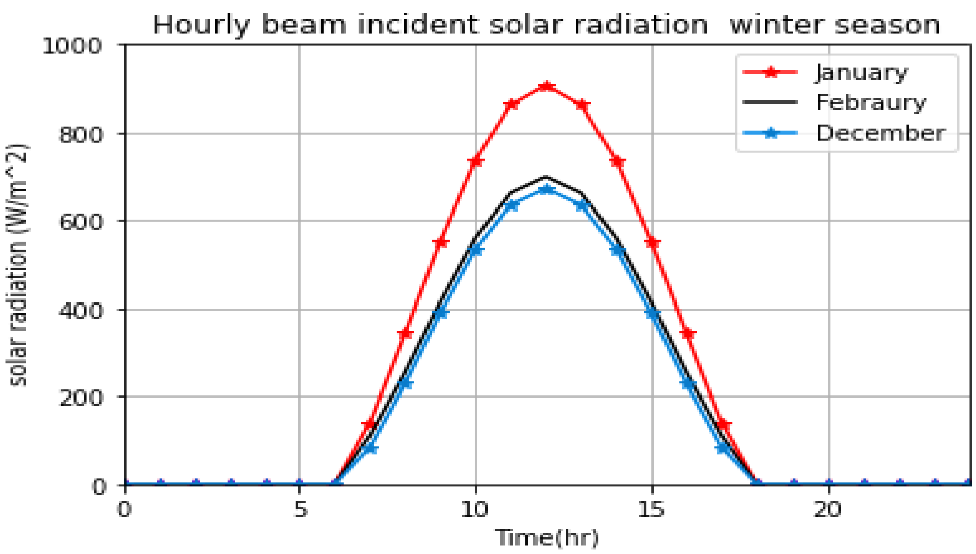

Figure 7. 8: Hourly beam incident solar radiation on Horizontal surface for the winter season

7.4. Variation of Outlet Temperature PTC

PYTHON transiently simulates the heat transfer fluid outlet temperature variation throughout the day for different seasons to find the outlet temperature of HTF. Based on hourly beam solar radiation incidence on the PTC, below the result of simulation of outlet temperature variation for the winter season is presented and other seasons presented ANNEX-A.2.

As shown in Figure, 7.8 show that outlet temperature of HTF can reach above 360 K, during solar radiation available. On the day, time the PTC starts to absorb solar radiation throughout the day start from sunrise to sunset hours. The fluid temperature continuously rises from sunrise to noontime and reaches a maximum at noon, then decreases continuously up to sunset hour.

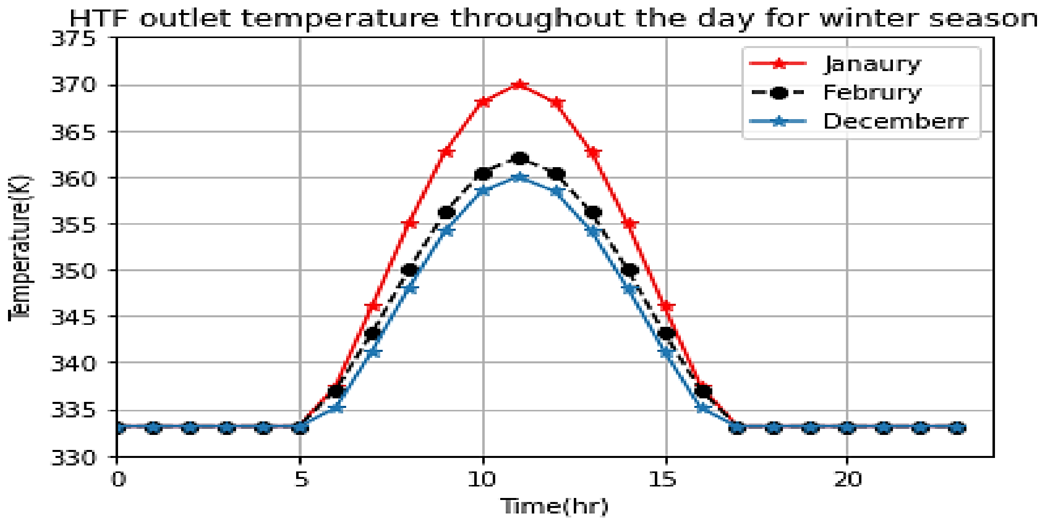

Figure 7. 9: HTF outlet temperature throughout the day of the winter season

7.4.1. PTCs modal validation of outlet Temperature

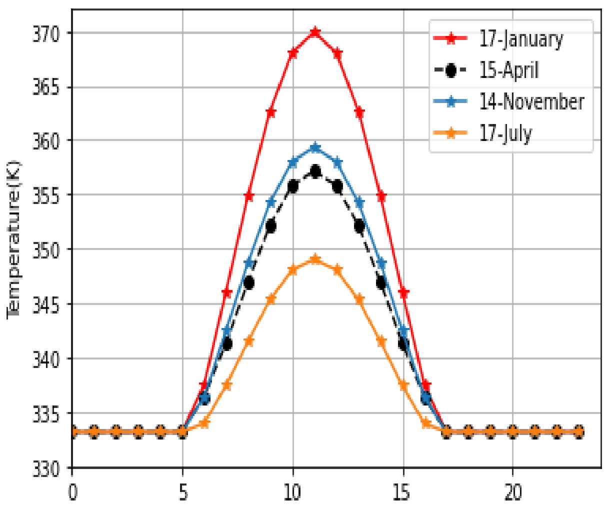

Figure 7. 10: HTF at the output of the on four day of year

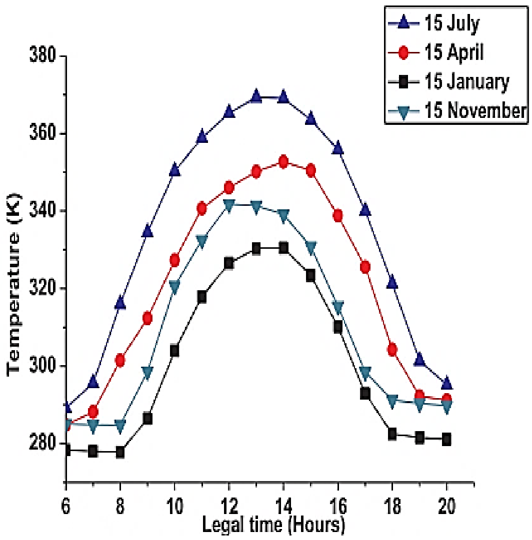

Figure 7. 11.Water temperature variation at the output of the absorber tube on four **(Lamrani et al., 2018)**

Figure 7.9 showed that water temperature variation at the output of the HTF on four days of the year. The simulation result by **Lamrani et al., (2018)** slightly agree with result found in this study. The same characteristics of the solar PTC are used in the present numerical model and obtained results show that results are in good agreement with numerical results (Figure 7.10). This study consider that these results validate to numerical model and the methodology that used developed. Therefore, it can be applied to this study of the thermal performance of the solar PTC under different operating conditions.

7.5. Instantaneous useful heat gained by PTC

Instantaneous Useful heat gained by collector calculated based on the thermal model developed. The result shows that it varies significantly from season to season. As it can be seen from Figure 7.11, instantaneous useful heat gained for a given day is maximum at solar noon. The instantaneous useful heat gained for winter are presented.

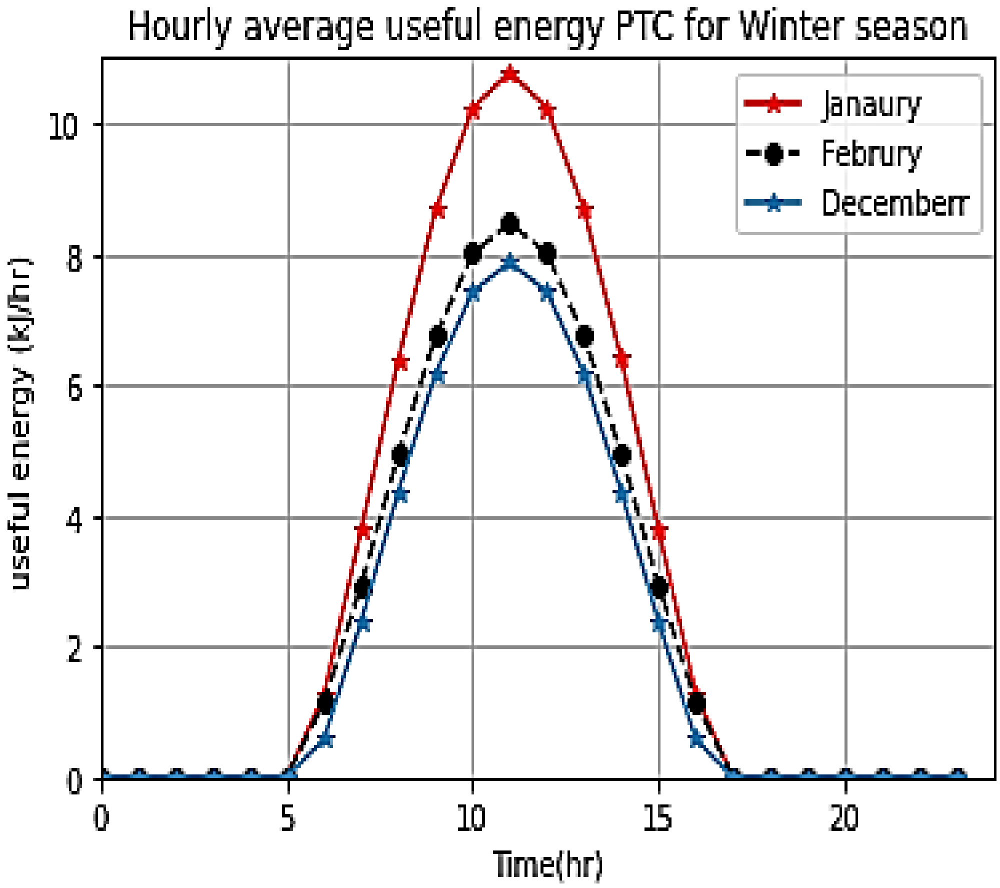

Figure 7. 12: Hourly average useful energy collected from a unit PTC during the winter season

7.6. Optical and Instantaneous thermal efficiency of PTC

Using the optical model developed in chapter 5 the maximum and minimum optical the efficiency of the collector calculated is equal to 0.76 and 0.697 respectively. Figure 7.12 indicates that lowest and highest efficiency observed during June and January respectively.

The instantaneous thermal efficiency of a PTC was analyzed from the instantaneous useful heat gained rate of a collector and the instantaneous total amount of beam solar radiation incidence on the collector surface. Figure 7.13 Instantaneous efficiency variation of a PTC from sunrise to sunset for January 17 is presented below.

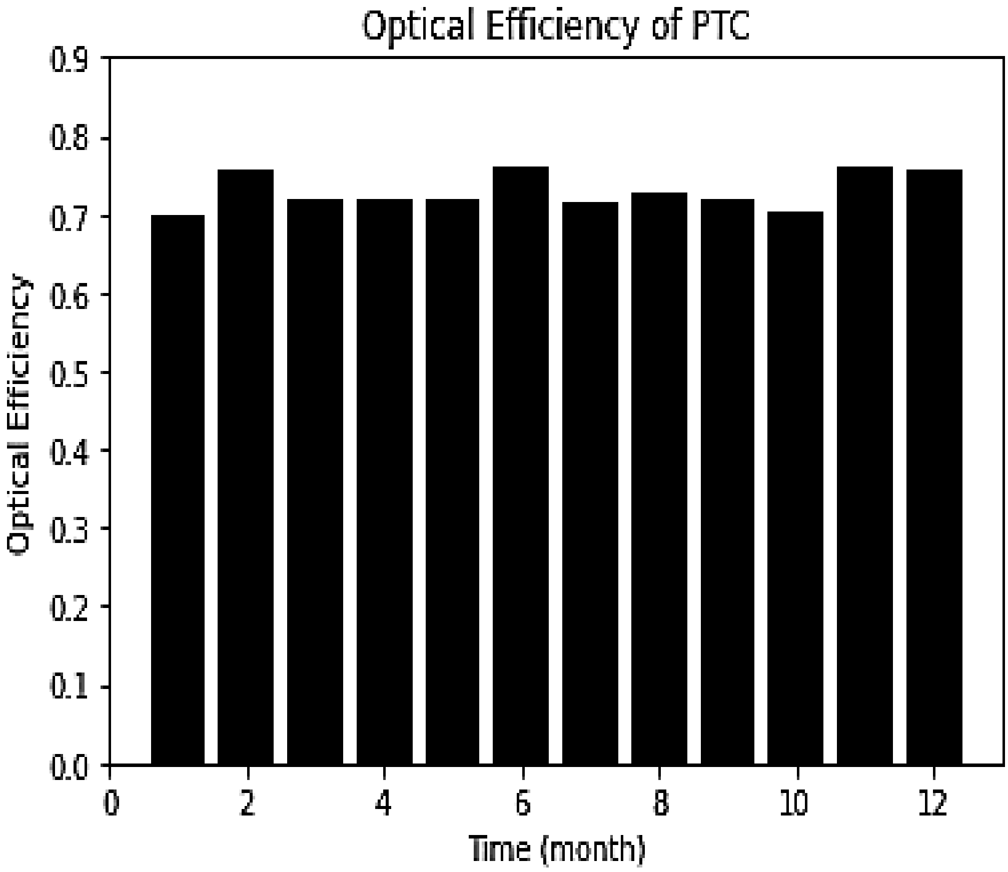

Figure 7. 13: Daily optical efficiency of the PTSC for representative days of each month

The result indicated that the lowest instantaneous thermal efficiency of a PTC occurs at sunrise and sunset hours in January. From figure 7.13, the highest value of efficiency occurs around noontime; because the sun comes to the overhead of the surface, due to this the major, part of the radiation is beam radiation.

7.6.1. Model validation Instantaneous thermal efficiency of PTC

Figure 7.13**,** shows the hourly thermal efficiency of the solar PTC. **(Lamrani et al., 2018)** thermal efficiency is maximum on 15 July and can reach 76.4%. During the winter, maximal value observed is about 69%. These results are corroborated by those of the hourly evolution of the solar flux received by the solar HTF. The same characteristics of the solar PTC are used in the present numerical model and obtained results show that results are in good agreement with numerical results (figure 7.15).

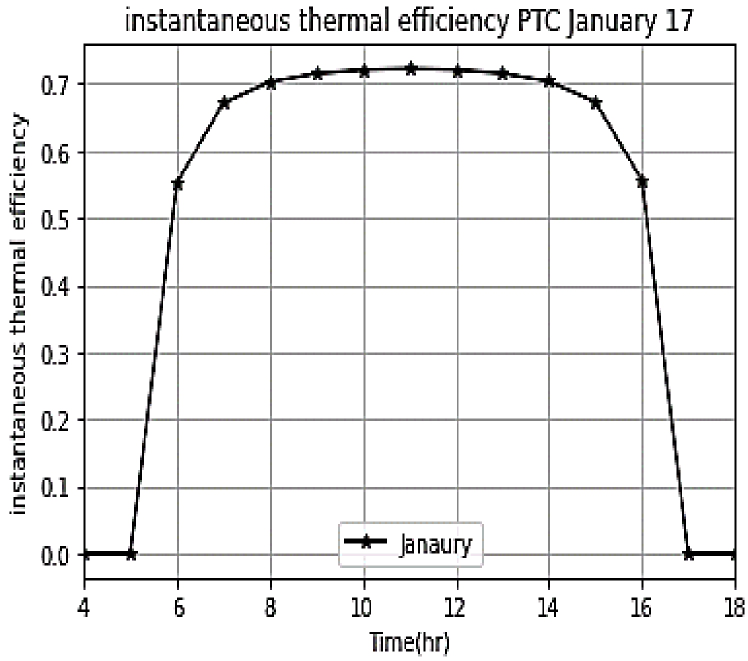

Figure 7. 14: Instantaneous efficiency variation of a PTC for January 17

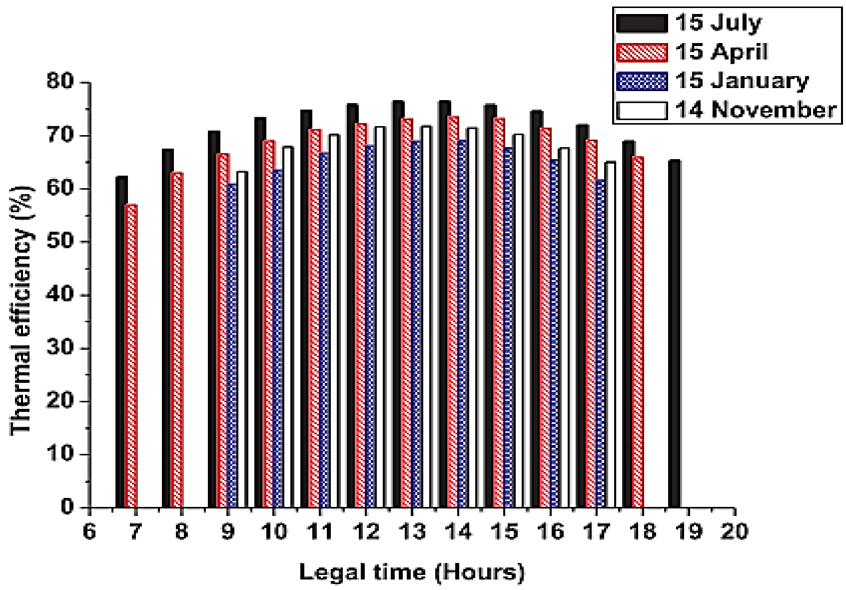

Figure 7. 15: Concentrator thermal efficiency on four days of the **year (Lamrani et al., 2018)**

7.7. Daily Average Useful Energy useful heat production of a unit collector

The total amount of energy that can be collected by a unit PTC throughout the day is analyzed for representative days of months. Below, the daily average useful energy collected by a unit PTC in different months is presented.

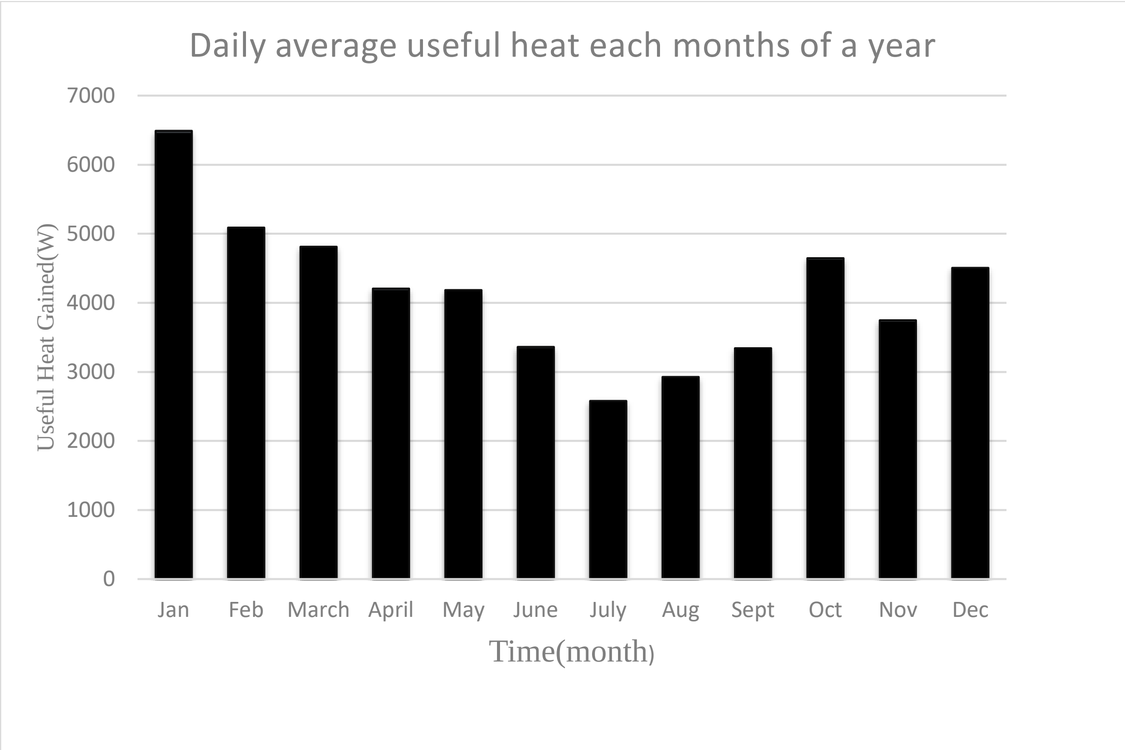

Figure 7. 16: Monthly average daily average useful energy collected by a PTC

Base on the result as shown in Figure 7.15, the average monthly instantaneous energy collected by the PTC varies from 6.5 kW in January to 2.6 kW in July. This is due to the significant difference in available solar radiation in these months. The annual average useful energy collected by a PTC is 4.157 kW.

7.7.1. Sizing of Parabolic Trough Solar Collectors

The average useful energy gained from PTC is variable for each month of the year. Therefore, the sizing of the PTC system is on basis of the average annual useful energy collected by PTC. In order to calculate the desired number of PTC, specifications in (Table 5.1) are considered as constant. The number of collectors required is calculated from the results, as shown above, 5 units of PTC are required to fulfill the average daily energy requirement of the digester. Since a single collector can meet the maximum, temperature and gain demanded thermal energy all PTC have to arrange in parallel. The total mass flow rate of heat transfer fluid is 0.35 kg/s.

7.8. Temperature Variation of Phase Changing Material on charging and discharging process.

MATLAB PDE solver is used to solving the two-coupled parabolic partial differential equation. The two-coupled parabolic equations (6.1) and (6.2) were solved simultaneously for new values of the temperature HTF and PCM at increasing time steps.

Charging mode: Initially, the temperature of the PCM and HTF in the bed was set at a constant 25ºC. The HTF entering was at a constant 80ºC. The charging process occurs for 9.4 hours' time duration, for the first 2.1 hours only a sensible heating process occurs. The phase-changing process occurs within a narrow temperature range (1-1.5ºC). This process occurs for 6.8 hours' time duration. After the phase, the changing process completes, a sensible heating process continues for a half-hour (figure 7.16).

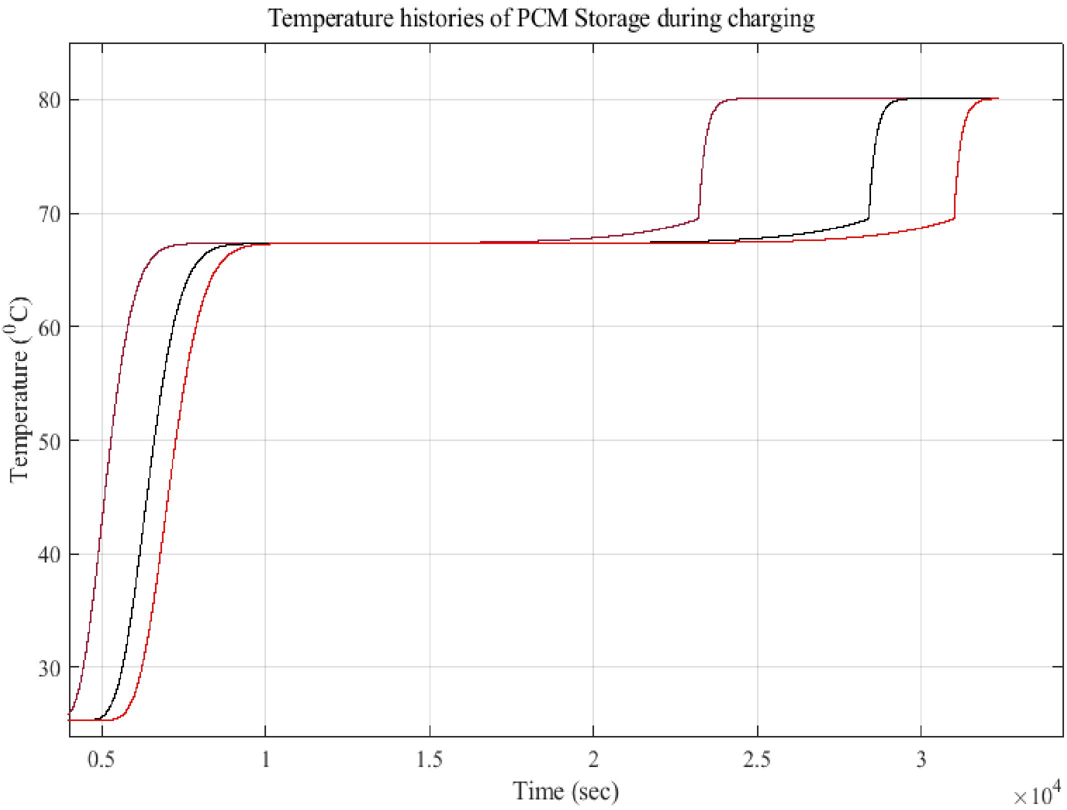

Figure 7. 17: Charging process temperature variation of phase-changing material for January 17

Discharging mode: Initially, the storage tank is assumed as a fully charged state, at 80ºC when t > 0, the temperature of the PCM and HTF at 80ºC. The cold fluid at 32°C flow from bottom of bed to the top to extracted heat energy. Figure 7.17 represents the temperature histories of PCM during discharging process. It is seen from the figure that the temperature drop is large until the PCM reaches its phase transition temperature as the hot water in the storage tank loses its sensible heat due to the mixing of inlet water at a temperature of 32°C. Figure 7.17 shows the temperature profile of PCM at particular locations. It is obviously seen that PCM undergoes three stages during discharging process. There are liquid sensible heat release, solidifying latent heat release and solid sensible heat release. The PCM temperature decreases rapidly at liquid sensible heat release stage, then it decreases slowly at temperature range of phase change until the solidifying process terminates. After the temperature range of phase change, the temperature decreases rapidly to reach the temperature of HTF at particular location as shown in figure 7.17.The discharging process is completed when the temperature of PCM is equal to the temperature of HTF.Result implies that the closer to the outlet location the longer the time required for fully discharged.

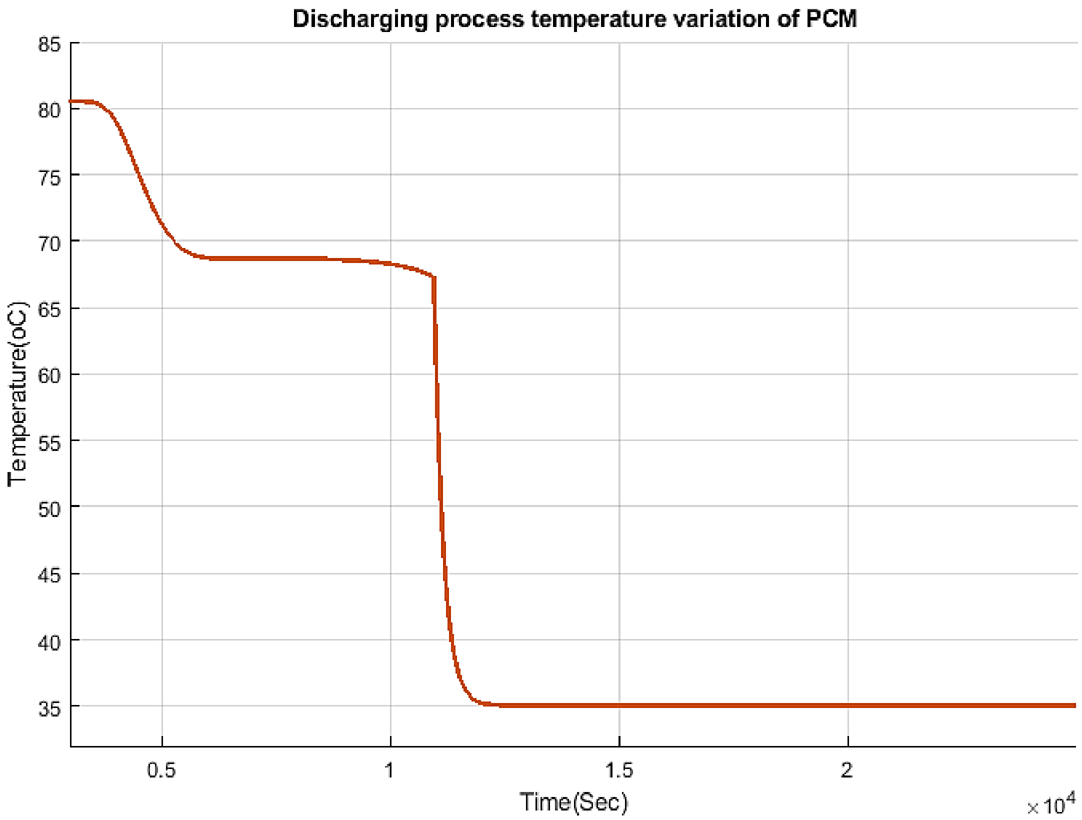

Figure 7. 18: Temperature histories of the PCM during Discharging January 17

To satisfy the heat demand of thermophilic anaerobic digester to maintain at desired temperature Level and produce biogas that demanded by 50-house holders for their cooking and lighting the size of PCM rectangular storage tank with height 3.04m and diameter of 2.03m is required. The spherical capsule with a diameter of 0.08m and porosity 0.5 through which the heat transfer fluid flows. The total number of spherical capsules required to store the desired quantity of heat was 18035.3. The result showed that 4.9m^3 of phase change material (paraffin Wax) required storing the energy consumption of digester for 16.5 hrs.

7.8.1. Model Validation

The selected numerical method that MATLAB pde computer code is validated against experimental by **Nallusamy et al. (2007)** and numerical simulation by **(Gao et al., 2020).**In order to validate the accuracy of the mathematical model, the experimental results of Nallusamy et al. (2007) are used for numerical simulation results. In the experimental system, the volume of the packed bed heat storage tank is $0.047 m^3$ the PCM is paraffin, the HTF is water, and the diameter of the packing ball is 55 mm. At three packed bed positions of *x*/*L*= 0.25, *x*/*L*= 0.75, and *x*/*L* =1.00, the change of PCM temperature is consistent with the temperature curve in the literature the same over time (Figure 7.18). Similarly, this numerical result was again validated against the numerical simulation results of **Gao. et al. (2020)** is used. In this numerical study, they investigated the effect of key design parameters on the thermal performance of the packed bed heat storage device. In their numerical simulation study of the temperature variation of initial (T_{ini}) and inlet (T_{in}), (303–323) K and (333–363) K, respectively, Mass flow rate (*m*) 20–40 L/min, and Sphere diameter (*D*c) 40–100 mm. The effect of sphere diameter result is used for validation figure 7.19. **(Xu et al., 2015)** in this work the discharging time of packed bed thermal storage tank is found by trial numerical simulation for industrial purpose figure 7.20.Result found during discharging process of this work has good agreement figure 7.17.

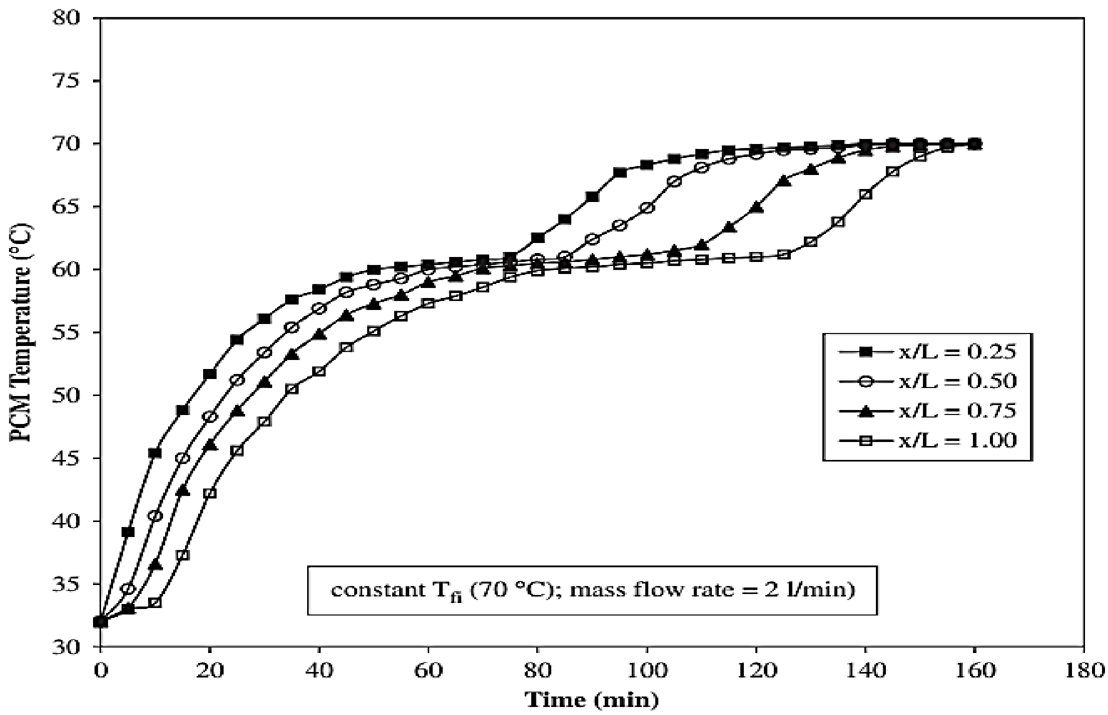

Figure 7. 19: Temperature histories of PCM during the charging process **(Nallusamy et al. 2007)**

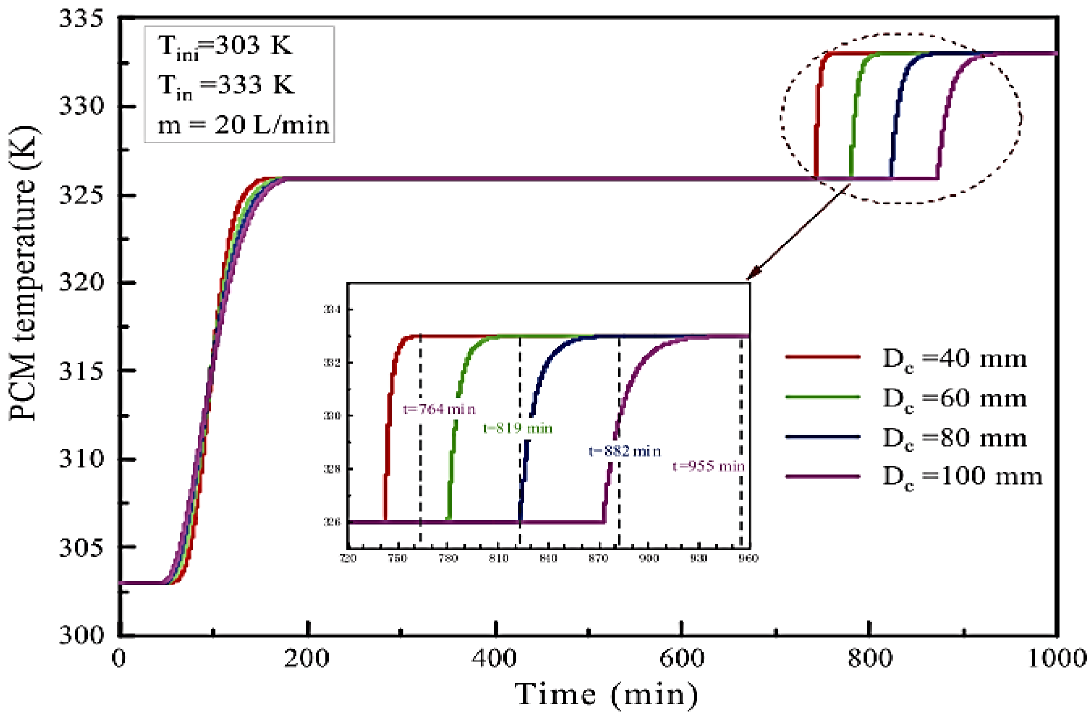

Figure 7. 20: Temperature histories of the PCM (Numerical simulation result) (**Gao et al., 2020).**

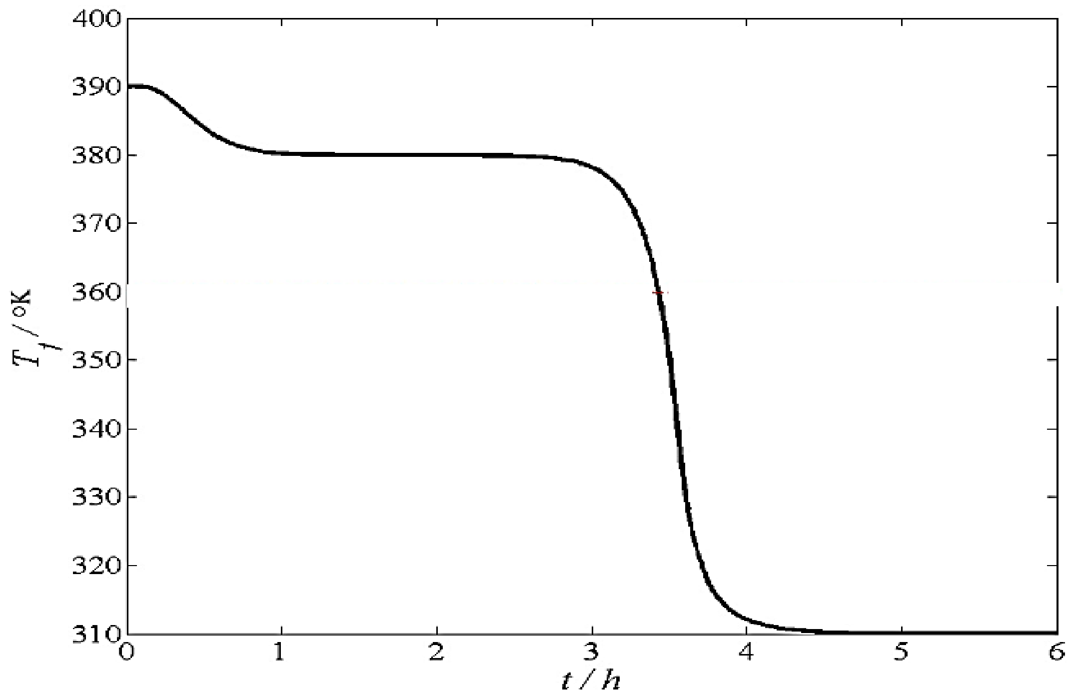

Figure 7. 21: Temperatures of PCM discharge based on the height of tank **(Xu et al., 2015)**

8. CONCLUSION, RECOMMENDATION, AND FUTURE WORK

8.1. Conclusion

In this study, a thermophilic anaerobic digestion system enhanced by PTC integrated with thermal storage to produce biogas consumed by 50-house holders round Bale Robe town. The necessary solar radiation and other weather data of Robe Town were obtained using the Ethiopian Metrology Agency (Adama). A 51 m^3 anaerobic system is heated by circulating hot water thermal storage tank heated by 5m length and 3.4 m length PTC**.** The numerically thermal performance of each system was evaluated based on the solar radiation received at the site as well as other climatic conditions such as ambient temperature.

The production of biogas is highly dependent on fermentation Temperature inside the digester. The overall biogas yield increase with the increase of operating temperature of anaerobic digestion system with perspective operating range (Thermophilic range in this case).To increase or maintain the desired level of temperature of the digestion system auxiliary source of energy can be applied. Solar energy for heating anaerobic digestion can be used as an auxiliary source of energy and solar energy could capable and environmentally friendly approach for anaerobic digester. The combination of solar energy and biogas production represents a kind of solar energy storage in the form of fuel gas. However, contrary, the incorporation of solar energy in the anaerobic digestion process may affect the process stability, which results from the daily fluctuations of the variable energy. Solar energy storage is a key issue to be addressed the intermittence of solar energy. Packed bed solar thermal energy storage with phase change material has a higher energy storage density and energy storage at constant temperature or within a small temperature range. Therefore, integrating a solar-assisted anaerobic digestion system with packed bed solar thermal energy storage with phase change material has a higher advantage in biogas technology.

In this study, the thermal performance of thermophilic anaerobic digestion enhanced by PTC system integrated paraffin wax latent thermal energy storage was studied. One dimensional heat transfer model of each system was developed. PYTHON code, MATLAB were used as numerical solvers, and those numerical results were validated by the experimental and numerical study of the previous researcher.

To determine the heat required by the digestion system, initially assumed the digester is at the optimum temperature of thermophilic condition. Simulation of partial differential equation energy balanced of each phase is solved using (ODE integrator) PYTHON Script in which return the result in 24 hr. The result showed that the highest temperature of digestate drop in June and the smallest value of temperature drop occur in February. Similarly ,temperature drop digester cover (Figure.7.2) the minimum average daily temperature drop of cover occurs in February and a maximum temperature drop occurs in June This drop is accounted for total heat lost from digestate varies $1.109867*10^6$ kJ/day on (2^{nd}) month or February to $1.306175*10^6$ kJ/day on the (6^{th}) month (June). The average heat delivered by heat exchanger is 17.7 KJ /sec. The main energy requirement is used to compensate for the energy loss from the digester by incoming digestate. The energy losses through the walls of the digester are only accounted for 7.63% to 8.7% of the total energy requirement of a digester

A one-dimensional model was developed to analyze PTC. A transient mathematical model was developed and solved using a finite difference method implemented by using the PYTHON code script the average monthly instantaneous energy collected by the PTC varies from 6.5W in January to 2.6 kW in July and 70.5 % instantaneous thermal efficiency in January. To replace the total heat energy requirement of digestion to be maintained at the desired level of temperature, 5 PTC units with 0.35 kg/s total mass flow rate is needed.

The charging and discharging mode of latent heat thermal storage system, the transient analysis of heat transfer is solved by developed MATLAB pde solver script.From this, we can conclude that 5 units of PTC with 4.9 m^3 of PCM can fulfill the energy requirement of the digestion system that is responsible for producing biogas for the energy consumption of 50 –householders for their cooking purpose and lighting per day.

8.2. Recommendation

The average monthly instantaneous energy collected by the PTC during July and August is less than the energy demanded by the thermophilic anaerobic digestion system. From figure 7.15 solar radiation, intensities reach the horizontal surface less due to seasonal weather conditions. To maintained temperature, thermophilic anaerobic digestion the following point will be recommended:

- Add one more parabolic trough solar collector to the system, which can fulfill all demanded heat energy.

- Applying another auxiliary source of energy to systems to be maintained at the desired level.

8.3. Future Works

The following points are recommended for future work:

- During the heat transfer model of the thermophilic digester, the same assumption was considered to reduce the mathematical complexity, but it will reduce the exactness of the result. The same work can be carried out by considering that assumption during heat transfer modeling of the digester.
- The thermo-physical property of PCM is taken as constant to simplify the study with the loss of some accuracy. The study by considering the variable property is considered as another possible future work.
- Studying the TES system with consideration of thermal loss to the environment can increase the accuracy of the model.
- On this work the effect of PCM on the temperature outlet of PTC and heat gain not included. So, Temperature and Heat Gain effect on PTC with PCM and without PCM may considered as future study
- Addition to what to done detail and experimental study will carry out on charging and discharging process of phase change material
- Cost analysis of the overall system can be used for future commercialization and financial feasibility.

References

Abebe.Ch, A., & Ababu Gemeda, B. (2018). Estimating Global Solar Radiation in Bale Robe Town Using Angstrom-Prescott and Hargreaves-Samani Models. *Ournal of Energy Technologies and Policy*, *8*(8), 14–40.

Alkhamis, T., El-khazali, R., Kablan, M., & Alhusein, M. (2000). Heating of a biogas reactor using a solar energy system with temperature control unit. *Solar Energy*, *69*(3), 239–247. https://doi.org/10.1016/s0038-092x(00)00068-2

Allouhi, A., Benzakour Amine, M., Kousksou, T., Jamil, A., & Lahrech, K. (2018). Yearly performance of low-enthalpy parabolic trough collectors in MENA region according to different sun-tracking strategies. *Applied Thermal Engineering*, *128*, 1404–1419. https://doi.org/10.1016/j.applthermaleng.2017.09.099

Al-Oran, O., & Lezsovits, F. (2020). Enhance thermal efficiency of parabolic trough collector using Tungsten oxide/Syltherm 800 nanofluid. *Pollack Periodica*, *15*(2), 187–198. https://doi.org/10.1556/606.2020.15.2.17

Amro, H., Duo, Z., & Ling, Q. (2011). Solar water heating model with sun tracking system for increasing biogas production. *Nongye Gongcheng Xuebao/Transactions of the Chinese Society of Agricultural Engineering.*, *27*(06), 256–261. https://doi.org/10.3969/j.issn.1002-6819.2011.05.000

Arabacigil, B., Yuksel, N., & Avci, A. (2015). The use of paraffin wax in a new solar cooker with inner and outer reflectors. *Thermal Science*, *19*(5), 1663–1671. https://doi.org/10.2298/tsci121022031a

Ashish, A. (2019). Design and Development of Portable Solar Parabolic Cooker with Inorganic PCM Storage. *International Journal of Innovative Technology and Exploring Engineering*, *9*(2S4), 528–531. https://doi.org/10.35940/ijitee.b1192.1292s419

Axaopoulos, P., Panagakis, P., Tsavdaris, A., & Georgakakis, D. (2001). Simulation and experimental performance of a solar-heated anaerobic digester. *Solar Energy, 70*(2), 155–164. https://doi.org/10.1016/s0038-092x(00)00130-4

Badr, O., Mohammed, A., & Azddine, F. (2017). Feasibility study of integrating solar energy into anaerobic digester reactor for improved performances using TRNSYS simulation: application Kenitra Morocco. *Energy Procedia*, *136*, 402–407. https://doi.org/10.1016/j.egypro.2017.10.255

Bale Robe. (2021, March 31). Wikipedia. https://en.wikipedia.org/wiki/Bale_Robe

Bellos, E., Tzivanidis, C., & Belessiotis, V. (2017). Daily performance of parabolic trough solar collectors. *Solar Energy*, *158*, 663–678. https://doi.org/10.1016/j.solener.2017.10.038

Bergman, T. L., Lavine, A. S., Incropera, F. P., & DeWitt, D. P. (2020). *Fundamentals of Heat and Mass Transfer* (8th ed.). Wiley.

Bhagat, S., & Verma, P. K. (2011). Analyses of a Phase Change Material based Thermal Energy Storage System. *Indian Journal of Applied Research*, *3*(2), 347–349. https://doi.org/10.15373/2249555x/feb2013/118

Chahine, K., Murr, R., Ramadan, M., Hage, H. E., & Khaled, M. (2018). Use of parabolic troughs in HVAC applications – Design calculations and analysis. *Case Studies in Thermal Engineering*, *12*, 285–291. https://doi.org/10.1016/j.csite.2018.04.016

Chen, Z., Qin, C., Li, Z., & Dai, W. (2011). The transient analysis of a household biogas digester with solar assisted heating system. *Taiyangneng Xuebao/Acta Energiae Solaris Sinica.*, *32*, 1139–1143.

Cheng, J. J. (2017). Anaerobic Digestion for Biogas Production. In Biomass to Renewable Energy Processes [E-book]. In *Biomass to Renewable Energy Processes* (2nd ed., Vol. 1, pp. 346–467). CRC Press. https://www.routledge.com/Biomass-to-Renewable-Energy-Processe

Cvetković, S., Kaluđerović Radoičić, T., Vukadinović, B., & Kijevčanin, M. (2016). A life cycle energy assessment for biogas energy in Serbia. *Energy Sources, Part A: Recovery, Utilization, and Environmental Effects*, *38*(20), 3095–3102. https://doi.org/10.1080/15567036.2015.1135207

Darwesh, M., & Ghoname, M. (2021). Experimental studies on the contribution of solar energy as a source for heating biogas digestion units. *Energy Reports*, *7*, 1657–1671. https://doi.org/10.1016/j.egyr.2021.03.014

Dawit, G. G., Mahanta, P., & Robi, P. S. (2019). Designing and Utilizing of the Solar Water Heater for Digestion of Lignocellulosic Biomass. *Advances in Waste Management*, *1*, 91–105. https://doi.org/10.1007/978-981-13-0215-2_7

Dejene, K. K. (2020, June). *Computational Modeling and Performance Analysis of Solar Thermal Storage Integrated with Parabolic Solar Concentrator for Cooking Application*. Thesis Submitted to the school of Graduate Studies of Addis Ababa University in Partial Fulfillment of the Requirements for the Degree of the Doctor of Philosophy in Mechanical Engineering (with Specialization in Thermal and Energy Systems Engineering). http://etd.aau.edu.et/handle/123456789/67/browse?type=author&value=Dejene%2C+Kebede

Dinker, A., Agarwal, M., & Agarwal, G. (2017). Heat storage materials, geometry and applications: A review. *Journal of the Energy Institute*, *90*(1), 1–11. https://doi.org/10.1016/j.joei.2015.10.002

Duffie, & Beckman. (2013). *Solar Engineering of Thermal Processes by Duffie, John A., Beckman, William A.(April 15, 2013) Hardcover* (2nd ed.). Wiley.

El-Husseini, S., Mostafa, M., El-Gindy, A., & Anwar, A. (2019). SOLAR HEATING SYSTEM USING PARABOLIC COLLECTOR FOR THERMAL OPTIMUM CONDITIONS OF BIOGAS PRODUCTION IN WINTER. *Arab Universities Journal of Agricultural Sciences*, *27*(1), 123–134. https://doi.org/10.21608/ajs.2019.43073

ELMASHAD, H. (2004). Effect of temperature and temperature fluctuation on thermophilic anaerobic digestion of cattle manure. *Bioresource Technology*, *95*(2), 191–201. https://doi.org/10.1016/j.biortech.2003.07.013

El-Mashad, H. M., van Loon, W. K., Zeeman, G., Bot, G. P., & Lettinga, G. (2004). Design of A Solar Thermophilic Anaerobic Reactor for Small Farms. *Biosystems Engineering*, *87*(3), 345–353. https://doi.org/10.1016/j.biosystemseng.2003.11.013

Feng, R., Li, J., Dong, T., & Li, X. (2016a). Performance of a novel household solar heating thermostatic biogas system. *Applied Thermal Engineering*, *96*, 519–526. https://doi.org/10.1016/j.applthermaleng.2015.12.003

Feng, R., Li, J., Dong, T., & Li, X. (2016b). Performance of a novel household solar heating thermostatic biogas system. *Applied Thermal Engineering*, *96*, 519–526. https://doi.org/10.1016/j.applthermaleng.2015.12.003

Gaballah, E. S., Abdelkader, T. K., Luo, S., Yuan, Q., & El-Fatah Abomohra, A. (2020). Enhancement of biogas production by integrated solar heating system: A pilot study using tubular digester. *Energy*, *193*, 116758. https://doi.org/10.1016/j.energy.2019.116758

Gao, L., Gegentana, Bai, J., Sun, B., Che, D., & Li, S. (2020). Parametric analysis of a packed bed thermal storage device with phase change material capsules in a solar heating system application. *Building Simulation*, *14*(3), 523–533. https://doi.org/10.1007/s12273-020-0686-2

Ghodbane, M., & Boumeddane, B. (2018). A numerical analysis of the energy behavior of a parabolic trough concentrator. *Journal of Fundamental and Applied Sciences*, *8*(3), 671. https://doi.org/10.4314/jfas.v8i3.2

Gupta, R., Rai, S., & Tiwari, G. (1988). An improved solar assisted biogas plant (fixed dome type): A transient analysis. *Energy Conversion and Management*, *28*(1), 53–57. https://doi.org/10.1016/0196-8904(88)90011-8

Gutiérrez-Castro, L., Quinto-Diez, P., Barbosa-Saldaña, J., Tovar-Galvez, L., & Reyes-Leon, A. (2014). Comparison between a Fixed and a Tracking Solar Heating System for a Thermophilic Anaerobic Digester. *Energy Procedia*, *57*, 2937–2945. https://doi.org/10.1016/j.egypro.2014.10.329

Hassanein, A. A., Qiu, L., Junting, P., Yihong, G., Witarsa, F., & Hassanain, A. (2015). Simulation and validation of a model for heating underground biogas digesters by solar energy. *Ecological Engineering*, *82*, 336–344. https://doi.org/10.1016/j.ecoleng.2015.05.010

Hreiz, R., Adouani, N., Jannot, Y., & Pons, M. N. (2017). Modeling and simulation of heat transfer phenomena in a semi-buried anaerobic digester. *Chemical Engineering Research and Design*, *119*, 101–116. https://doi.org/10.1016/j.cherd.2017.01.007

Ibn, A., Baba, S. U., & Ismail. (2012). Anaerobic digestion of cow dung for biogas production. *ARPN Journal of Engineering and Applied Sciences*, *7*.

K. G. Gebremedhin, B. Wu, C. Gooch, P. Wright, & S. Inglis. (2005). HEAT TRANSFER MODEL FOR PLUG-FLOW ANAEROBIC DIGESTERS. *Transactions of the ASAE*, *48*(2), 777–785. https://doi.org/10.13031/2013.18320

Kalogirou, S. A. (2012). A detailed thermal model of a parabolic trough collector receiver. *Energy*, *48*(1), 298–306. https://doi.org/10.1016/j.energy.2012.06.023

Kalogirou, S. A. (2014). *Solar Energy Engineering: Processes and Systems* (1st ed.). Academic Press.

Kamp, L. M., & Bermúdez Forn, E. (2016). Ethiopia′s emerging domestic biogas sector: Current status, bottlenecks and drivers. *Renewable and Sustainable Energy Reviews*, *60*, 475–488. https://doi.org/10.1016/j.rser.2016.01.068

Karimov, K. S., & Abid, M. (2012). Biogas Digester with Simple Solar Heater. *IIUM Engineering Journal*, *13*(2). https://doi.org/10.31436/iiumej.v13i2.123

KARTHIKEYAN, S. (2011, December). *NUMERICAL AND EXPERIMENTAL INVESTIGATIONS ON A PACKED BED LATENT HEAT STORAGE SYSTEM FOR LOW TEMPERATURE AIR HEATING APPLICATIONS* (600 025). FACULTY OF MECHANICAL ENGINEERING ANNA UNIVERSITY, in partial fulfilment for the award of the degree of DOCTOR OF PHILOSOPHY.

KOUSKSOU, T., STRUB, F., CASTAINGLASVIGNOTTES, J., JAMIL, A., & BEDECARRATS, J. (2007). Second law analysis of latent thermal storage for solar system. *Solar Energy Materials and Solar Cells*, *91*(14), 1275–1281. https://doi.org/10.1016/j.solmat.2007.04.029

Kumar, A., & Shukla, S. (2015). A Review on Thermal Energy Storage Unit for Solar Thermal Power Plant Application. *Energy Procedia*, *74*, 462–469. https://doi.org/10.1016/j.egypro.2015.07.728

Kumar, D., & Kumar, S. (2015). Year-round performance assessment of a solar parabolic trough collector under climatic condition of Bhiwani, India: A case study. *Energy Conversion and Management*, *106*, 224–234. https://doi.org/10.1016/j.enconman.2015.09.044

Lamrani, B., Khouya, A., Zeghmati, B., & Draoui, A. (2018). Mathematical modeling and numerical simulation of a parabolic trough collector: A case study in thermal engineering. *Thermal Science and Engineering Progress*, *8*, 47–54. https://doi.org/10.1016/j.tsep.2018.07.015

Lemi, W. N., Koteswararao, B. K. B., Zeru, B. A., & P.V. (2020). Design and CFD Simulation of Solar Water Heater Used in Solar Assisted Biogas System. *International Journal of Innovative Technology and Exploring Engineering*, *9*(3), 371–380. https://doi.org/10.35940/ijitee.b7463.019320

Lin, W., Ma, Z., Ren, H., Gschwander, S., & Wang, S. (2019). Multi-objective optimisation of thermal energy storage using phase change materials for solar air systems. *Renewable Energy*, *130*, 1116–1129. https://doi.org/10.1016/j.renene.2018.08.071

Lu, Y., & Lu, H. (2016). Experimental Study of a Thermal Storage Technique with Phase Change Material Closure for Solar-Biogas Hybrid Fermentation System. *Fermentation Technology*, *05*(01). https://doi.org/10.4172/2167-7972.1000126

Lu, Y., Tian, Y., Lu, H., Wu, L., & Li, X. (2015). Study of solar heated biogas fermentation system with a phase change thermal storage device. *Applied Thermal Engineering*, *88*, 418–424. https://doi.org/10.1016/j.applthermaleng.2014.12.065

Madamwar, D., Patel, A., & Patel, V. (1990). Effect of temperature and retention time on methane recovery from water hyacinth-cattle dung. *Journal of Fermentation and Bioengineering*, *70*(5), 340–342. https://doi.org/10.1016/0922-338x(90)90146-n

Marefati, M., Mehrpooya, M., & Shafii, M. B. (2018). Optical and thermal analysis of a parabolic trough solar collector for production of thermal energy in different climates in Iran with comparison between the conventional nanofluids. *Journal of Cleaner Production*, *175*, 294–313. https://doi.org/10.1016/j.jclepro.2017.12.080

Mohammed, I. (2012). DESIGN AND DEVELOPMENT OF A PARABOLIC DISH SOLAR WATER HEATER. *Materials Science*. Published.

M.Sain, S., & Anita A, N. (2014). Thermal Simulation of Biogas Plants Using Mat Lab. *Journal of Engineering Research and Applications*, *4*(10), 24–28.

Nallusamy, N., Sampath, S., & Velraj, R. (2006). Study on performance of a packed bed latent heat thermal energy storage unit integrated with solar water heating system. *Journal of Zhejiang University-SCIENCE A*, *7*(8), 1422–1430. https://doi.org/10.1631/jzus.2006.a1422

Okuo, D., Waheed, M., & Bolaji, B. (2014). Evaluation of Biogas Yield of Selected Ratios of Cattle, Swine, and Poultry Wastes. *International Journal of Green Energy*, *13*(4), 366–372. https://doi.org/10.1080/15435075.2014.961460

Ouagued, M., Khellaf, A., & Loukarfi, L. (2013). Estimation of the temperature, heat gain and heat loss by solar parabolic trough collector under Algerian climate using different thermal oils. *Energy Conversion and Management*, *75*, 191–201. https://doi.org/10.1016/j.enconman.2013.06.011

Padilla, R., Demirkaya, G., Stefanakos, E., & Rahman, M. (2011). Heat transfer analysis of parabolic trough solar receiver. *Applied Energy - APPL ENERG*, *88*, 5097–5110. https://doi.org/10.1016/j.apenergy.2011.07.012.

Patel, V., Patel, A., & Datta, M. (1992). Effects of adsorbents on anaerobic digestion of water hyacinth - cattle dung. *Bioresource Technology*, *40*(2), 179–181. https://doi.org/10.1016/0960-8524(92)90206-d

Pollard, A. M., & Blanchard, R. (2014, January). *A Hybrid Biogas System for Kolkata*. International Conference on Non Conventional Energy (ICONCE). https://doi.org/10.1109/ICONCE.2014.6808701

Quinto, P., Aguilar, H., López, R., & Reyes, A. (2016). Potential of biogas production in an anaerobic digester solar assisted. *Renewable Energy and Power Quality Journal*, 580–582. https://doi.org/10.24084/repqj14.399

Rennuit, C., & Sommer, S. (2013). Decision Support for the Construction of Farm-Scale Biogas Digesters in Developing Countries with Cold Seasons. *Energies*, *6*(10), 5314–5332. https://doi.org/10.3390/en6105314

Reta, B. (2020, October). *Investigating the Performance of Parabolic Trough Solar Collector with Thermal Energy Storage System for Injera Baking Applications*. ASTU. https://etd.astu.edu.et

Reza Vakhshouri, A. (2020). Paraffin as Phase Change Material. *Paraffin - an Overview*. Published. https://doi.org/10.5772/intechopen.90487

Sharma, A., Tyagi, V., Chen, C., & Buddhi, D. (2009). Review on thermal energy storage with phase change materials and applications. *Renewable and Sustainable Energy Reviews*, *13*(2), 318–345. https://doi.org/10.1016/j.rser.2007.10.005

Shobo, A. B., & Mawire, A. (2015). *Numerical investigation of a packed bed thermal energy storage system for solar cooking using encapsulated phase change material*. 11–13.

Sitotaw, N. A. (2019, September). *Numerical Investigation of Solar Vapor Absorption Refrigeration System Integrated with Phase Change Material for Industrial Application*. Adama Science and Technology University. http://etd.astu.edu.et/handle/123456789/29

Surendra, K., Takara, D., Hashimoto, A. G., & Khanal, S. K. (2014). Biogas as a sustainable energy source for developing countries: Opportunities and challenges. *Renewable and Sustainable Energy Reviews*, *31*, 846–859. https://doi.org/10.1016/j.rser.2013.12.015

Tadesse Lulie.(2010).Study on current status of instutional Biogas Plant in Ethiopia

Tarekegn Kibret, L. (2018). Investigation of Thermal Performance of a Solar Assisted Anaerobic Digestion System Integrated With Solar Thermal Energy Storage

Packed With Phase Change Material. *Adama Science and Technology University Master Thesis*. Published.

Terradas-Ill, Georgina, P., Cuong, Jin, T., M.-H., & Sommer, S.G.., J. (2014). Thermic Model to Predict Biogas Production in Unheated Fixed Dome Digesters Buried in the Ground. *Environmental Science & Technology*, *7*, 3253–3262. https://doi.org/10.1021/es403215w.

Thermophilic digester. (2019, October 30). Wikipedia. https://en.wikipedia.org/wiki/Thermophilic_digester

Tian, Y., & Zhao, C. (2013). A review of solar collectors and thermal energy storage in solar thermal applications. *Applied Energy*, *104*, 538–553. https://doi.org/10.1016/j.apenergy.2012.11.051

Varel, V. H., Hashimoto, A. G., & Chen, Y. R. (1980). Effect of Temperature and Retention Time on Methane Production from Beef Cattle Waste. *Applied and Environmental Microbiology*, *40*(2), 217–222. https://doi.org/10.1128/aem.40.2.217-222.1980

Varel, V. H., Isaacson, H. R., & Bryant, M. P. (1977). Thermophilic methane production from cattle waste. *Applied and Environmental Microbiology*, *33*(2), 298–307. https://doi.org/10.1128/aem.33.2.298-307.1977

Wassie, Y. T., & Adaramola, M. S. (2020). Analysing household biogas utilization and impact in rural Ethiopia: Lessons and policy implications for sub-Saharan Africa. *Scientific African*, *9*, e00474. https://doi.org/10.1016/j.sciaf.2020.e00474

Xu, B., Li, P., Chan, C., & Tumilowicz, E. (2015). General volume sizing strategy for thermal storage system using phase change material for concentrated solar thermal power plant. *Applied Energy*, *140*, 256–268. https://doi.org/10.1016/j.apenergy.2014.11.046

Yiannopoulos, A. C., Manariotis, I. D., & Chrysikopoulos, C. V. (2008a). Design and analysis of a solar reactor for anaerobic wastewater treatment. *Bioresource Technology*, *99*(16), 7742–7749. https://doi.org/10.1016/j.biortech.2008.01.067

Yiannopoulos, A. C., Manariotis, I. D., & Chrysikopoulos, C. V. (2008b). Design and analysis of a solar reactor for anaerobic wastewater treatment. *Bioresource Technology*, *99*(16), 7742–7749. https://doi.org/10.1016/j.biortech.2008.01.067

Yılmaz, B. H., & Mwesigye, A. (2018). Modeling, simulation and performance analysis of parabolic trough solar collectors: A comprehensive review. *Applied Energy*, *225*, 135–174. https://doi.org/10.1016/j.apenergy.2018.05.014

Yousuf, A., Khan, M. R., Pirozzi, D., & Ab Wahid, Z. (2016). Financial sustainability of biogas technology: Barriers, opportunities, and solutions. *Energy Sources, Part B: Economics, Planning, and Policy*, *11*(9), 841–848. https://doi.org/10.1080/15567249.2016.1148084

Youzhou, J., Pengfei, L., Li, G., Zhang, Q., Ding, P., Wang, S., Gao, Z., Du, S., & He, C. (2016). Design and preliminary experimental research on a new biogas fermentation system by solar heat pipe heating. *International Journal of Agricultural and Biological*, *9*(2), 153–162. https://doi.org/10.3965/j.ijabe.20160902.1935

Yuan, S., Rui, T., & Hong, Y. X. (2011a). Research and Analysis of Solar Heating Biogas Fermentation System. *Procedia Environmental Sciences*, *11*, 1386–1391. https://doi.org/10.1016/j.proenv.2011.12.208

Yuan, S., Rui, T., & Hong, Y. X. (2011b). Research and Analysis of Solar Heating Biogas Fermentation System. *Procedia Environmental Sciences*, *11*, 1386–1391. https://doi.org/10.1016/j.proenv.2011.12.208

Yune, H. S. (2019, September). *Investigating the Thermal Performance of a Solar Water Heating System Integrated with Phase Change Material as a Thermal Energy Storage: A Case of Adama Hospital Medical College*. Adama Science and Technology University.

In partial fulfillment of the degree of Masters of Science in Thermal Engineering

Zupančič, G., & Roš, M. (2003). Heat and energy requirements in thermophilic anaerobic sludge digestion. *Renewable Energy*, *28*(14), 2255–2267. https://doi.org/10.1016/s0960-1481(03)00134-4

APPENDIX

ANNEX –A.1: Hourly beam incident solar radiation

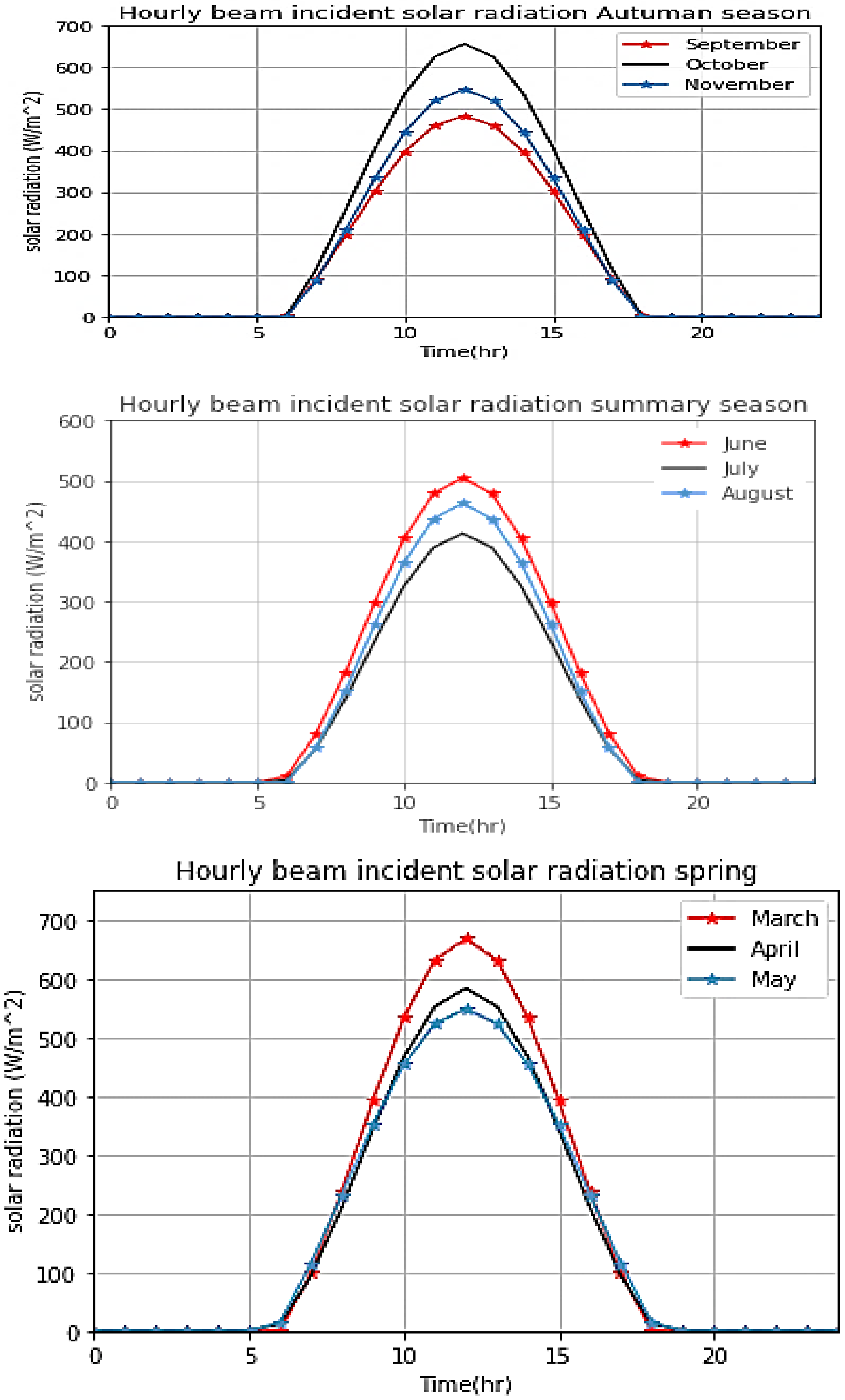

Figure ANNEX A. 1: Hourly beam incident solar radiation of autumn, summer and spring.

ANNEX- A.2. HTF outlet temperature throughout the day of the rest of season

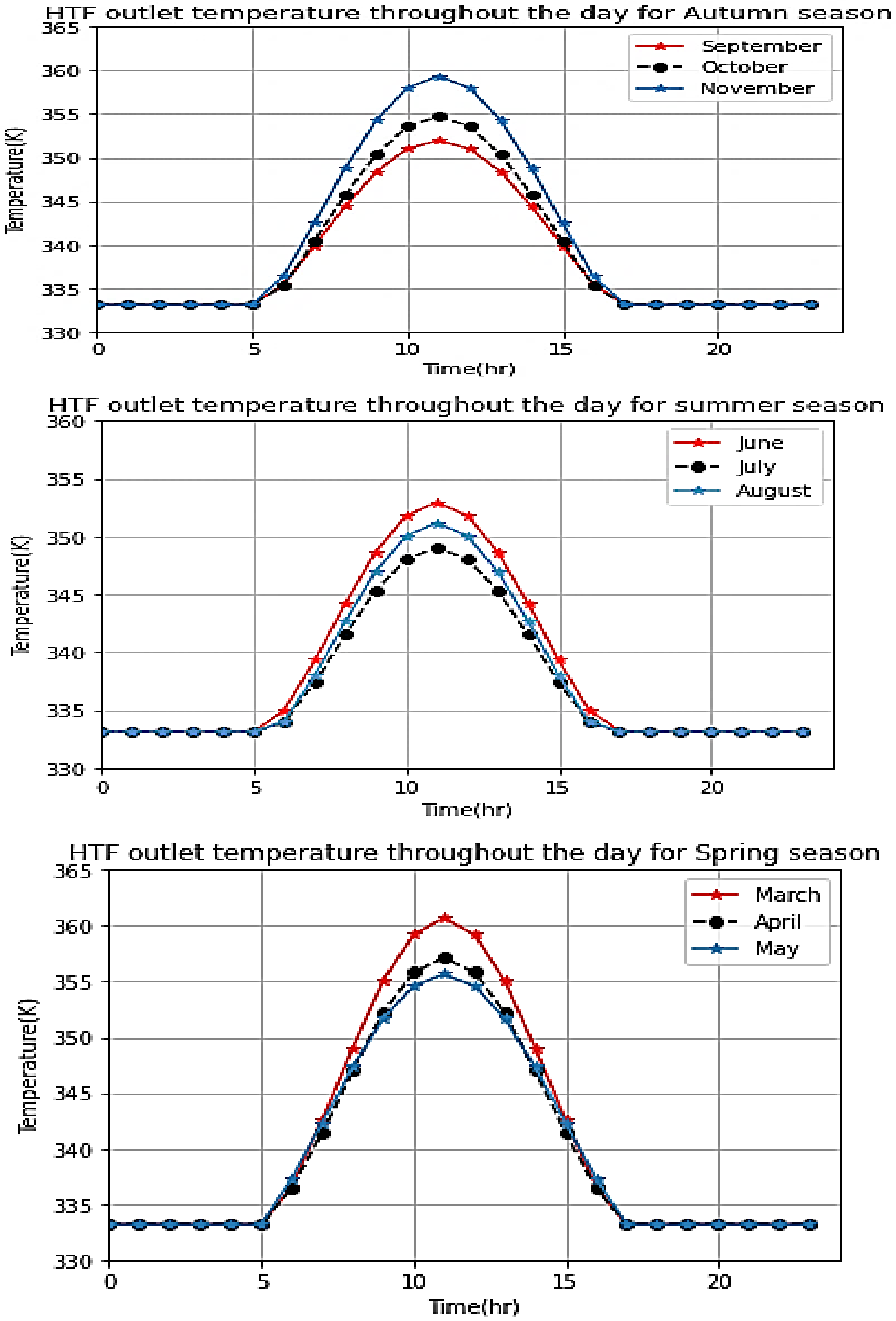

Figure ANNEX A. 2: HTF outlet temperature throughout the day of the autumn, summer, spring.

ANNEX B: PYTHON program of Transient Thermal Simulation of a Digester

```
# -*- coding: utf-8 -*-
"""Created on Sat Apr 3 16:24:34 2021
Atmospheric hourly temperature variation and biogas digester simulation. This code is developed to determine the transient analysis of thermophilic biogas digester. The program is written to simulated biogas digester maintain (60 ºC) and with variation ambient temperature. Plot code is removed for clarity's of document.
""""""
@author: Beyisa Bogale
""""
Import matplotlib.pyplot as plt
from scipy.integrate import odeint
## Atmospheric temperature variation
Tmax=float (input ('enter the maximum temperature of the day the month'))
Tmin=float (input ('enter the minimum temperature off the day the month '))
xax=np.linspace(0,12,12)                    #graduation of x axis
def hourly_temp(t):
    TW = Tmax - ((Tmax-Tmin)/2)*(1 - np.sin((np.pi*t-10*np.pi)/12))
    return TW
TW = np.array ([0.0]*(24))
for i in range (1,25):
    TW[i-1] = hourly_temp(i)
## Transient analysis of thermophilic biogas digester
"" INPUT VARIABLE"""
for simplification, the density and heat capacity of the feed (slurry and manure) were considered similar to that of water (983. kg m-3 and 3976.7J kg-1K-1 respectively, evaluated at 60 °C). Rho=983.20    , density of digest state in kg/m^3 for simplification density of water is taken at 60 Vdg=100            #volume of digestate in m^3.
Cdg=3976.7                    # heat capacity of digestate in J/kgK
A=rho*vdg*Cdg
Mf= 5083.5                    # mass of feed kg (Feeding and leaving rate are equal)
Cw=4179                       # specific heat of water J/kgK
```

```
B=mf*Cw
hDg_Bg=0.269                  #convective heat transfer between digeste and biogas calculated form give data and formula
SDg_Bg=10.45                  # SDg_Bg the digestate free surface (equals the digester’s cross-section, 10.45 m2)
C=hDg_Bg*SDg_Bg
Sigma = 5.67e-8                              #Boltzman constant
epsdg=0.9                                     # thermal emissivity of digester
epsco=0.9                                    # thermal emissary of cover
Sco=20.9                                          #Cover cross sectional
U=(1-epsdg)/(epsdg*SDg_Bg)+(1-epsco)/(epsco*Sco)            #Heat transfer convection
D=sigma/U
hDg=0.269
Lwall=0.2                                      # thickness of concrate wall in m
Adg=94.8                                      # surface area of cylinerical digester
Kwall=1.5                                     # thermal conductivity of digester
UDg_soil=(Kwall*hDg)/(Kwall+(hDg*Lwall))
E=UDg_soil*Adg
"""intial Temp """
Tamb=TW                                      #float (input ("insert average ambient temp of first month in K"))
Tamb=float(input("insert average ambient temp of first month in K"))
Tsoil=17.898+0.98*Tamb
```

""Digestate Phase"""

```
def digestate(TDg,t):
    TBg= (TDg-10)
    dTDgdt = 1/A*((B*(Tamb-TDg)-C*(TDg-TBg)-D*(TDg**4-TBg**4)-E*(TDg-Tsoil)))
    return dTDgdt
td = np.linspace(0,24,24)                         # Time values
Tdg = odeint(digestate,333.15,td)                  # Temperature of digester
lostd = -((B*(Tamb-(Tdg))-C*(Tdg-TBg)-D*(Tdg**4-TBg**4)-E*(Tdg-Tsoil)))/A   #Heat lost from digester
```

"""Biogas phase"""

```
AA=1.075*30.5*1376.5                             # Density*Volume Biogas*heat capacity
```

```
BB=1.075*30.5                                  # mass of biogas
hDg_co=0.269                      # convective heat transfer between biogas and digestate
Sco=20.9                           # cross sectional area cover by biogas
DD=hDg_co*Sco
 def biogas(TBg,t):
        dTBgdt = 1/AA*((BB*(TDg-TBg)+C*(TDg-TBg)-DD*(TBg-Tco)))
            return dTBgdt
tb=np.linspace(0,24,24)
Tbiogas = odeint(biogas,313.56,tb)                        # Return value of temperature of
biogas
lostb=-BB*(Tdg-Tbiogas)+CC*(Tdg-Tbiogas)+DD*(Tbiogas-Tco)      # loss of biogas
```

"""Cover phase"""

```
rho_co=1125                              # density of cover kg/m3
V_co=30                                  # Volume of cover
C_co=1900                                #specific het capacity of of cover
CA=rho_co*V_co*C_co
Sco=20.9                                 # surface area of cover
CB=hDg_co*Sco
rho_air=1.1924                           #Density of air
C_at=1006                                # specific heat capacity
U_wind=3.5                                  #wind speed
hco_at=0.025*rho_air*C_at*U_wind**0.3
cD=hco_at*Sco
epdg=0.9
epco=0.9
Qr_co=1588.174926
Ts=60+273
CE=(1-epdg)/(epdg*SDg_Bg)+((1-epco)/(epco*Sco))*sigma
def cover (Tco,t):
   dTcodt   =   1/CA*((CB*(Tdg-Tco)-cD*(Tco-Tamb)-cD*(Tbiogas-Tco)-CE*(Tdg**4-
Tco**4)))
 return dTcodt
 tc = np.linspace(0,24,24) # Time values in hr
 Tcover = (odeint(cover,(45+273),tc))
```

```
lostc=-((CB*(Tdg-Tcover)-cD*(Tcover-Tamb)-cD*(Tbiogas-Tcover)-CE*(Tdg**4-
Tcover**4)))+Qr_co
```

ANNEX C-: MATLAB program for PCM thermal storage system

```
function paraffinWaxc_pcm
global H e v r_f l_f c_f mu_f r_s1 r_s2 c_s1 c_s2 l_s1 l_s2 lh Vst Dst
global u_m1 u_m2 h_f u1 u2 dp Re Pr tend
Vst=9.8;                          %Volume of storgae Tank
Dst=2.03;                         % diameters of tank
H=3.04;                           % Length of tank in m
e=0.5;                            % Porosity
v=4.715E-04;                      % Fluid velocity in m/s
l_f=0.654;                        % Fluid thermal conductivity of water
r_f=983.21;                       % Fluid density
mu_f=0.466E-3;                    % Fluid dynamic viscosity
dp=0.08;                          % Diameter of of spherical particle
r_s1=912;                         % Density of solid PCM
r_s2=781;                         % Density of liquid PCM
c_s1=1855;                        % Specific heat of solid PCM
c_s2=2387;                        % Specific heat of liquid PCM
l_s1=0.217;                       % Thermal conductivity of solid PCM
l_s2=0.156;                       % Thermal conductivity of liquid PCM
lh=260000;                        % Latent heat of fusion for PC
u_m1=67;                          % Lower limit temperature for phase change in oC
u_m2=68.5;                        % Upper limit temperature for phase change in oC
tend=32400;                       % seconds
Re=(r_f*dp*e*v)/mu_f;     % Reynold number
Pr=(c_f*mu_f)/l_f;        % Prandtl Number

h_f=(((6*(1-e))*(2+(1.1*(Re^0.6)*(Pr^(1/3)))*l_f))/(dp^2)); % Heat transfer coefficient
m = 0;                            %% symmetry constant of solving pde equation
x = linspace(0,H,700);            % Space discretization
t = 0:1:tend;                     % Time discretization
```

```
sol = pdepe(m,@tes1pde,@tes1ic,@tes1bc,x,t);

u1 = sol(:,:,1);                    % Solution for fluid phase
u2 = sol(:,:,2);                  % Solution for solid phase

% Plot of temperature variation with time for fluid
figure(1)
plot(t,u2(:,1),'r');
figure(2)
plot(t,u1(:,100),'r-')
hold all
figure,plot(t,u2(:,100),'b',t,u1(:,100),'b:')
hold all
plot(t,u2(:,200),'y',t,u1(:,200),'y:')
hold all
plot(t,u2(:,300),'c',t,u1(:,300),'c:')
hold all
figure(3)
plot(t,u2(:,400),'c')%,t,u1(:,400),'c:')
hold all
plot(t,u2(:,500),'g')%,t,u1(:,500),'g:')
plot(t,u2(:,550),'c')%,t,u1(:,500),'c:')
hold all
plot(t,u2(:,600),'c')%,t,u1(:,600),'c:')
hold all
plot(t,u2(:,650),'c')%,t,u1(:,650),'c:')
hold all
plot(t,u2(:,700),'c')%,t,u1(:,700),'c:')
legend('N=400','N=500','N=550','N=600','N=650','N=N');
title('Temperature Profile of PCM storage')
xlabel('Time,t')
ylabel('Temperature,T')
grid on;
title('Temperature histories of PCM Storage during charging')
```

```
xlabel('Time (sec)')
ylabel('Temperature (^0C)')
function [c,f,s] = tes1pde(x,t,u,DuDx)
global l_f v r_f c_f h_f e c_s1 c_s2 r_s1 r_s2 lh u_m1 u_m2 l_s1 l_s2
    if (u(2)<u_m1)
        c = [(e*r_f*c_f); ((1-e)*r_s1*c_s1)];
    elseif (u(2)>=u_m1 && u(2)<u_m2)
        c = [(e*r_f*c_f); ((1-e)*((r_s1+r_s2)./2)*(((c_s1+c_s2)/2)+(lh./(u_m2-u_m1))))];
    else
        c = [(e*r_f*c_f); ((1-e)*r_s2*c_s2)];
    end
    if (u(2)<u_m1)
        f = [(e*l_f*DuDx(1))-(e*v*r_f*c_f*u(1)); (1-e)*l_s1*DuDx(2)];
    elseif (u(2)>=u_m1 && u(2)<u_m2)
        f = [(e*l_f*DuDx(1))-(e*v*r_f*c_f*u(1)); (1-e)*((l_s1+l_s2)/2)*DuDx(2)];
    else
        f = [(e*l_f*DuDx(1))-(e*v*r_f*c_f*u(1)); (1-e)*l_s2*DuDx(2)];
    end
        s = [-(h_f*(u(1)-u(2))); (h_f*(u(1)-u(2)))];
function u0 = tes1ic(x)
u0 = [25;25];
function [pl,ql,pr,qr] = tes1bc(xl,ul,xr,ur,t)
global e v r_f c_f
pl = [e*v*r_f*c_f*80; ul(2)];
ql = [1; 1];
pr = [e*v*r_f*c_f*ur(1); ur(2)];
qr = [1; 1];
```